1974

Solid transformations and premelting phenomena in fluorite structures and the system $SrCl_2BaCl_2$

Damri Sukhotanang

SOLID TRANSFORMATIONS AND PREMELTING PHENOMENA IN FLUORITE STRUCTURES AND THE SYSTEM $SrCl_2$-$BaCl_2$

by

DAMRI SUKHOTANANG, 1949-

A DISSERTATION

Presented to the Faculty of the Graduate School of the

UNIVERSITY OF MISSOURI - ROLLA

In Partial Fulfillment of the Requirements for the Degree

DOCTOR OF PHILOSOPHY

in

CERAMIC ENGINEERING

1974

Charles A Sorrell — J. B. Clark

Advisor

Harlan L. Anderson — L. D. Moore

W. A. Yolton

ABSTRACT

Thermal expansion and phase transformations in CaF_2, BaF_2, $SrCl_2$, and $BaCl_2$ were studied by high temperature x-ray diffractometry, differential thermal analysis, and thermodilatometric analysis. Thermal expansion characteristics of CaF_2, BaF_2 and $SrCl_2$ are very similar. The structures expand normally at lower temperatures and depart substantially from linearity at higher temperatures, because of formation of defects and disordering of anions. At high temperatures CaF_2 and BaF_2 react with water vapor, even at low humidities, forming oxides and emitting HF, leading to difficulty in observation of phase transformations. $SrCl_2$ undergoes the transformation from the cubic fluorite to a hexagonal structure in the temperature range 660°-750°C, with nucleation and grain growth. $BaCl_2$ occurs in three forms: cubic, orthorhombic, and hexagonal. The cubic form is stable below about 165°C and transforms irreversibly to the orthorhombic form; at 920°C the orthorhombic form is changed to a highly disordered hexagonal structure, similar to the hexagonal form of $SrCl_2$.

Cubic fluorite compounds can change to the orthorhombic $PbCl_2$ structure, to a hexagonal structure, or to a disordered structure, depending on pressure, temperature, and the chemistry of compound. The mechanism of the transformation is related to movement of anions in the open fluorite structure, followed by changes in

first-coordination.

The study of phase relationships of the system $SrCl_2$-$BaCl_2$ shows that at high temperatures $SrCl_2$ forms a complete solid solution series with $BaCl_2$, having hexagonal structure, with a freezing point minimum of 845°C at about 28 mole percent $BaCl_2$. At lower temperatures the samples with more than 35 mole percent $BaCl_2$ form orthorhombic solid solutions and those with less than 25 mole percent $BaCl_2$ form cubic solid solutions. Orthorhombic solid solutions invariably persist at room temperature rather than inverting to the stable cubic structure.

ACKNOWLEDGEMENT

The author wishes to acknowledge the aid and advice of Dr. Charles A. Sorrell, major advisor. He is also grateful to Dr. Harlan U. Anderson for his helpful discussion and to Dr. Robert E. Moore for his interest and encouragement. Computer program for calculating the thermal expansion written by R. R. Ramey was helpful.

Part of the thesis investigation was completed during a semester with the High-Temperature Chemistry Group, under the supervision of Dr. Robert J. Thorn, to whom appreciation is extended. The author is particularly grateful to Dr. Raymond J. Ackermann, Argonne National Laboratory, for his help, advice, and the use of a high-temperature X-ray unit.

The financial support provided by the Civil Service Commission of Thailand is greatly appreciated. Some additional support during a semester at Argonne National Laboratory by U. M. R. is appreciated.

TABLE OF CONTENTS

LIST OF ILLUSTRATIONS

LIST OF TABLES

I. INTRODUCTION

The fluorite structure involves a face centered cubic arrangement of cations, with anions located in all available tetrahedral sites.[1-4] The structure can be described alternatively as a simple cubic anion array, with half the 8-fold positions occupied by cations in an alternative arrangement. More than 100 compounds have been reported with the fluorite structure, including such important ceramic oxides as UO_2, PuO_2, and ThO_2.

High-temperature calorimetric measurements on some fluorite-type materials, such as CaF_2, $SrCl_2$, and UO_2, show anomalies in the heat content curve before melting.[5-12] The same phenomenon also occurs in the anti-fluorite type of compound.[13] It has also been reported that the entropies of fusion of some salts with the fluorite and anti-fluorite structures are unusually low in comparison with those of other salts such as MgF_2, or $CaBr_2$.[6] The low entropies of fusion were found to be the result of anomalously high entropies of the solids at or near the melting points, in which case heat capacity curves exhibit lambda-type maxima well below the melting points. The reasons for this phenomenon are not yet fully understood. Some have explained this phenomenon in terms of formation of Schottky and Frenkel defects with increasing temperature.[8] Bredig[11] interpreted the anomaly as an order-disorder (lambda) transition. Several investigators[6-8,11] refer to the anomaly as a diffuse transition, suggesting that it

is attributable to the gradual redistribution of anions (x), with rising temperature, over both octahedral and tetrahedral lattice positions.

The transition before melting also occurs in some lead-chloride type structure compounds, such as $BaCl_2$, $SrBr_2$.[6,12] These compounds show large "first order" transition entropies just below the melting points. The high temperature forms of $BaCl_2$ and $SrBr_2$ are believed to have the fluorite type of structure. The mechanism and the characteristics of these transformations are not yet fully determined.

There are two main purposes in this study. The first is to characterize the premelting transition of some compounds having the fluorite structure. CaF_2, BaF_2 and $SrCl_2$ were chosen for study because of their low melting points. The explanation of premelting phenomena in these compounds could very well be extended to those that may occur in the important fluorite-type ceramic oxides at much higher temperatures. The second is examination of premelting transition characteristics of $BaCl_2$ and phase equilibria in the system $SrCl_2$-$BaCl_2$. A new form of $SrCl_2$ was found and sub-solidus equilibria in the system $SrCl_2$-$BaCl_2$ at high temperature were determined during this investigation. Experimental methods included x-ray diffraction, high-temperature x-ray diffraction, differential thermal analysis (DTA), and dilatometry.

II. LITERATURE REVIEW

A. Crystal Structure of the Fluorite Type Materials

The fluorite structure was first described by Bragg[1] in 1914. It is a cubic face-centered structure in which each cation is surrounded by eight anions at the corners of a cube and each anion is tetrahedrally surrounded by four cations.[1-4] There are four formular units (AX_2) per unit cell, with the atoms are in a and c Wyckoff positions of O_h^5 ($Fm3m$):[14]

(A) Cation: (4a) 000; 0 1/2 1/2; 1/2 0 1/2; 1/2 1/2 0

(X) Anion : (8c) $\pm$ (1/4 1/4 1/4; 1/4 3/4 3/4; 3/4 1/4 3/4; 3/4 3/4 1/4)

The (100) projection of the unit cell of the fluorite structure is shown in Figure 1.

The fluorite structure normally occurs in the compounds that are predominantly ionic and contain rather large cations, but it can occur in intermetallic compounds as well. The geometric basis of the crystal structure shows that 8:4 co-ordination will occur when the radius ratio is greater than 0.73, that is, when r(A)/r(X) is greater than or equal to 0.73.

Wyckoff[2] pointed out that there are four kinds of the fluorite-like crystals.

1. Halides of the larger divalent cations.

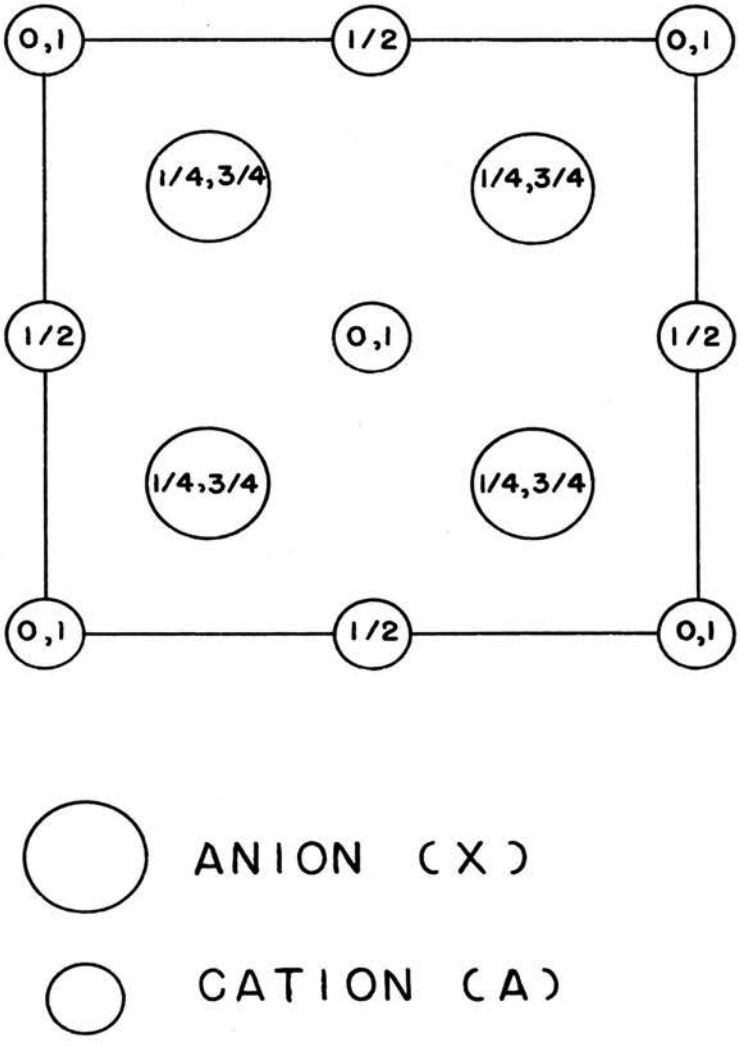

Figure 1. Projection of Fluorite Structure on (100)

2. Oxides, sulfides, etc. of univalent ions, mostly alkalies, with structures called anti-fluorite structure, because of the reverse arrangement of cation and anion. In this structure, the anions rather than cations are in (4a) Wyckoff positions; the radius ratio is commonly greater than unity.

3. Oxides of large quadrivalent cations.

4. Intermetallic compounds.

Some metal halides and oxides with the fluorite type structure[2-4] are tabulated in Table I. The radius ratios and the lattice parameters are also included. It can be seen that in some fluorite structures the radius ratios are smaller or much greater than 0.73. This may be attributed to polarization of the ions and involvement of the covalent bond in the structure.

The fluorite structures investigated in this study are CaF_2, BaF_2, $SrCl_2$ and $BaCl_2$. The lattice parameters of these materials were carefully measured and reported by Swanson and coworkers.[15-17] The lattice constants of CaF_2, BaF_2 and $SrCl_2$ at 25°C. are 5.4626 Å, 6.2001 Å, and 6.9767 Å, respectively. Cubic $BaCl_2$ was reported as an unstable form that persisted at room temperature with 7.311 Å lattice constant.[17]

TABLE I

Metal Halides and Oxides with the Cubic Fluorite Structure[2-4]

Compound	Radius Ratio r(A)/r(X)	a, Å	
AmO_2	0.61	5.376	
$BaCl_2$	0.75	7.34	(25°C)
BaF_2	0.99	6.2001	(25°C)
CaF_2	0.73	5.46295	(28°C)
CdF_2	0.71	5.3880	
CeO_2	0.72	5.4110	(26°C)
CmO_2	-	5.372	
EuF_2	-	5.796	
HfO_2	0.56	5.115	
HgF_2	0.81	5.54	
NpO_2	0.63	5.4341	
PaO_2	0.65	5.505	
β-PbF_2	0.88	5.92732	(18°C)
α-PoO_2	-	5.687	(5.626 at-190°C)
PrO_2	0.66	5.4694	
PuO_2	0.62	5.3960	
RaF_2	1.05	6.368	
$SrCl_2$	0.63	6.9767	(26°C)
SrF_2	0.83	5.7996	(26°C)
TbO_2	0.58	5.220	
ThO_2	0.68	5.5997	

TABLE I (Cont.)

Compound	Radius Ratio r(A)/r(X)	a,Å
UO_2	0.64	5.4682 (26°C)
ZrO_2	0.57	5.07

B. Reported Transformations in Fluorite Structures

In 1945 Naylor[5] measured high temperature heat contents of magnesium and calcium fluorides by the "drop" method.[18] He observed that calcium fluoride shows an anomalous heat content in the region between 1320 and 1440 °K (1047°-1167°C). To fit equations to the heat content curve, the alpha (α) and beta (β) forms were designated as low and high temperature forms of CaF_2, respectively, with a transition temperature of 1424 °K (1151°C). The mechanism of the transition has not been delineated.

In 1946 Croatto and Bruno,[19] studied the transition in $SrCl_2$ by x-ray methods. X-ray diffraction patterns showed a few very faint lines, indicating lattice disorder with increase in temperature. They suggested that the lattice disorder was due to the anions tending to abandon statistically their regular lattice positions to occupy new positions, corresponding statistically to a partial 1/2 1/2 1/2 lattice with centered faces. Heat content and entropy of $SrCl_2$ were measured by Dworkin, and Bredig[6-7] with a copper block drop calorimeter. Variation of heat content of $SrCl_2$ with temperature was found to be similar to that shown in CaF_2. The transition occurs gradually between 940° and 1040°K (667° and 767°C), with no discontinuity in the heat content curve. A solid-solid transition in $SrCl_2$ was confirmed by Janz and coworkers[12] in 1963, and by Efremova and Matizen[20] in 1970. Efremova and Matizen also reported similar variations in enthalpy data for SrF_2 and

BaF_2. They reported transition temperatures in the solid state as follows: BaF_2, 1240° and 1480°K (967° and 1207°C), $SrCl_2$, 990°K (717°C), SrF_2 (one transition) 1421-84°K (1148-1211°C). These transitions were assumed to reflect gradual disordering of the anion sublattice, and was called a diffuse transition.

The high-temperature calorimetric heat content measurements on UO_2 was first interpreted by Szwarc[8] as a result of formation of point defects and a theoretical treatment was presented in the usual terms of a limited concentration of non-interacting Frenkel defects in the oxygen lattice.

It was noted that fusion entropies of the fluorite and anti-fluorite compounds, such as CaF_2 (1.40 cal deg^{-1} gram ion^{-1}), $SrCl_2$ (1.13), and K_2S (1.16), were low in comparison with those of other simple salts, such as MgF_2 (3.0), $CaBr_2$ (2.3).[6-7,11-13] These were found to be the result of entropies of the transitions occurring below the melting points. These transitions were interpreted in terms of an order-disorder (lambda) type of transition by Bredig[11] in 1972. He also pointed out the effect of ion size on the transition by correlating excess entropy for the order-disorder transition with the relative sizes of the A and X ions. Dworkin and Bredig[13] suggested that the occurrence of a diffuse transition is a general characteristic of compounds with fluorite and anti-fluorite structures. The heat contents and entropies of K_2S, with an anti-fluorite structure, exhibit the same features as those of CaF_2

and $SrCl_2$. Heat content and molar heat capacity curves of CaF_2 and $SrCl_2$ are shown in Figure 2.

It was postulated that disordering of the anions is a characteristic feature of the special geometry of the fluorite (and anti-fluorite) structure, in which half of the octahedral sites are unoccupied. In 1965 Willis[21] found that at room temperature the neutron intensities of the Bragg reflexions of CaF_2 show a slight displacement of fluorine atoms toward the centers of the interstitial holes at 1/2 1/2 1/2. A similar structural feature was reported for BaF_2,[22] SrF_2,[23] UO_2, and ThO_2[24] at high temperatures. A model for description of the phase transition in fluorite type lattice was proposed by Belosludov, Efremova and Matizen[25] in 1974. Many investigators[26-30] have studied lattice disorder of fluorite structures by measuring ionic conductivity of pure crystals and/or of crystals containing known concentrations of aliovalent cations. They have generally concluded that the predominant imperfections at high temperatures are anionic Frenkel defects, and that transport of the anions takes place by either an interstitialcy or a vacancy mechanism. The model of anion disorder has received support from transport and diffusion studies, showing that diffusion coefficients for cations in the fluorite type materials are very small compared with those of the anions.[26,28,31] The mechanism and the characteristics of these transitions, however, are not yet fully understood. No high temperature x-ray diffraction data

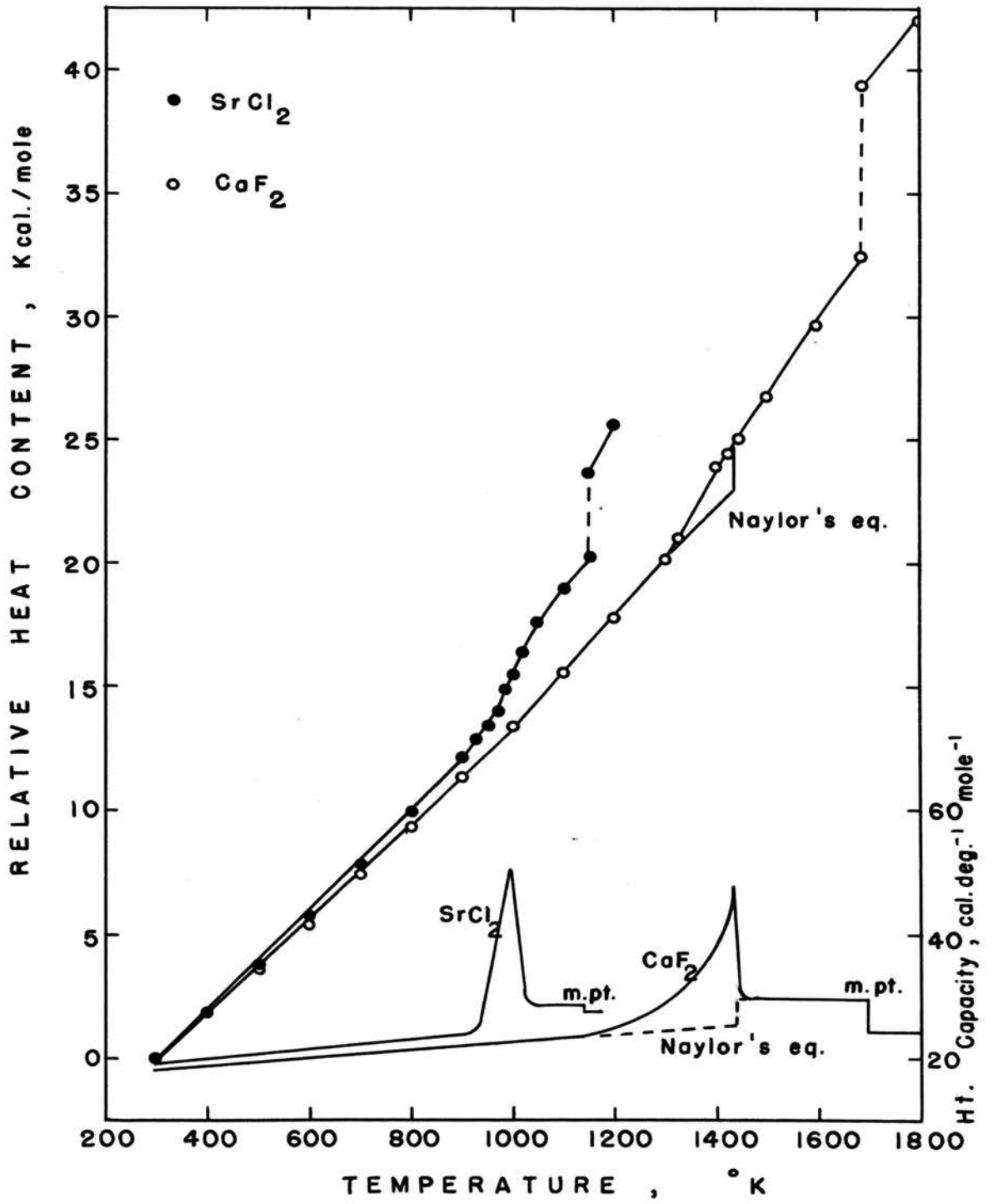

Figure 2. Heat Contents and Molar Heat Capacities of CaF_2 and $SrCl_2$: From [5,7]

have been published.

C. Crystal Structures of $BaCl_2$ Polymorphs

1. Orthorhombic $BaCl_2$

The earliest study of the crystallography and the polymorphism of $BaCl_2$ was done in 1913 by Gemsky,[32] by means of cooling curves and optical methods. He indicated that at 930°C the singly refracting modification of barium chloride which crystallises out at 955°C is transformed into a doubly refracting form. Monoclinic symmetry was suggested for the low temperature form. The principal x-ray diffraction investigation of $BaCl_2$ was done by Döll and Klemm[33] in 1939. They showed that $BaCl_2$ has an orthorhombic modification, with the lead chloride structure stable at room temperature. They reported lattice parameters for orthorhombic $BaCl_2$ as a=4.705 Å, b=7.823 Å, and c=9.338 Å. The structure was refined by Brackett, Brackett and Sass[34] and Sahl,[35] both in 1963. Solans-Huguet and Font-Altaba[36] reported the lattice parameters of orthorhombic $BaCl_2$ as a=4.733 Å, b=7.870 Å, and c=9.417 Å; Brackett et al.[34] reported a=7.865 Å, b=4.731 Å, and c=9.421 Å with a reversal of the a and b axes from those of the previous investigators.[33] Swanson et al.[17] reported the lattice constants of orthorhombic $BaCl_2$ as a=7.872 Å, b=9.425 Å, and c=4.7322 Å with a reversal of the b and c axes from those of Brackett et al. The monoclinic symmetry suggested by Gemsky[32] has not been confirmed.

The orthorhombic structure of $BaCl_2$ can be described as a considerably distorted close-packed arrangement of chlorine ions with the barium ions accommodated in the same plane. There are nine chlorine ions surrounding each barium ion, three on the same crystallographic mirror plane and three each on the two equivalent mirror planes above and below. Brackett et al.[34] showed that seven chlorine ions are arranged at closer distances; one each at 2.86, 3.15, and 3.18 Å, two each at 3.17, and 3.25 Å, and two other chlorine ions at much greater distances (3.58 Å). Sahl[35] also reported the same, with modified distances, of course. There are four molecules (AX_2) per unit cell, where all atoms are in special positions,

(4c): ± (u,v,1/4; 1/2-u, v+1/2, 1/4),

of D_{2h}^{16} (Pnma), with the parameters u(Ba)=0.2514, v(Ba)= 0.1209. u(Cl,1)=0.1504, v(Cl,1)=0.4130, u(Cl,2)=0.0290, v(Cl,2)=0.8392 (parameters rearranged from [34]). The orthorhombic structure of $BaCl_2$ is shown in Figure 3.

2. Cubic $BaCl_2$

Cubic barium chloride was observed in 1948 by Vainshtein.[37] From electron diffraction determination on layers of barium chloride 10^{-6} cm. thick on celluloid film, he reported that the structure is cubic, with a=7.34 Å. In 1963 Brackett et al.[34] heated the dihydrate of barium chloride under vacuum at 60°C overnight,

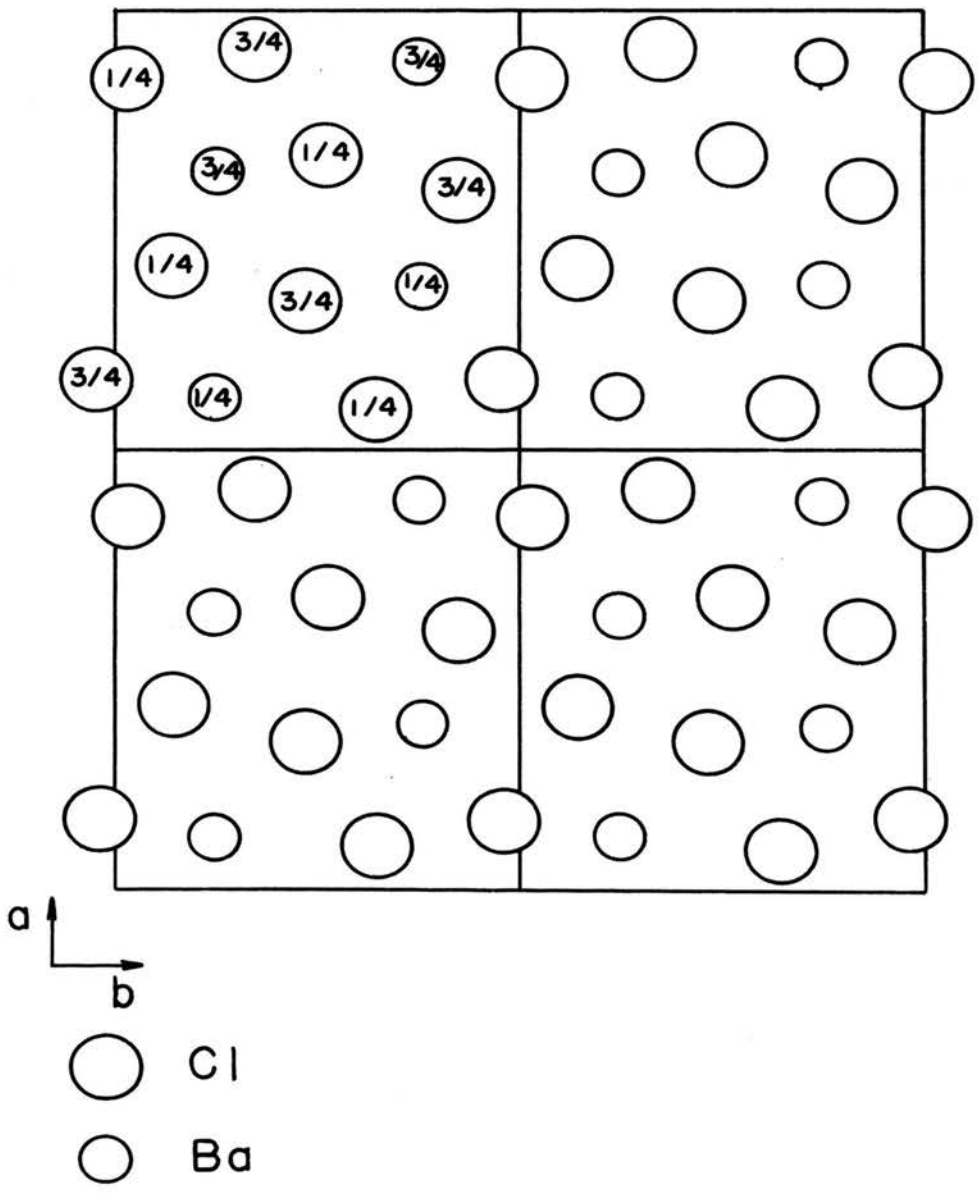

Figure 3a. Projection of Orthorhombic $BaCl_2$ on (001)

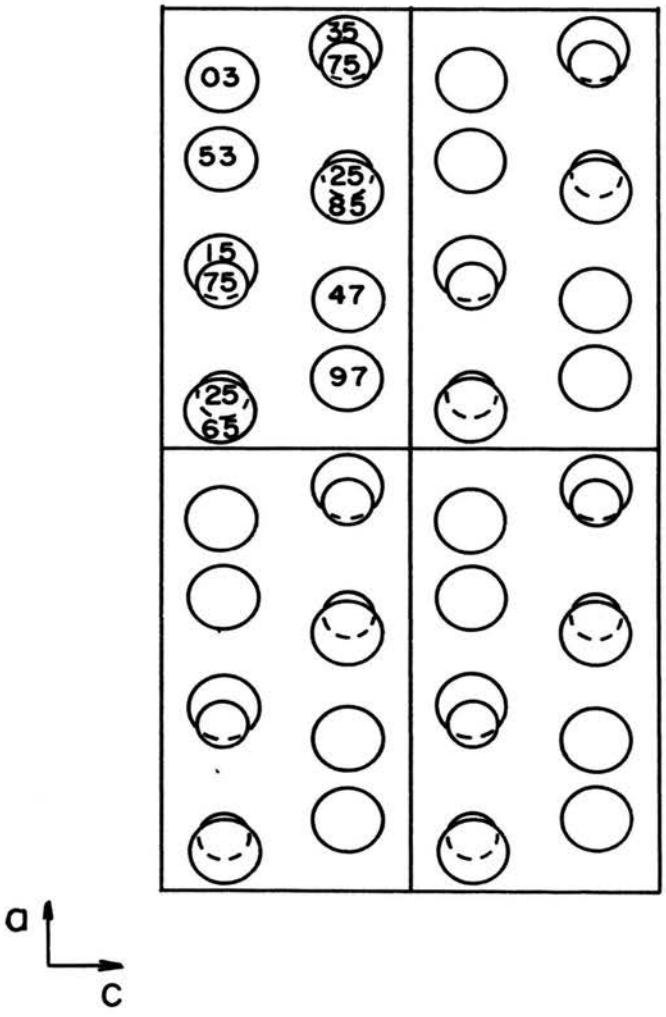

Figure 3b. Projection of Orthorhombic $BaCl_2$ on (010)

producing a cubic form with a=7.324 Å. They reported that the cubic form did not convert appreciably to the orthorhombic form at room temperature, but at 200°C the conversion was complete after two days. In 1971 Swanson et al.[17] reported the lattice parameter of cubic $BaCl_2$, prepared by the same method as described by Brackett et al., as a=7.311 Å. Cubic $BaCl_2$ is face centered cubic with the fluorite structure (Fm3m). The cubic form was interpreted as the stable modification of $BaCl_2$ in the temperature range 925-960°C, with reference to Gemsky's work.[32]

The high-temperature calorimetric heat-content measurements on $BaCl_2$ indicate a first order transition below the melting point,[6,12] with the orthorhombic-cubic transformation presumed to be the cause, though the mechanism of the transformation has not been elucidated.

Derrington and O'Keeffe[38] reported that the ionic conductivity of the high temperature phase of $BaCl_2$ is higher than that of the low temperature phase (orthorhombic) by several orders of magnitude, and changes only slightly on melting. The high temperature phase has been referred to as a cubic fluorite phase with disordered anions.

D. The System $SrCl_2$-$BaCl_2$

The first investigation of the system $SrCl_2$-$BaCl_2$ was by Vortisch[39] in 1914, using cooling curve method and microscopic observation. He reported complete miscibility in both liquid and solid phases, with a freezing point minimum at 847°C at 30 mole percent $BaCl_2$. He also reported that, on cooling, solid solutions of the high form (β) are transformed to solid solutions of the low form (α) as in pure $BaCl_2$. The phase diagram of $SrCl_2$-$BaCl_2$ of Vortisch[39] is shown in Figure 4. Levin et al.[40] pointed out that the phase diagram as shown in Figure 4 does not obey the phase rule. In 1949 Bergman and Bukhalova[41] studied the diagram by means of thermal visual methods and reported the same results as Vortisch. Schei and Flood[42] redetermined the liquidus curve of the system $SrCl_2$-$BaCl_2$ by thermal analysis and by high-temperature filtration, and the solidus curve by a tracer technique. They reported that the system shows complete miscibility in both liquid and solid phases, with a freezing point minimum of 852°C at about 68 mole percent $SrCl_2$.

The first x-ray analyses of phases in the system were done by Brauer and Müller[43] in 1958. They reported that at 500°C, $SrCl_2$ forms cubic solid solutions with up to 23.5 mole percent $BaCl_2$. Beyond 30 mole percent $BaCl_2$, solid solutions have the $BaCl_2$ (α) structure. However complete phase equilibria of the system $SrCl_2$-$BaCl_2$ have not been reported in the literature.

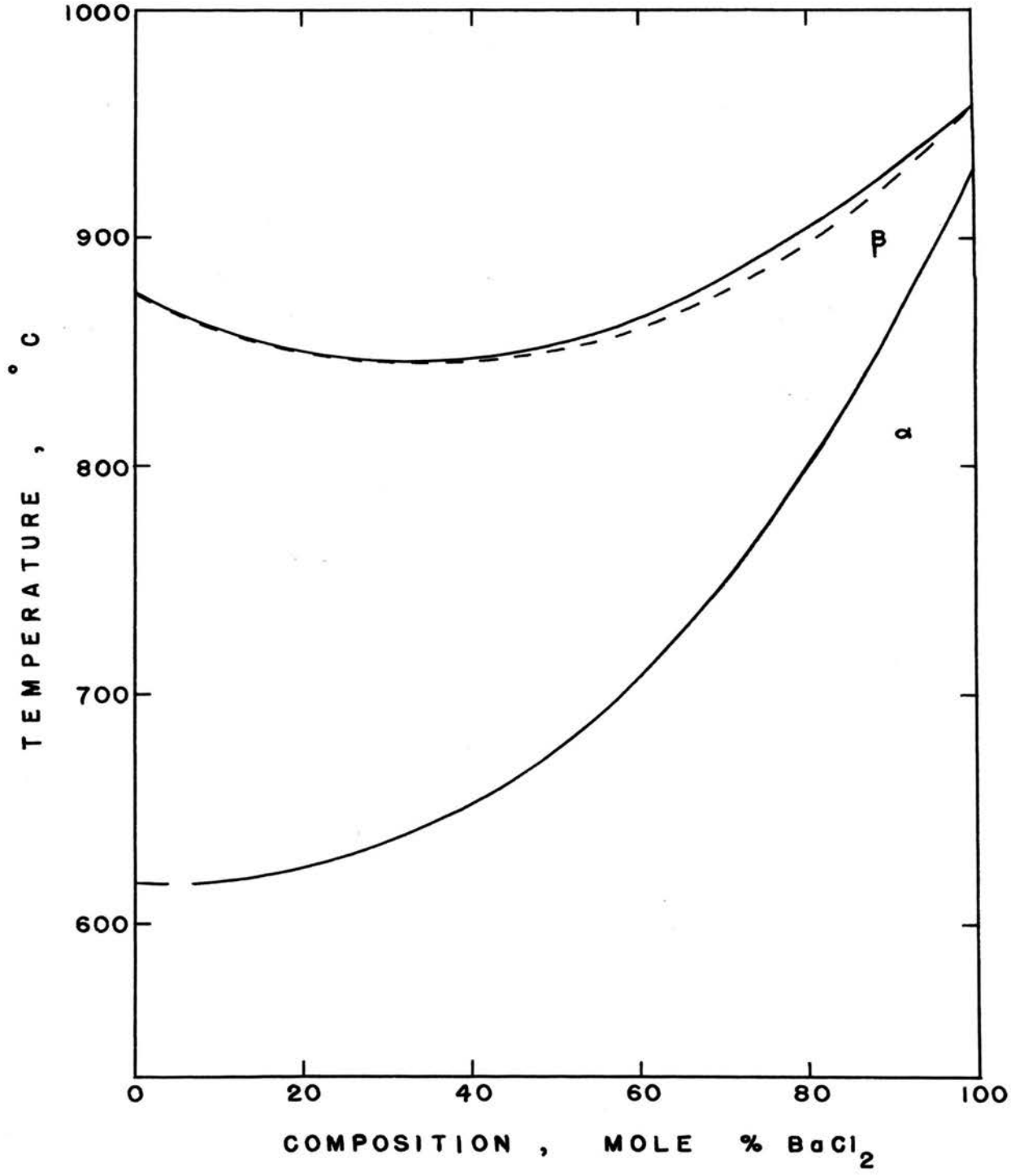

Figure 4. Phase Diagram $SrCl_2$-$BaCl_2$: From Vortisch[39] (1914)

III. EXPERIMENTAL PROCEDURE

A. Specimen Preparation

CaF_2 for this investigation was obtained from Fisher Scientific Company. Pure grade SrF_2 was obtained from Matheson Coleman & Bell Company. $SrCO_3$ and $BaCO_3$ were reacted with HCl to form $SrCl_2$ and $BaCl_2$ for this investigation. $BaCO_3$ and HCl (Technical 22° Baume') were obtained from Fisher Scientific Company. $SrCO_3$ was obtained from Baker & Adamson Products, Allied Chemical Corporation. Table II, III, and IV show the Suppliers' analyses of CaF_2, $SrCO_3$, and $BaCO_3$ respectively.

Ten gram samples were prepared for $SrCl_2$-$BaCl_2$ phase equilibria study by weighing the dry carbonates in proper proportions to the nearest milligram. The samples were mixed and reacted with excess HCl, forming chlorides. Excess HCl was evaporated; the chloride samples were dried in air at 110°C and mixed in a laboratory ball mill for 25 minutes. The compositions of the samples are shown in Table V.

Approximately 1 gram of each sample was placed into a platinum crucible and heated in a resistance muffle furnace controlled at fixed temperatures with a set point controller, equipped with an on-off relay. Maximum variation from the mean temperature was $\pm$ 5°C. Temperatures were measured with a Pt-Pt 13% Rh thermocouple. Heating-Quenching techniques were used to determine phase relationships. The samples were heated until the x-ray patterns of samples

TABLE II

Chemical Analysis of CaF_2 (Fisher Certified A.C.S.)

	Percent
Chloride (Cl)	0.01
Ammonia (as NH_3)	0.01
Sulfate (SO_4)	0.05
Barium (Ba)	0.01
Heavy Metals (as Pb)	0.005
Iron (Fe)	0.005

TABLE III

Chemical Analysis of $SrCO_3$ (Allied Chemical)

		Percent
Assay ($SrCO_3$)	min.	99.0
Insoluble in HCl		0.010
Chloride (Cl)		0.005
Sulfate (SO_4)		0.005
Heavy Metals (as Pb)		0.002
Iron (Fe)		0.002
Substances not precipitated by $(NH_4)_2CO_3$ (as Sulfates)		0.20

TABLE IV

Chemical Analysis of $BaCO_3$ (Fisher Certified A.C.S.)

	Percent
Oxidizing substances (as NO_3)	0.003
Chloride (Cl)	0.0005
Iron (Fe)	0.002
Insoluble in dilute HCl	0.010
Substances not ppt'd. by H_2SO_4	0.02
Calcium (Ca)	0.02
Heavy metals (as Pb)	0.0005
Strontium (Sr)	0.15

TABLE V

$SrCl_2$-$BaCl_2$ Compositions

Sample No.	Composition (mole % $BaCl_2$)
000	0.0
100	10.0
200	20.0
250	25.0
260	26.0
280	28.0
300	30.0
320	32.0
350	35.0
400	40.0
500	50.0
600	60.0
700	70.0
750	75.0
800	80.0
900	90.0
1000	100.0

exhibited no further change, after which intensities and lattice parameters of phases were measured. Samples were heated at 650°, 710°, 800° and 850°C for 125, 72, 24, and 12 hours. These samples were also used for high temperature x-ray, dilatometry, and DTA studies.

High temperature x-ray techniques were used to determine thermal expansion and phase transformation mechanisms of the fluorite type materials and the high temperature phases of $SrCl_2$-$BaCl_2$ system.

B. X-ray Diffraction

A G. E. XRD-5 recording diffractometer, using CuKα radiation at 50 KV. and 15 ma., was utilized to study phase relationships. During heating and quenching cycles, samples were scanned at the rate of 2° 2θ per minute with a recording chart speed of 24 in. per hour. A scanning rate of 0.2° 2θ per minute was used to determine the lattice parameters of the phases. The 2θ scans were from 20° to 60° 2θ. Corundum (α-Al_2O_3) was used as an internal standard. Before scanning, the sample was covered with transparent tape to prevent rehydration of sample. The 2θ values of the (012), (104), (110), and (113) lines of Al_2O_3, the (111), (220), and (311) lines of the cubic solid solutions, and the (200), (002) and (040) lines of the orthorhombic solid solutions were measured and corrected. The lattice parameters of cubic solid solutions and orthorhombic solid solutions were determined from the corrected 2θ values.

A high temperature, controlled atmosphere, x-ray diffractometer attachment, mounted on a Norelco Wide-Range Diffractometer, was used to measure thermal expansion of CaF_2, BaF_2, $SrCl_2$ and $BaCl_2$, and to study phase equilibria at high temperature in the $SrCl_2$-$BaCl_2$ system. The detailed description and operation of the high-temperature x-ray diffractometer attachment have been described in detail by Maurer and Ackermann.[44]

A thin powder specimen was deposited on a platinum resistance strip-heater by applying a CCl_4 suspension of

the specimen on the heater and then evaporating the CCl_4, providing a specimen less than 0.001 in. thick. Alignment of the specimen on the goniometer axis was achieved by using the (200) reflection of the platinum strip-heater as the internal standard. Using the lattice constant at 25°C for platinum, 3.9231 Å,[45] and the linear coefficient of thermal expansion, 10.2×10^{-6} deg^{-1},[46] the 2θ value for any (hkl) reflection of platinum can be calculated at any desired temperature. Thus expansion, contraction, or tilting of the platinum strip-heater with the specimen can be compensated for by adjusting the alignment mechanisms.

Two thermocouples of 0.002 in. diam. Pt and Pt-10% Rh wire were welded to the heater surface. One was used to measure sample temperature via a millivolt potentiometer. The other thermocouple was used to furnish the input emf to the temperature control system. The temperature control accuracy was determined, by measurement of melting points of a number of halides, to be within approximately five degrees of the reported melting temperatures. It was also checked by observing the α-β transformation temperature of quartz to be 573 $\pm$ 1°C,[47] precisely that accepted in the literature.[48] In general, operational temperatures were stabilized within $\pm$ 1°C.

Copper Kα radiation at 40 KV. and 18 ma. was used in the investigation. The 2θ values of the sample were detected by a scintillation counter, amplified, and recorded on a strip chart. To observe the high temperature phases,

the samples were scanned at the rate of 1° 2θ per minute with a recording chart speed of 0.5 inches per minute. To determine the lattice parameters of the phases, samples were scanned at the rate of 1/8° 2θ per minute. For cubic fluorite structures the 2θ values of the (111), (200), (220), and (311) lines were measured and used for calculation of the lattice parameters. The lattice parameters of the orthorhombic $BaCl_2$ structure were calculated from the 2θ values of the (200), (002), and (040) lines.

C. Differential Thermal Analysis (DTA)

All differential thermal analyses were made on a controlled atmosphere DTA apparatus of R. L. Stone Company model KA-H recorder-controller assembly using an F-1D furnace. A heating rate of 10°C per minute with a SH-77BP2-INZ cup sample holder was employed. During the investigation it was noted that the chlorides of Ba and Sr reacted with the stainless steel and nickel cups. The platinum cup was found to be inert to these chlorides and was used for all work. Reagent grade anhydrous Al_2O_3 was used as a standard for all DTA runs. Pt-Pt 13% Rh thermocouples were used to measure and control the temperature of the DTA furnace. The differential temperature was plotted on a strip chart at a ΔT sensitivity of 48 to 96 micro-volts per inch.

Samples were heated at 10°C per minute to above fusion temperatures and then cooled down at the same rate. Transition and solidus temperatures were obtained on heating and liquidus temperatures were obtained on cooling. These event temperatures were determined by noting temperatures at which endothermic or exothermic peaks departed from the base line. The premelting transformations affected the endothermic peaks of fusion so that the solidus temperatures could not be determined accurately (see V. Discussion).

D. Thermodilatometric Analysis (TDA) or Dilatometry

Thermal expansion measurements were made with a recording dilatometer, consisting of a linear variable differential transformer (LVDT) and a Daytronic 300D type 72F transducer-amplifier-indicator unit. The dilatometer details have been given by Sorrell, Anderson, and Ackermann.[49]

A powdered specimen was packed in a sealed-bottom gold tube, 2 mm. inside diameter and 0.002 inches thick, and presintered at 800°C for 4 hours in a resistance muffle furnace. The gold tube with the presintered specimen was then placed into a flat-bottom fused silica tube, 8 mm. inside diameter, which extended vertically into a resistance muffle furnace. The fused silica sample holder and transformer were connected at a common water-cooled base. Changes in length of the specimen were detected via a pushrod by a linear variable differential transformer (LVDT). The pushrod was a fused silica rod, 1.5 mm. in diameter, resting on the specimen. The transformer core was attached directly to the pushrod, with displacement producing an output voltage proportional to the linear displacement. The instrument was designed to measure expansion and contraction continuously over the entire temperature range, and was calibrated so that 1 inch chart displacement corresponded to 0.0001 inch sample displacement. Measured displacements were corrected for expansion of the tube, and of the gold plate, using coefficients of

0.5×10^{-6} deg^{-1} for fused silica and 14.2×10^{-6} deg^{-1} for gold.

A cam controlled saturable core reactor was used in programming heating and cooling of the furnace. A heating and cooling rate of 7.5°C per minute in the temperature range 25-780°C was employed. A Pt-Pt 13% Rh thermocouple with the bead placed near the surface of the specimen was used to measure sample temperature with the aid of a millivolt potentiometer.

IV. RESULTS

A. Thermal Expansion of CaF_2 and BaF_2

Thermal expansions of CaF_2 and BaF_2 were determined from 25°C to 1150°C and from 25°C to 1070°C, respectively. The measurements of the lattice constants of CaF_2 and BaF_2, as a function of temperature, were carried out in a dry N_2 atmosphere with less than 0.1% water vapor. The lattice parameters of the cubic fluorite type structure were determined from the (111), (200), (220), and (311) lines, obtained with CuKα radiation at a scanning rate of 1/8° 2θ per minute. The calculated lattice parameters from these lines were in good agreement within $\pm$ 0.001 Å. The lattice parameters versus temperature of CaF_2 and BaF_2 are shown in Figures 5 and 6. The original data are tabulated in Appendix A. The x-ray patterns of the cubic fluorite phases are shown in Appendix B.

In the low temperature regions, the lattice parameters of CaF_2 and BaF_2 are shown to expand in a normal manner. At higher temperatures, 500°-1150°C for CaF_2 and 300°-1170°C for BaF_2, the lattice parameters are seen to depart substantially from linearity. The interpolation polynomials, determined by least squares, can be expressed by the equations:

$$a\ (CaF_2) = 5.4622 + 0.9366 \times 10^{-4}T + 0.5527 \times 10^{-7}T^2$$

$$a\ (BaF_2) = 6.2018 + 0.8095 \times 10^{-4}T + 0.8360 \times 10^{-7}T^2$$

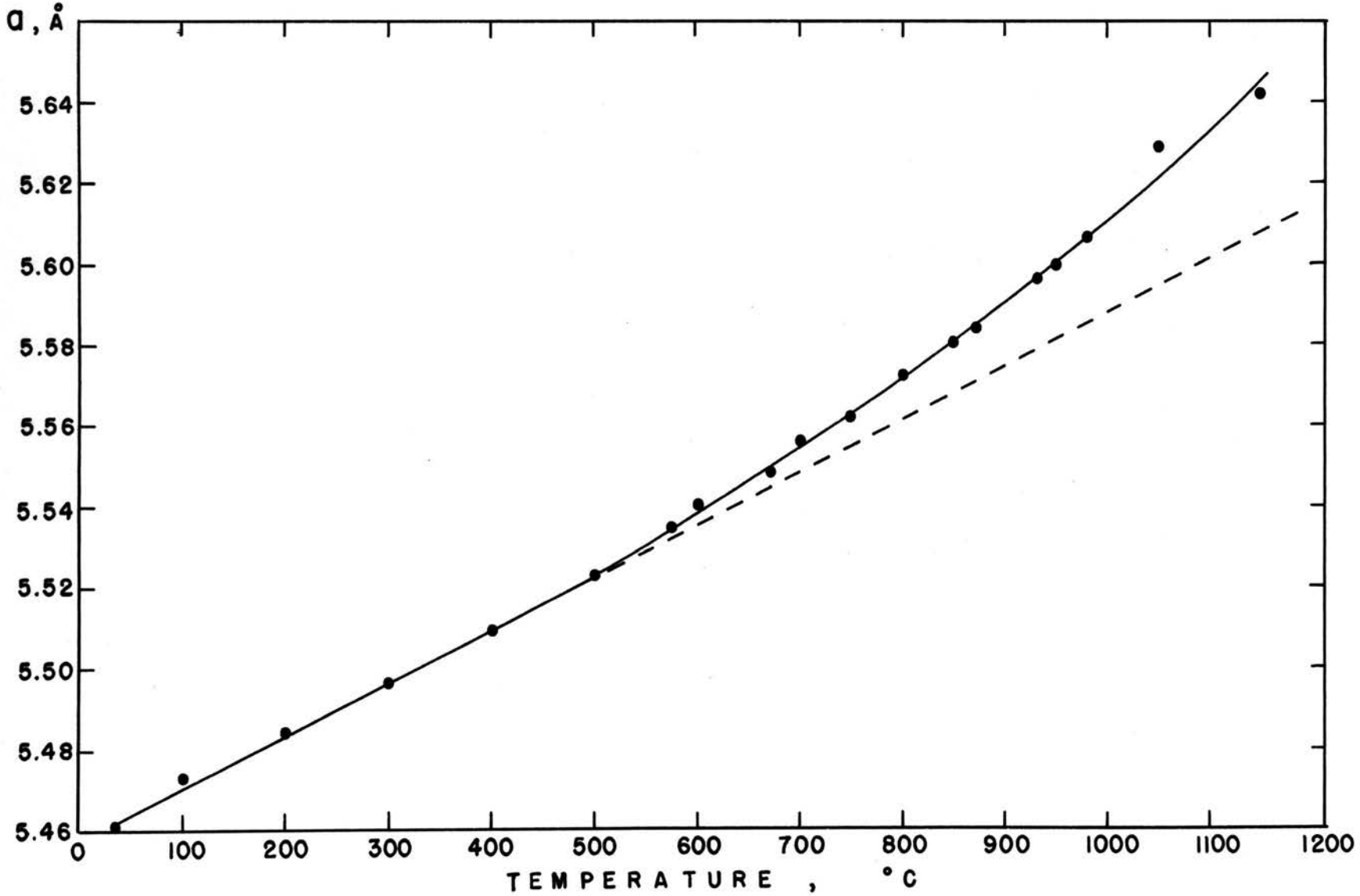

Figure 5. CaF_2 Lattice Parameter as a Function of Temperature

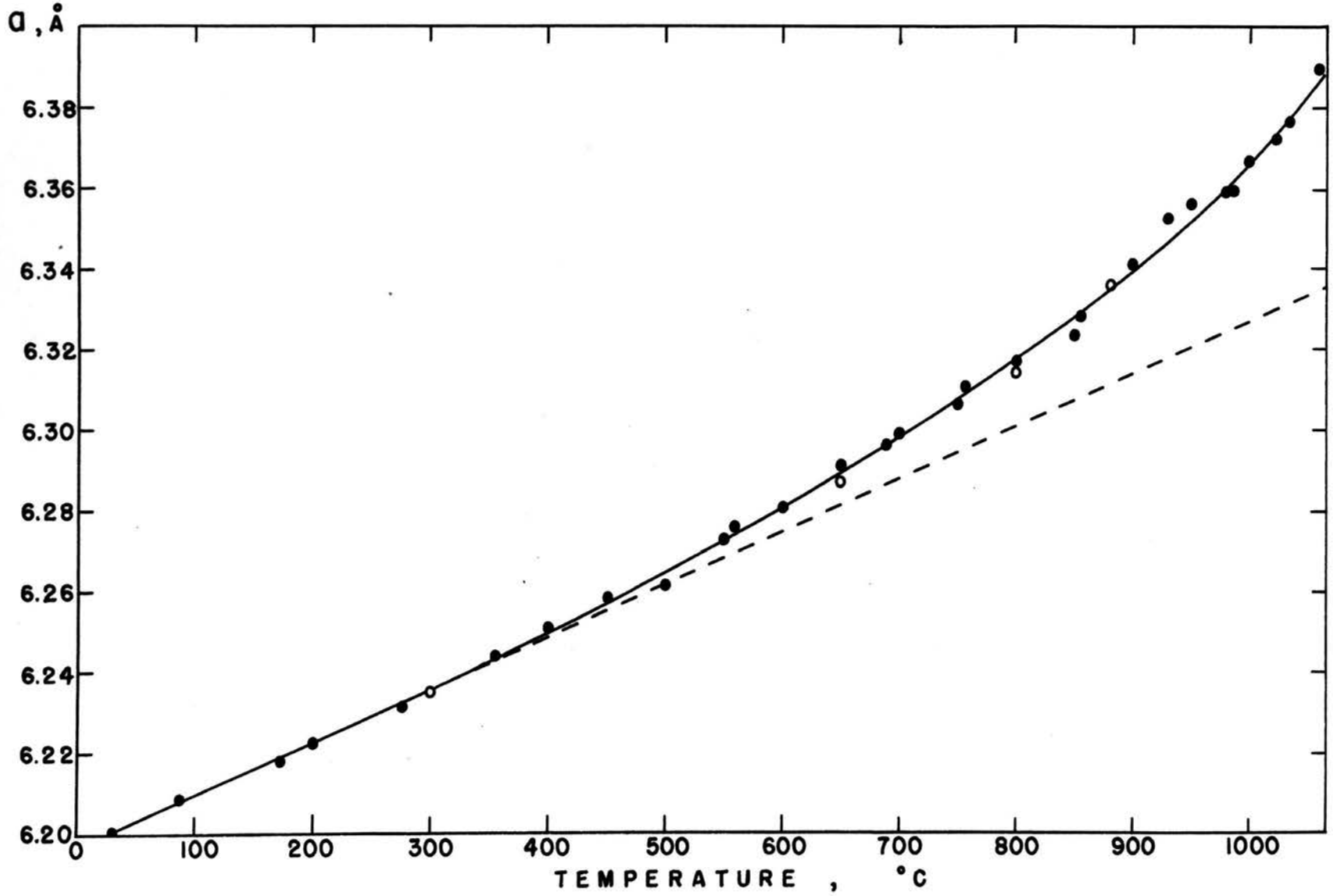

Figure 6. BaF_2 Lattice Parameter as a Function of Temperature

The coefficients of T^2 are significant at the 95% confidence level for all variations analyzed. The correlation coefficients of these equations for CaF_2 and BaF_2 are 0.9991 and 0.9988, respectively.

The linear thermal expansion coefficient, $\alpha(T)$, for both CaF_2 and BaF_2 compounds are calculated from the equation:

$$\alpha(T) = \Delta l/l(T)\ \Delta T$$

Where T is the average temperature, ΔT is the temperature interval, l is the lattice constant measured, and Δl is the change in the lattice constant. The results of this work for CaF_2 are in good agreement with those of Whittemore and Ault,[50] who determined the thermal expansion of presintered CaF_2 by using a telescope method in the temperature range from room temperature to 1000°C. The values of the linear thermal expansion coefficient, $\alpha(T)$, for CaF_2 as reported by Whittemore and Ault, and for CaF_2 and BaF_2 from this study are given in Table VI.

At high temperature, CaF_2 and BaF_2 reacted with water vapor, forming CaO and BaO, respectively, and emitting HF. Thermodynamically, the reactions of these fluorides with water vapor are favored even at low humidities. In this investigation, CaO was observed at 930°C, when CaF_2 was heated in dry N_2 with less than 0.1% water content. Lower reaction temperatures and faster rates of reaction were seen when the CaF_2 sample was heated in air.

TABLE VI

Linear Thermal-Expansion Coefficients of CaF_2 and BaF_2

Sample	Temp. Range (°C)	$\alpha(T) \times 10^6$ deg^{-1}
CaF_2 as reported by Whittemore and Ault	25- 300	22.3
	25- 600	24.8
	25- 900	26.1
CaF_2 this work	25- 500	23.0
	500- 950	30.2
	950-1150	37.8
BaF_2	25- 300	20.4
	300- 850	25.7
	850-1070	47.8

X-ray diffraction lines of BaF_2 at high temperature, over 800°C, became diffuse and lost intensity. In the transition temperature ranges, reported by Efremova and Matizen[20] as 967° and 1207°C, all of the x-ray diffraction lines of cubic fluorite structures were observed to lose intensities. Fast scan, 2° 2θ per minute, of BaF_2 in dry N_2 at 1150°C from 22° to 55° 2θ showed development of new x-ray diffraction lines at 25.3, 28.3, 38.4, 40.6, 51.9, and 53.6 2θ. The new lines, which can be indexed on a simple cubic unit cell, persisted at room temperature after quenching. A sample of BaF_2, heated to 1050°C for 20 minutes and then quenched to room temperature, exhibited powder patterns of BaF_2, with a small amount of BaO. So that all of new x-ray diffraction lines observed over the high temperature range are possibly those of an oxyfluoride phase. No attempt was made to determine the significance of the new x-ray lines of the BaF_2 sample.

B. Thermal Expansion and Transformations of $SrCl_2$ and $BaCl_2$

1. Thermal Expansion and Transformation of $SrCl_2$

Measurements of the lattice constants of $SrCl_2$ were carried out over a temperature range of 25°C to 860°C in dry N_2 atmosphere. The (111), (220), and (311) reflections were used to evaluate the lattice parameter of the cubic fluorite phase. In some instances, the (400) reflection was also used. These reflections were obtained with CuKα radiation at a scanning rate of 1/8° 2θ per minute, using a platinum resistance strip-heater. The lattice parameter of the cubic fluorite phase versus temperature, in the temperature range 25°C to 735°C, is shown in Figure 7. The original data from which this figure was drawn are also contained in Appendix A. Appendix B shows the x-ray diffraction pattern of the cubic phase of $SrCl_2$.

The lattice of cubic $SrCl_2$ expands normally at low temperatures, from 25°C up to approximately 225°C. At high temperature, between 225° and 735°C, the lattice parameter of $SrCl_2$ is seen to act the same way as those of CaF_2 and BaF_2, departing substantially from linearity. A quadratic function was fitted to the thermal expansion data, using the standard method of least squares, with temperature as the independent variable and the lattice parameter as the dependent variable. This function can be expressed by the equation:

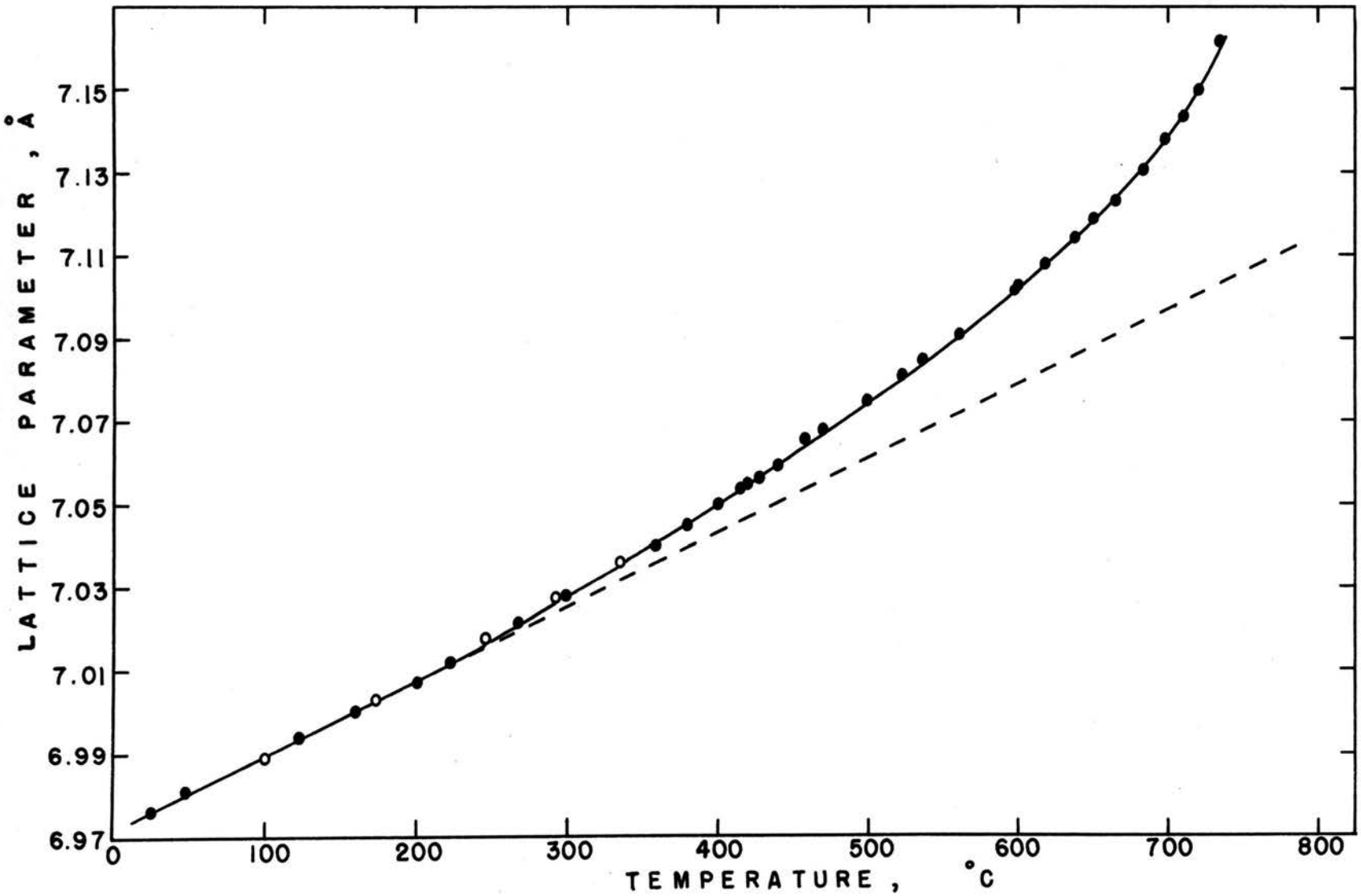

Figure 7. Cubic $SrCl_2$ Lattice Parameter as a Function of Temperature

$$a(\text{Cubic } SrCl_2) = 6.9762 + 1.1727 \times 10^{-4} T + 1.6428 \times 10^{-7} T^2$$

The coefficient of T^2 is significant at the 95% confidence level with a 0.9984 correlation coefficient.

The x-ray diffraction pattern of $SrCl_2$, starting at about 480°C, shows a few very faint lines in addition to those for cubic fluorite structure. These indicate a lattice disorder of the cubic fluorite structure as suggested by Croatto and Bruno.[19] At about 650°C, the x-ray diffraction lines of the cubic phase of $SrCl_2$ are seen to decrease in intensity with an increase in the intensities of some new lines. The intensities of the new diffraction lines increase with increasing temperature and also increase with increasing time. This phenomenon is seen to occur in the temperature range from 650° to 730°C. In fact, it is precisely this region in which the specific heat and the heat content[6,7,12,20] show a peak and an anomalous phenomenon, respectively. This phenomenon also occurred during heating samples of cubic $SrCl_2$ on a gold resistance strip-heater and on an Al_2O_3-based platinum strip-heater. The new x-ray diffraction lines are not those of SrO. In a thermodynamic sense, the reaction of $SrCl_2$ with water vapor is not favored, especially in dry N_2 atmosphere. The new lines can be indexed on a hexagonal unit cell. Prolonged heating of cubic $SrCl_2$ at 716°C resulted in complete conversion to the hexagonal form. Observed 2θ values, obtained by scanning the sample at 716°C from 15° to 85° 2θ, $\sin^2\theta$ values, and calculated $\sin^2\theta$ values, indexed (hk·l), and

$\sin^2\theta$ differences are presented in Table VII. The hexagonal phase persisted on cooling on either a platinum strip-heater or a gold strip-heater. The quenched sample with the hexagonal phase was scraped from the strip-heater, ground, and remounted; the x-ray diffraction pattern showed only cubic fluorite lines.

The sample of cubic $SrCl_2$ was pressed as pellets of different thicknesses, heated at 750°C for 2 to 3 hours in a resistance muffle furnace, and rapidly quenched to room temperature. Without grinding, the specimens were scanned on a G.E. XRD-7 recording diffractometer at the rate of 2° 2θ per minute, using CuKα radiation. X-ray diffraction lines of the thick pellet showed the cubic fluorite phase, and those of the thin showed the hexagonal phase. The pellet with the hexagonal phase was then ground and rerun, for which only cubic fluorite lines were observed.

The observed 2θ and (hk·l) data for the metastable hexagonal form at room temperature over the range from 10° to 90° 2θ were used to determine a space group. The general and special reflections, used to determine the lattice type and the microsymmetry, are tabulated in Table VIII. The table indicated that the hexagonal phase has a primitive (P) lattice type with a 6_3 screw axis and a c glide plane in $(1\bar{1}.0)$. The space group can be, therefore, either $P6_3/mmc$ (D^4_{6h}) or $P6_3mc$ (C^4_{6v}). The x-ray pattern of the hexagonal phase is shown in Figure 8.

TABLE VII

Observed 2θ, Indexed (hk·l), Observed $\sin^2\theta$, Calculated $\sin^2\theta$, and $\sin^2\theta$ Differences

2θ	(hk·l)	observed $\sin^2\theta$	calc. $\sin^2\theta$	difference
16.05	10.1	0.01946	0.01962	-0.00017
21.31	20.0	0.03413	0.03432	-0.00019
24.24	00.2	0.04401	0.04417	-0.00016
24.56	20.1	0.04516	0.04536	-0.00020
30.91	21.1	0.07089	0.07111	-0.00021
32.52	20.2	0.07827	0.07849	-0.00022
34.56	30.1	0.08809	0.08827	-0.00018
37.46	22.0	0.10294	0.10297	-0.00003
37.68	21.2	0.10411	0.10423	-0.00012
38.38	10.3	0.10786	0.10796	-0.00010
42.92	20.3	0.13362	0.13370	-0.00008
45.14	22.2	0.14706	0.14713	-0.00007
45.30	40.1	0.14805	0.14833	-0.00028
46.63	31.2	0.15639	0.15572	0.00068
47.10	21.3	0.15932	0.15944	-0.00012
49.36	32.1	0.17402	0.17407	-0.00006
49.74	30.3	0.17660	0.17660	0.00000
50.48	40.2	0.18149	0.18146	0.00003
51.92	41.1	0.19128	0.19123	0.00005
54.20	32.2	0.20717	0.20720	-0.00003
54.75	20.4	0.21107	0.21099	0.00008

TABLE VII (Cont.)

2θ	(hk·l)	observed $\sin^2\theta$	calc. $\sin^2\theta$	difference
56.75	50.1	0.22549	0.22556	-0.00007
57.62	33.0	0.23187	0.23168	0.00019
58.29	21.4	0.23682	0.23673	0.00009
61.68	32.3	0.26234	0.26241	-0.00007
64.55	10.5	0.28467	0.28463	0.00004
67.76	20.5	0.31027	0.31037	-0.00010
68.90	60.1	0.31951	0.31994	-0.00043
71.38	32.4	0.33978	0.33970	0.00008
72.12	52.1	0.34591	0.34569	0.00022
82.51	52.3	0.43422	0.43402	0.00020

TABLE VIII

General and Special Reflections of Hexagonal $SrCl_2$

hk•l	h0•0	00•1	hk•0	h0•1	hh•1	hh•0
21•1	10•0	00•2	21•0	10•1	11•2	22•0
21•2	20•0	00•4	31•0	20•1	22•2	33•0
31•1	30•0		32•0	20•2	22•4	44•0
31•2	40•0		42•0	30•1	44•2	
21•3	50•0		53•0	10•3		
32•1	70•0			30•2		
41•1				20•3		
32•2				40•1		
41•2				30•3		
21•4				20•4		
32•3				50•1		
51•1				40•3		
42•2				50•2		
43•1				10•5		
42•3				20•5		
32•4				60•1		
52•1				70•1		
43•2				20•6		
51•3				70•2		
31•5						
43•3						
42•4						

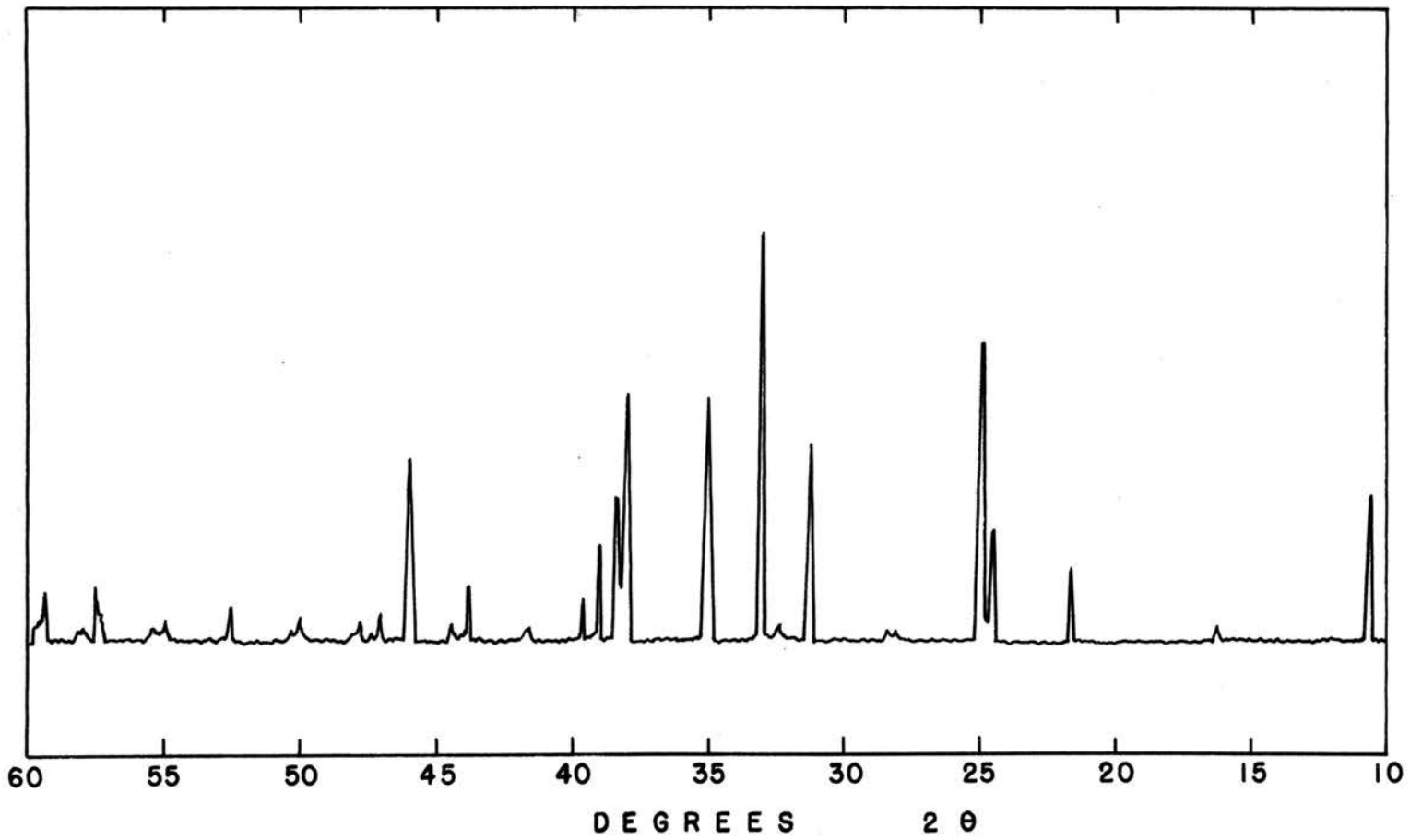

Figure 8. X-Ray Pattern of Hexagonal $SrCl_2$ as a Metastable Form at Room Temperature; CuKα Radiation

Because of the persistence of the hexagonal form on cooling, the lattice parameters at different temperatures were measured over a temperature range from 860°C to 25°C. On cooling, the (20.1) and (30.1) lines of the hexagonal phase were observed to split into two peaks. The reason for this is unknown. Values of the lattice parameters were evaluated primarily from the (20.0), and (00.2) reflections, obtained from CuKα radiation scanned at a rate of 1/8° 2θ per minute, using the platinum resistance strip-heater. The a and c parameters of the hexagonal phase versus temperatures are shown in Figures 9 and 10, respectively. Raw 2θ angles, d-spacings, and calculated lattice parameters at different temperatures for the hexagonal $SrCl_2$ are contained in Appendix C.

The lattice of hexagonal $SrCl_2$ contracted linearly in both the a and c directions down to room temperature. At high temperatures, near the melting point of $SrCl_2$, the c parameter exhibits a rather sharp increase in expansion, where as the a parameter expansion continues linearly. Thermal expansion of the hexagonal phase, based on heating and cooling data, can be expressed by the linear equations:

$$a \text{ (hex. } SrCl_2) = 9.4694 + 2.25 \times 10^{-4} T$$

$$c \text{ (hex. } SrCl_2) = 7.2063 + 1.9 \times 10^{-4} T$$

Density measurements of metastable hexagonal form of $SrCl_2$ by the pycnometer method gave a value of 2.91 gm/cm^3. The number of molecules per unit cell is calculated from

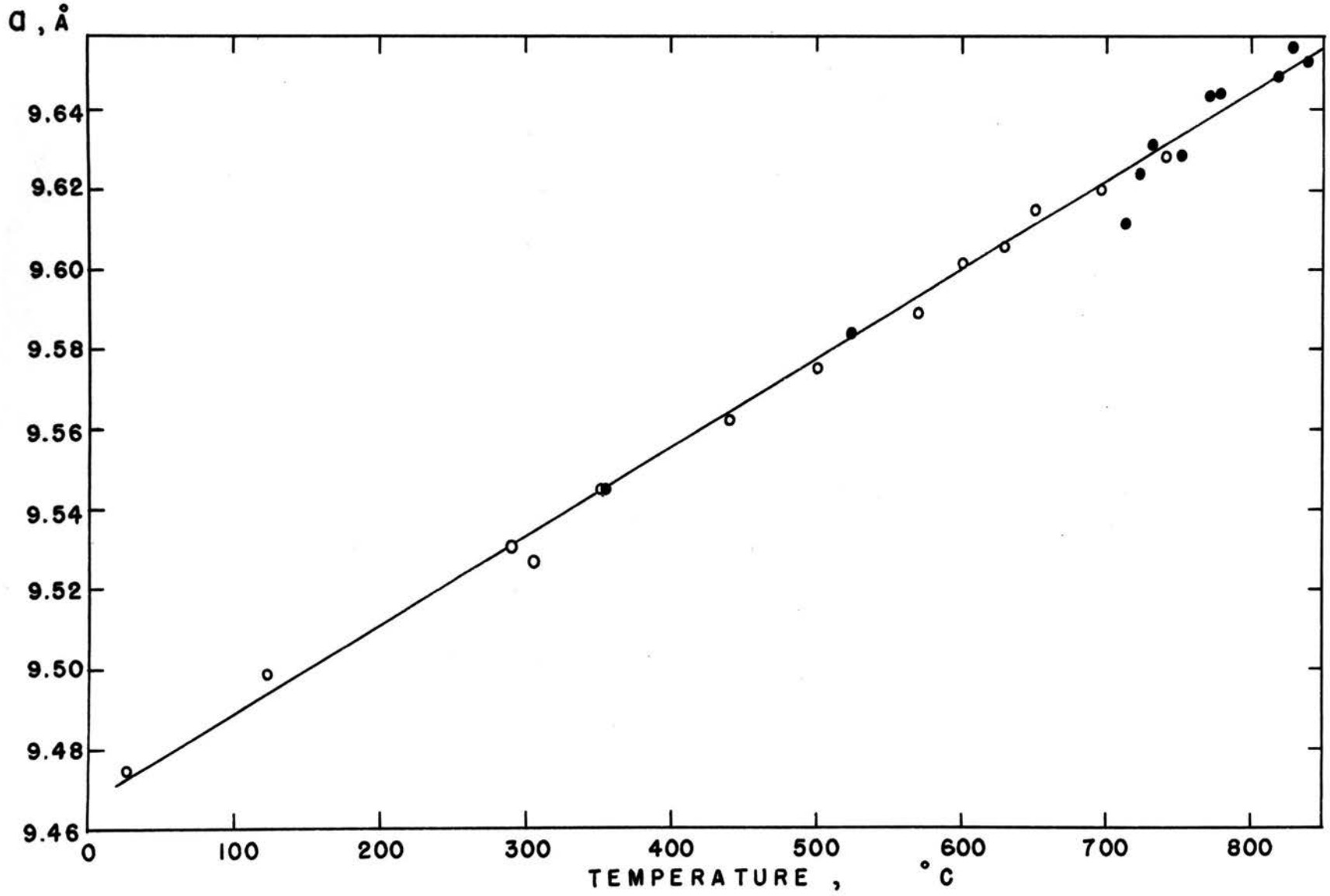

Figure 9. The a Parameter of Hexagonal $SrCl_2$ as a Function of Temperature

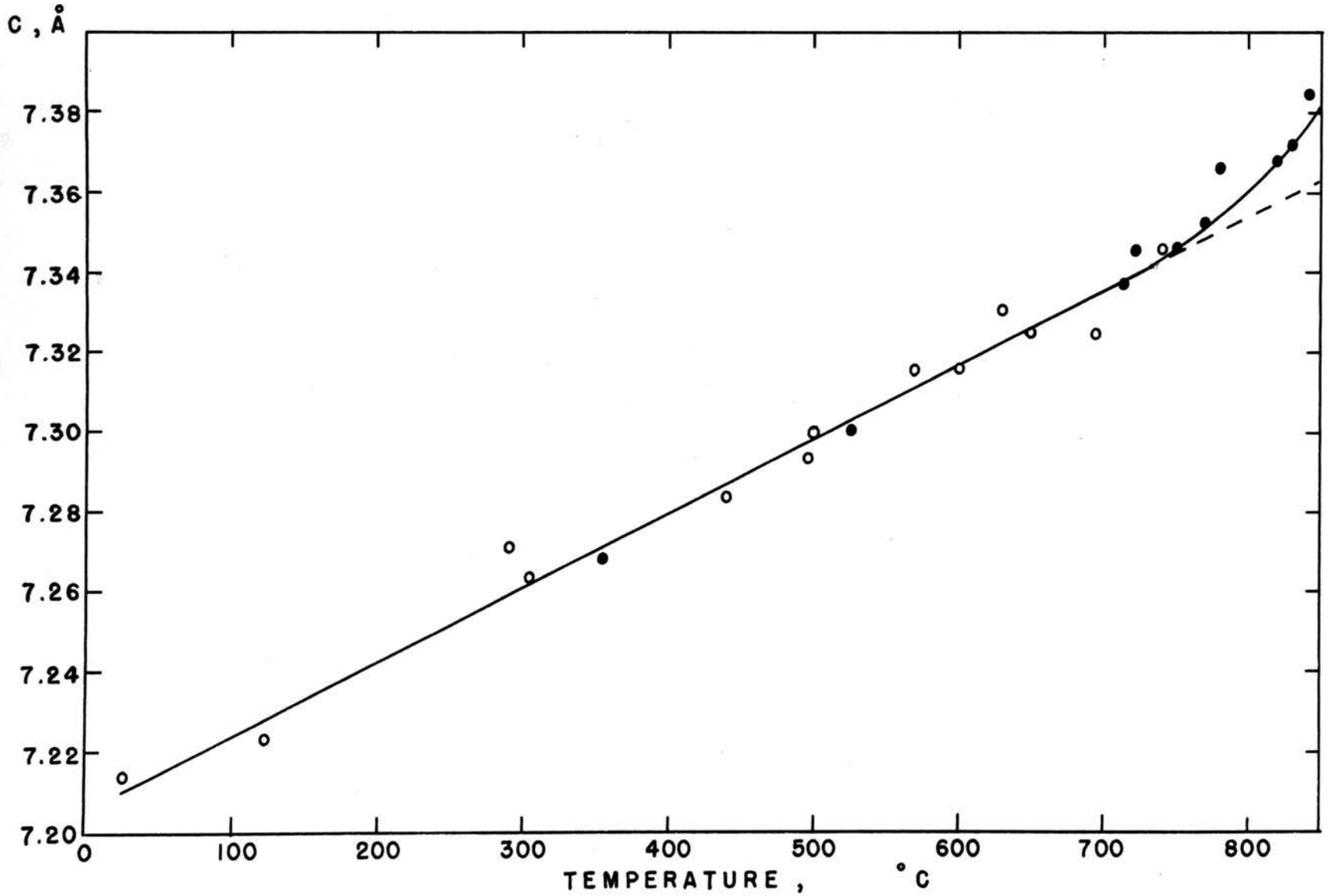

Figure 10. The c Parameter of Hexagonal $SrCl_2$ as a Function of Temperature

the equation:

$$\rho = \frac{n \times M.W.}{N \times V}$$

Where:

ρ = Density

n = the number of $SrCl_2$ units per unit cell

M.W. = Molecular Weight (158.52 for $SrCl_2$)

N = Avogadro's number (6.023×10^{23} $mole^{-1}$)

V = Volume of unit cell

For the hexagonal structure V is equal to $0.866 \times a^2 \times c$. The calculated number of molecules per unit cell is equal to 6.2; so it is reasonable to assume that there are 6 molecules per unit cell of hexagonal lattice. The calculated density of the hexagonal form, from extrapolated a and c parameters, at the melting point is equal to 2.66 gm./cm.^{3}, less than that of liquid $SrCl_2$, 2.717 gm./cm.^{3} [51]

Calculation of the molar volumes of the cubic and hexagonal polymorphs from their lattice parameters shows that the molar volume of hexagonal phase is larger than that of cubic. The molar volumes of both polymorphs versus temperature are shown in Figure 11. The original data are tabulated in Appendix D. The molar volumes versus temperature for both phases are seen to be parallel in the low temperature range. In the region 625°-735°C, the molar

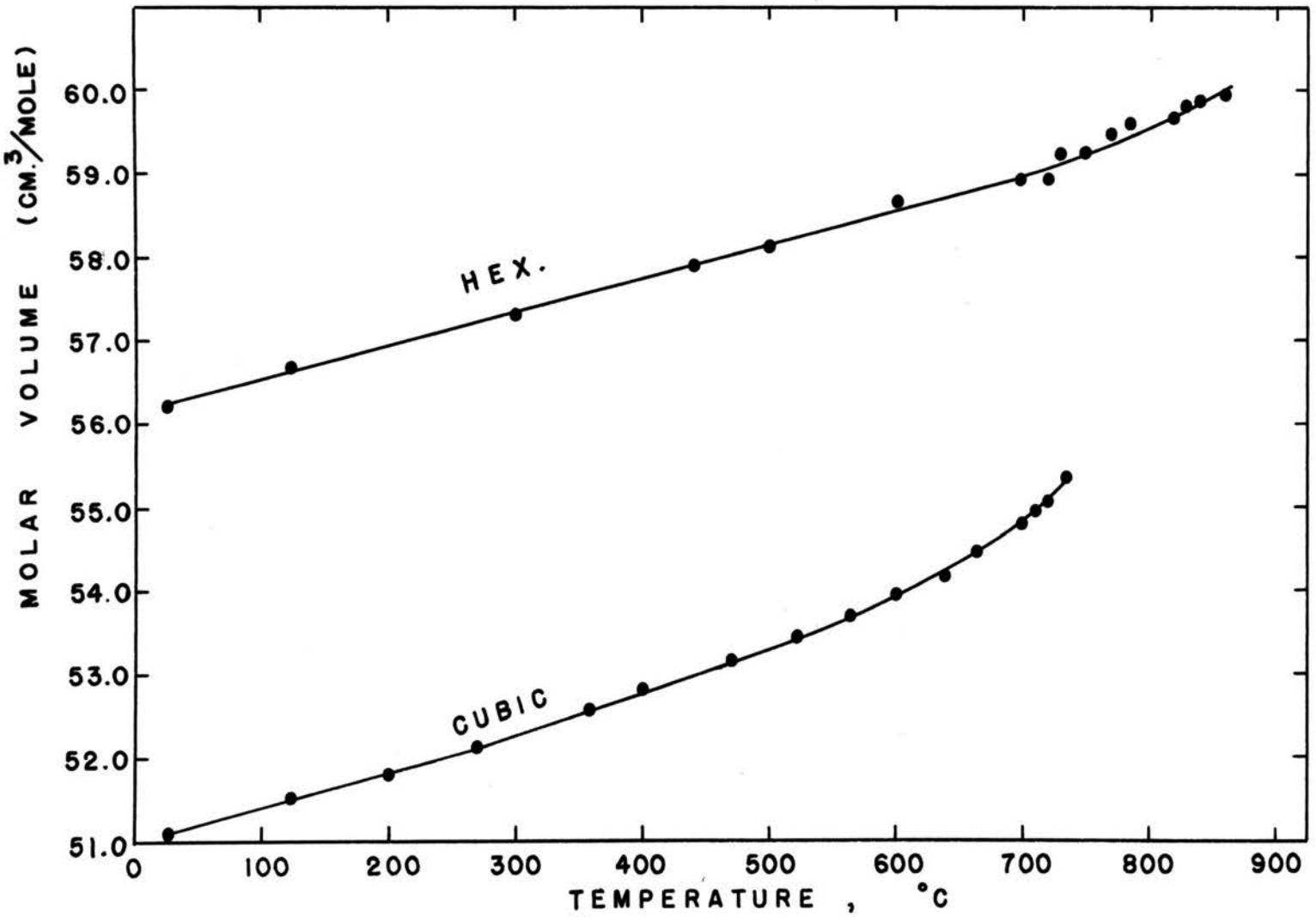

Figure 11. Molar Volumes of Cubic and Hexagonal $SrCl_2$ as a Function of Temperature

volume of the cubic phase shows a rather sharp increase toward the molar volume of the hexagonal phase. The molar volumes of the hexagonal phase at 25°, 650°, and 735°C are 10.1, 8.15, and 7.18% larger than those of cubic phase, respectively.

The thermal expansion of $SrCl_2$ was also determined by means of thermodilatometric analysis (TDA), or dilatometry, in air, in the temperature range from 25° to 750°C. The results are shown in Figure 12 as $L_T/L_{25°}$ versus temperature. Original data from which the figure was drawn are contained in Appendix E. The sample expands normally to approximately 625°C. At higher temperatures, a sintering effect plays a major role so that the size of the sample is decreased with increasing temperature. The sample is seen to reexpand in the temperature range 685° to 735°C, the transformation range. The measurement of the second run gives the result shown in Figure 13. Original data are included in Appendix E. It is seen that after running the sample through the first heating and cooling cycle, it does not expand discontinuously in the transformation range. This indicates that the hexagonal form persists at low temperature as a metastable form.

The linear thermal expansion coefficients of the cubic form and hexagonal forms of $SrCl_2$, calculated from measurements of lattice parameters with the high-temperature x-ray method and by thermodilatometric analysis, are shown in Table IX. It is seen that the results from the

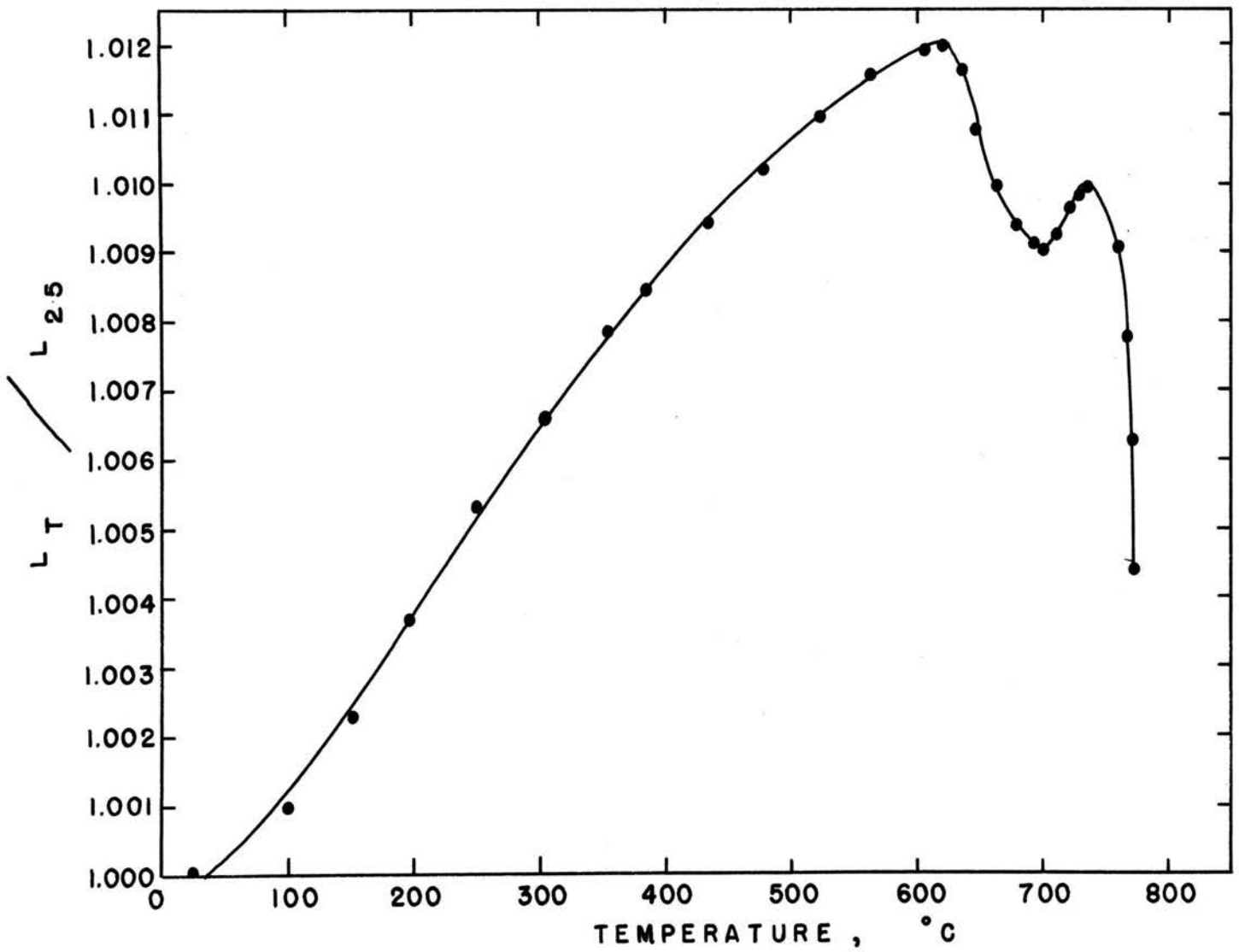

Figure 12. Thermal Expansion of Pure $SrCl_2$ on the First Run Measured by TDA

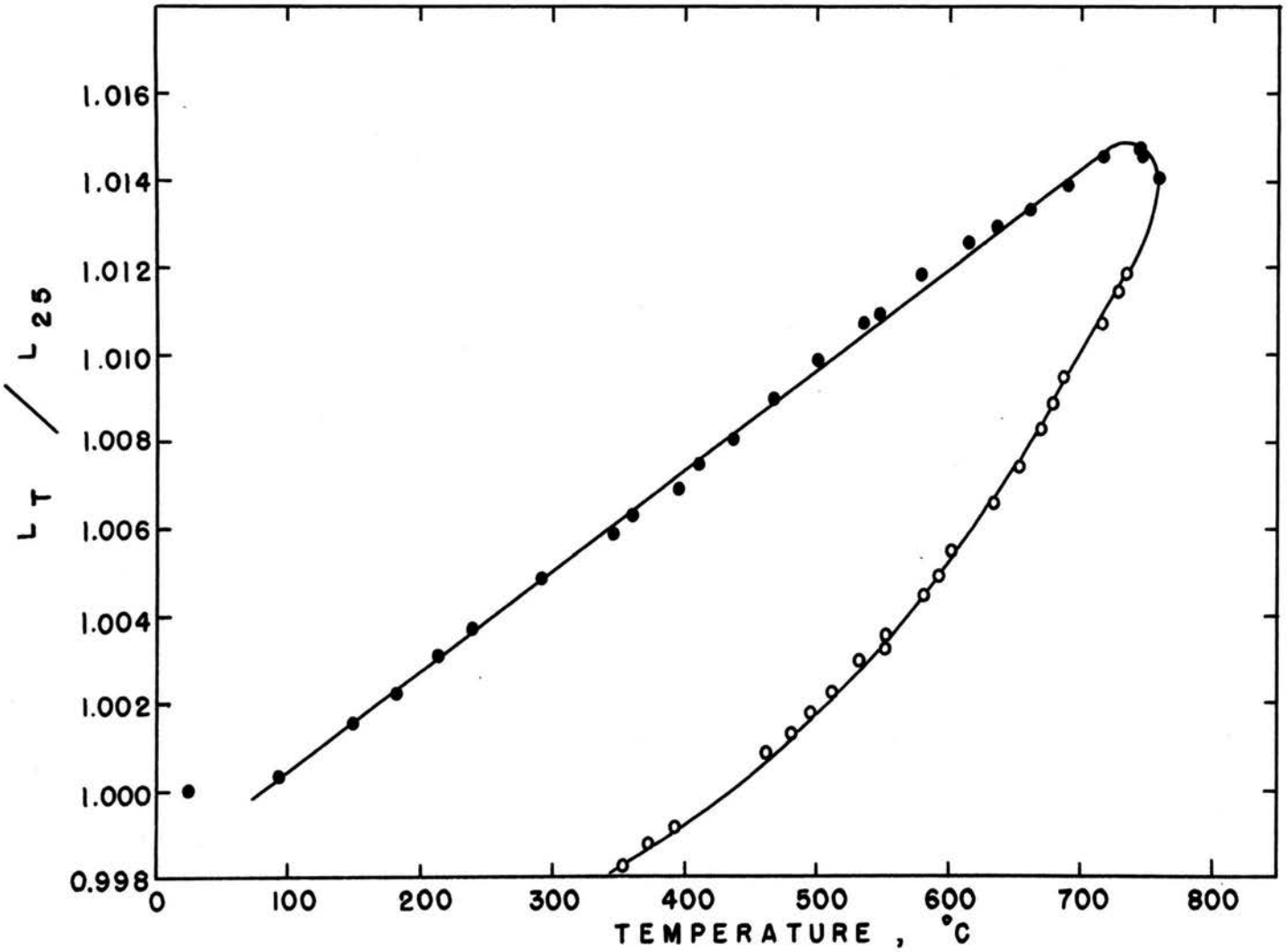

Figure 13. Thermal Expansion of Pure $SrCl_2$ on the Second Run Measured by TDA

TABLE IX

Linear Thermal-Expansion Coefficients of $SrCl_2$

Sample and Method of Detn.	Temp. Range (°C)	$\alpha(T) \times 10^6$ deg^{-1}
Cubic $SrCl_2$ by x-ray	25-225	26.0
	225-525	32.9
	680-735	73.5
Hex. $SrCl_2$ by x-ray	25-825	23.6 (a)
	25-750	25.2 (c)
$SrCl_2$ by dila. 1st run	100-350	27.3
	200-450	24.0
$SrCl_2$ by dila. 2nd run	100-725	23.0

thermodilatometric analysis correspond well with those from the high temperature X-ray analysis, especially in the low temperature range. At higher temperature, the sintering phenomenon is exhibited by the dilatometric sample, producing complicated results.

A thermogram from the DTA study of pure $SrCl_2$ is shown in Figure 14. It was obtained for both heating and cooling of the sample in air, using a platinum cup sample holder. Deviations downward are endothermic and deviations upward are exothermic effects. A thermogram shows an endothermic effect in the temperature range 665°-785°C with the minimum point at 725°C. That is the region in which X-ray analysis shows a transformation. The transformation does not appear to be sharp or first order since it shows a broad endothermic peak. Following the transformation peak is the melting endotherm. The melting point as determined at the minimum point of the endothermic peak (875°C) agrees well with a reported value of 873°C.[6,12] The freezing point as determined on cooling is about 5° to 10°C lower than that determined on heating, indicating that the liquid was supercooled before recrystallization. The DTA thermogram shows one small endothermic effect, sometimes undetectable, in the low temperature range, 420° to 490°C. This is the region in which X-ray data reveals a very few faint lines in addition to those for the cubic phase. The hexagonal→cubic transformation on cooling is shown by the thermogram to start at about 750°C, with a

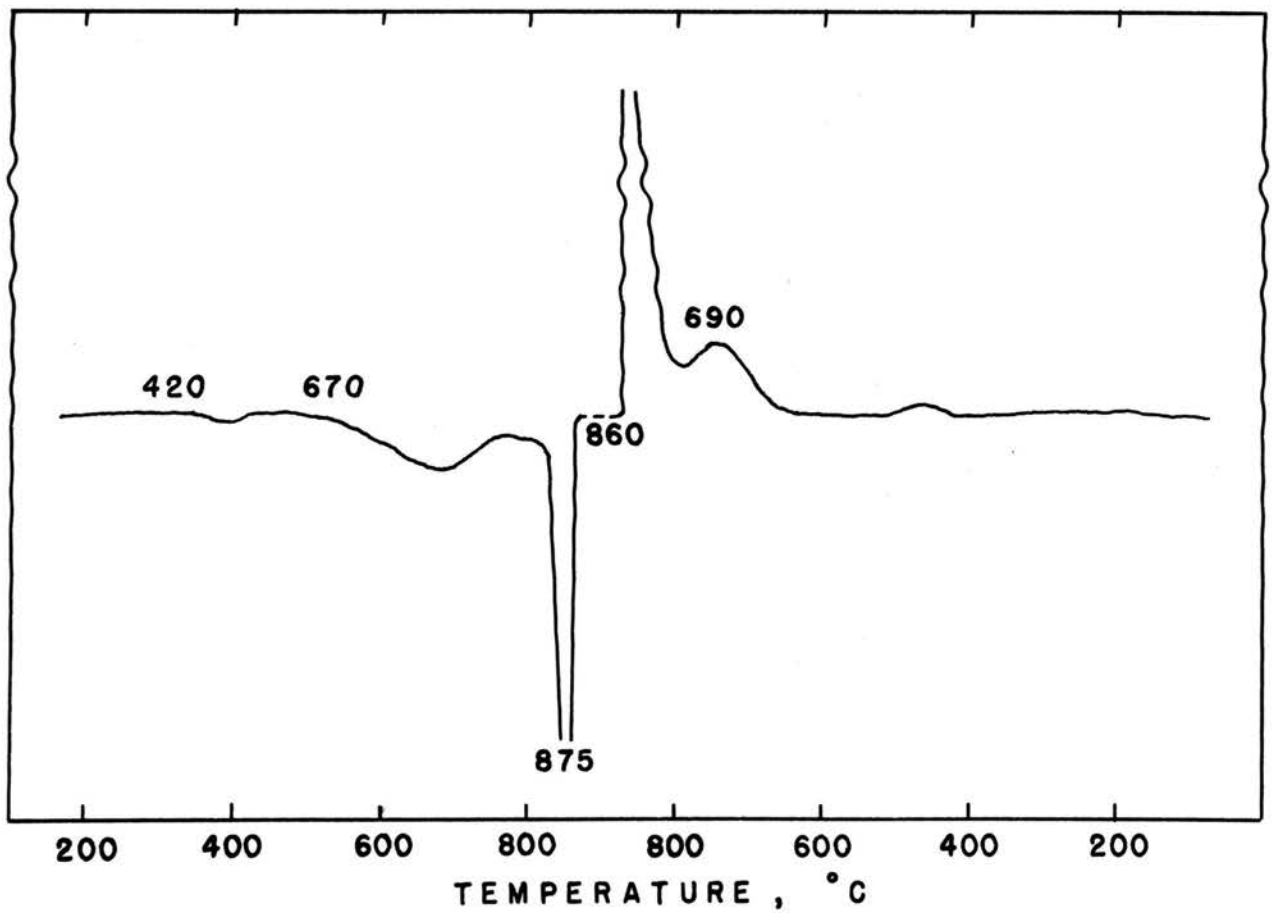

Figure 14. DTA Thermogram for $SrCl_2$

broad peak over 200°C range.

2. Thermal Expansion and Transformation of $BaCl_2$

Thermal expansion of $BaCl_2$ was investigated by using a platinum resistance strip-heater in dry N_2 atmosphere. The sample was preheated overnight at 875°C in a resistance muffle furnace and mounted on a platinum strip-heater. X-ray diffraction at room temperature shows an orthorhombic structure (Pnma). Measurement of the lattice constants of $BaCl_2$, as a function of temperature, was carried out over a temperature range 25° to 870°C. Values of the three lattice parameters were evaluated primarily from the (200), (040), and (002) lines, obtained with CuKα radiation at a scanning rate of 1/8° 2θ per minute. The results are shown in Figure 15; original data are included in Appendix A. The x-ray pattern of the orthorhombic phase is shown in Appendix F. The thermal expansion data can be expressed by linear equations as follows:

$$a = 7.8605 + 3.17 \times 10^{-4} T$$

$$b = 9.4260 + 1.75 \times 10^{-4} T$$

$$c = 4.7251 + 1.91 \times 10^{-4} T$$

The linear thermal expansion coefficients in the temperature range 25°-800°C for a,b, and c are 4.04×10^{-5}, 1.86×10^{-5}, and 4.05×10^{-5} deg^{-1}, respectively.

The lattice expands normally in three directions to 870°C. At higher temperatures, between 870° and 920°C, the x-ray lines of the orthorhombic phase are seen to lose

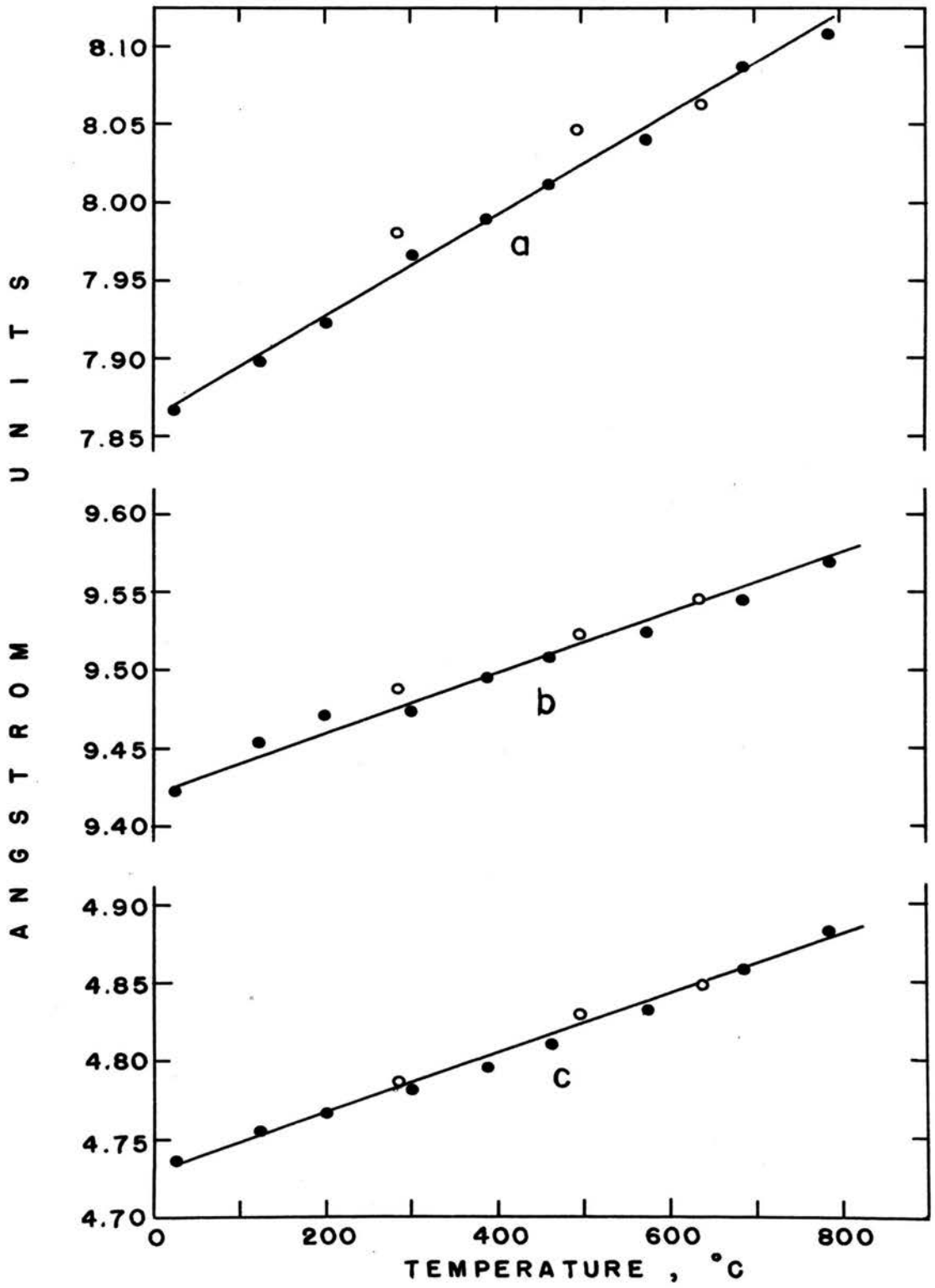

Figure 15. Lattice Parameters of $BaCl_2$ as a Function of Temperature

intensity. Above the transformation temperature, 920°C,[6,12,38] the sample behaves like a liquid, flowing on the strip-heater under the influence of gravity. The x-ray pattern above 920° shows strong peaks at 20.17°, and 30.38° 2θ and several small peaks. Values of $\sin^2\theta$ of these two strong peaks show that the peak at 20.17° is a second order one and that at 30.38° is a third order line, suggesting that at this temperature range the sample has a layer-like structure or shows a preferred orientation effect. If the sample creeps on the platinum strip-heater, it reacts with rhodium in Pt-Rh wire of the thermocouple giving a dark green reaction product. Due to the difficulty in keeping the $BaCl_2$ sample on a strip-heater within the transformation temperature range, a detailed x-ray analysis can not be done by this technique.

Determination by means of differential thermal analysis shows that $BaCl_2$ undergoes endothermic reactions near 920° and 960°C. These correspond to the phase transformation and the melting of $BaCl_2$ respectively. After several cycles of heating and cooling, the two endothermic peaks come together, forming one peak at 900°C on heating, while on cooling, the thermogram still shows two peaks, at 960° and 920°C. Thermograms from DTA studies of $BaCl_2$ are shown in Figure 16. Thermograms 1,2, and 3 are representative of $BaCl_2$, run during first, fourth, and seventh cycles, respectively. The value of the transformation temperature (920°C) agrees well with the results of Derrington

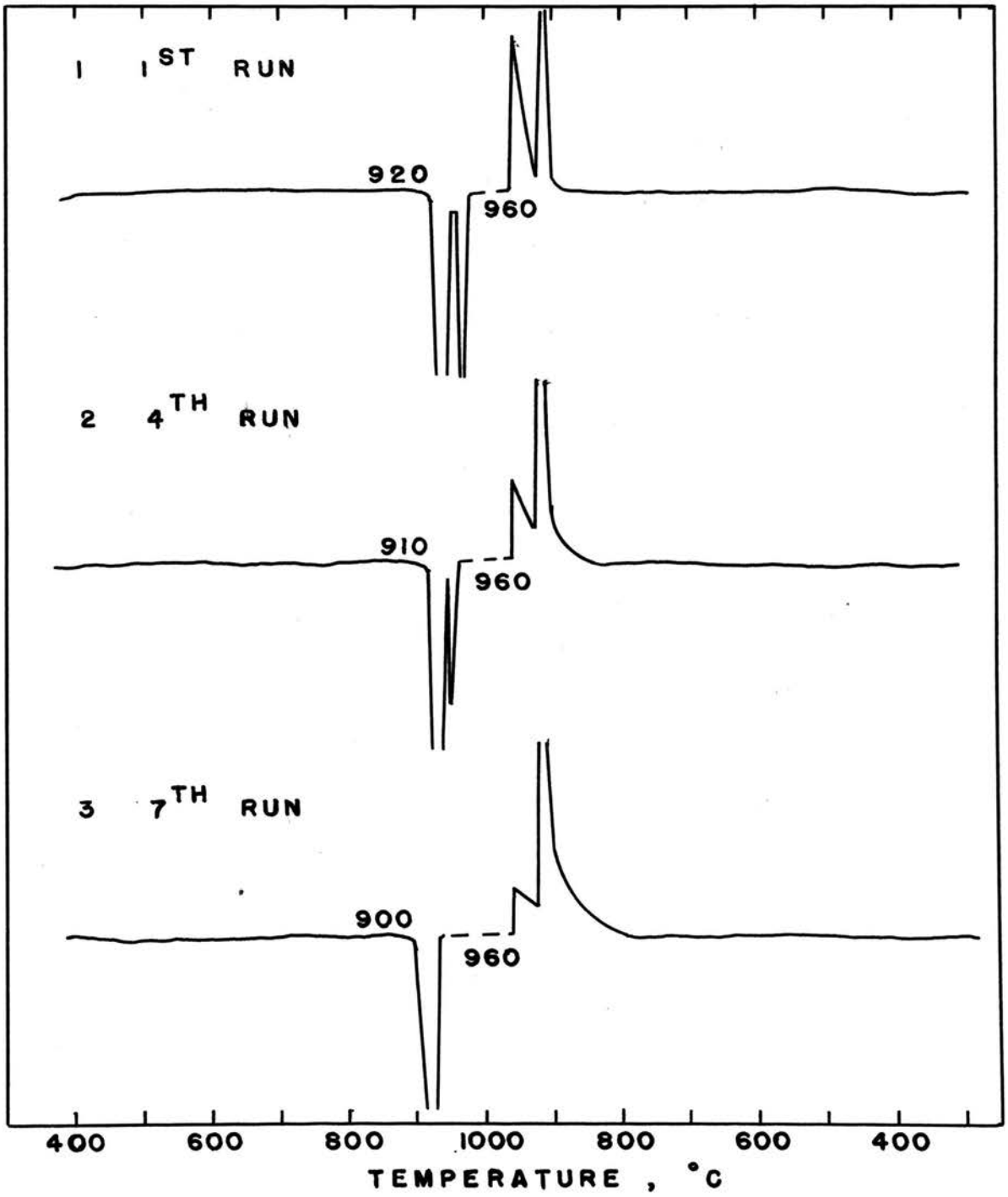

Figure 16. DTA Thermograms for $BaCl_2$

and O'Keeffe[38] (920°C) who determined it by measuring the ionic conductivity and those of several investigators[6,12] (920°, 925°C) who determined it by measuring the heat content. The transformation appears to be sharp corresponding to the abrupt change in ionic conductivity and in heat content. On cooling, the thermograms show an exothermic reaction at 960°C followed suddenly by a larger exothermic peak at the transformation temperature, 920°C.

Thermal expansion of orthorhombic $BaCl_2$ was also determined dilatometrically from 25° to 760°C in air. The calculated $L_T/L_{25°}$ values at different temperatures are tabulated in Table E III of Appendix E. The $L_T/L_{25°}$ values are plotted versus temperature and shown in Figure 17, with closed circles representing heating and opened circles cooling. There are no transformations observed over the temperature range covered except for sintering at high temperature. The linear thermal expansion coefficient, in temperature range 25°-530°C, is 2.33×10^{-5} deg^{-1}, higher than that of b parameter but lower than those of a and c parameters of the orthorhombic form.

This investigation was also concerned with cubic $BaCl_2$. A sample was prepared by mounting the dihydrate of barium chloride on a platinum strip-heater and heating at 70°C in vacuum. The x-ray pattern showed a cubic fluorite structure, as shown in Appendix B, with a 7.3145 Å lattice constant at room temperature (25°C). This value agrees well with the results of other investigators.[17,34,37]

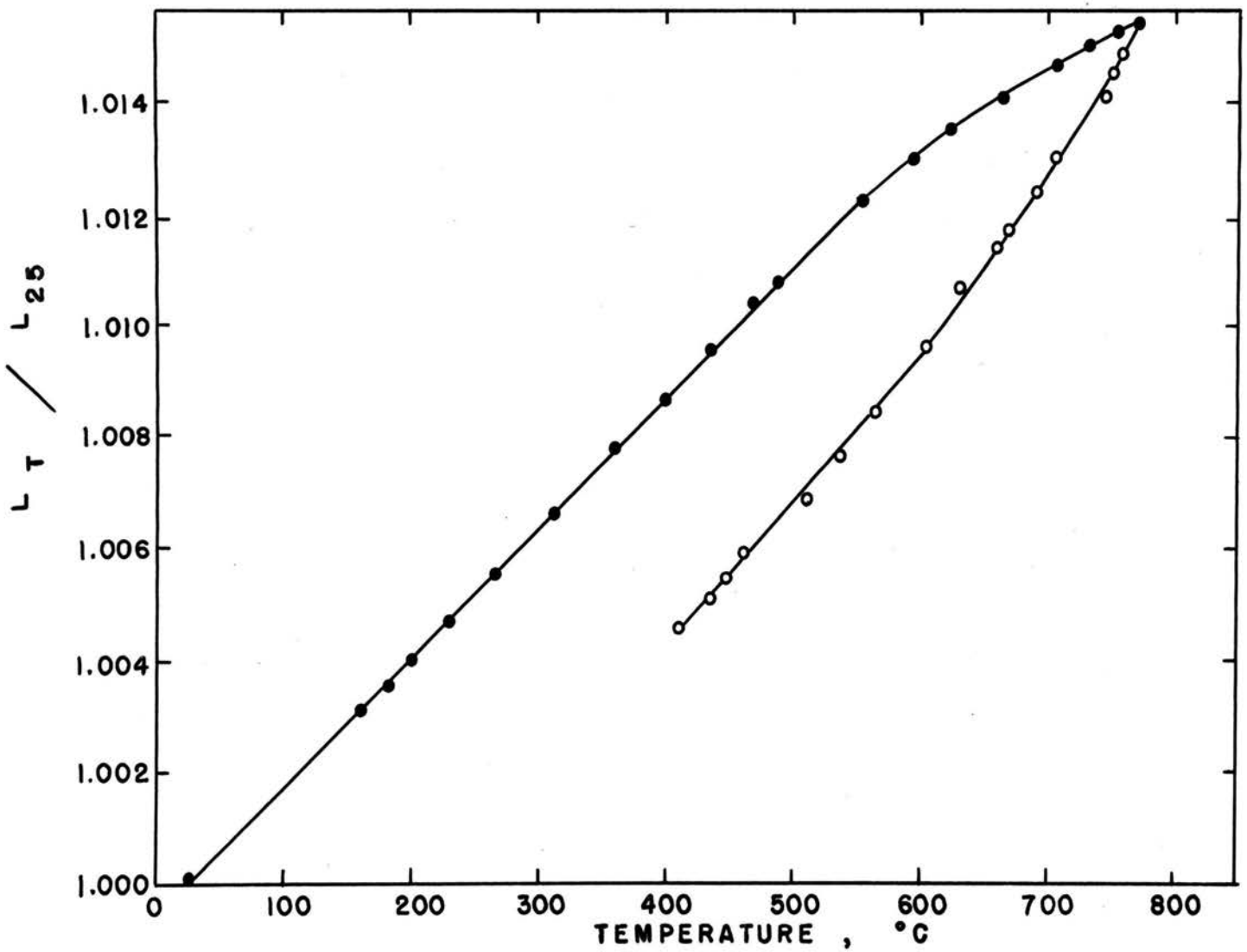

Figure 17. Thermal Expansion of Orthorhombic $BaCl_2$ Measured by TDA

The cubic form did not convert to the orthorhombic form at room temperature, in agreement with the observation of Brackett et al. (1963).[34] Thermal expansion of cubic $BaCl_2$ was investigated by heating the sample in a dry N_2 atmosphere. The (111), (220), and (311) lines were used for calculation of lattice parameter. At 165°C the x-ray diffraction lines of orthorhombic $BaCl_2$ became detectable, the intensities of the orthorhombic lines increasing with increasing temperature and/or time. At about 330°C all of cubic phase converted to the orthorhombic phase within 5 minutes. Figure 18 shows a plot of the experimental values of the lattice parameter versus temperature. It is seen that the cubic $BaCl_2$ expands normally in the investigated temperature range, 25°-330°C. The thermal expansion data can be expressed by the linear equation:

$$a \text{ (cubic } BaCl_2) = 7.3102 + 1.93 \times 10^{-4} T$$

The linear thermal expansion coefficient is equal to 2.61×10^{-5} deg^{-1}.

An attempt was made to obtain cubic $BaCl_2$ by heating $BaCl_2 \cdot 2H_2O$ in air. Two procedures were used. The first was by heating $BaCl_2 \cdot 2H_2O$ in a platinum crucible at 125°C for a long period of time. In the second procedure, aqueous solution of the dihydrate of $BaCl_2$ was sprayed onto a glass slide and then dried at 70°C for about 2 hours. The first procedure yielded the orthorhombic form but the second yielded the cubic fluorite form.

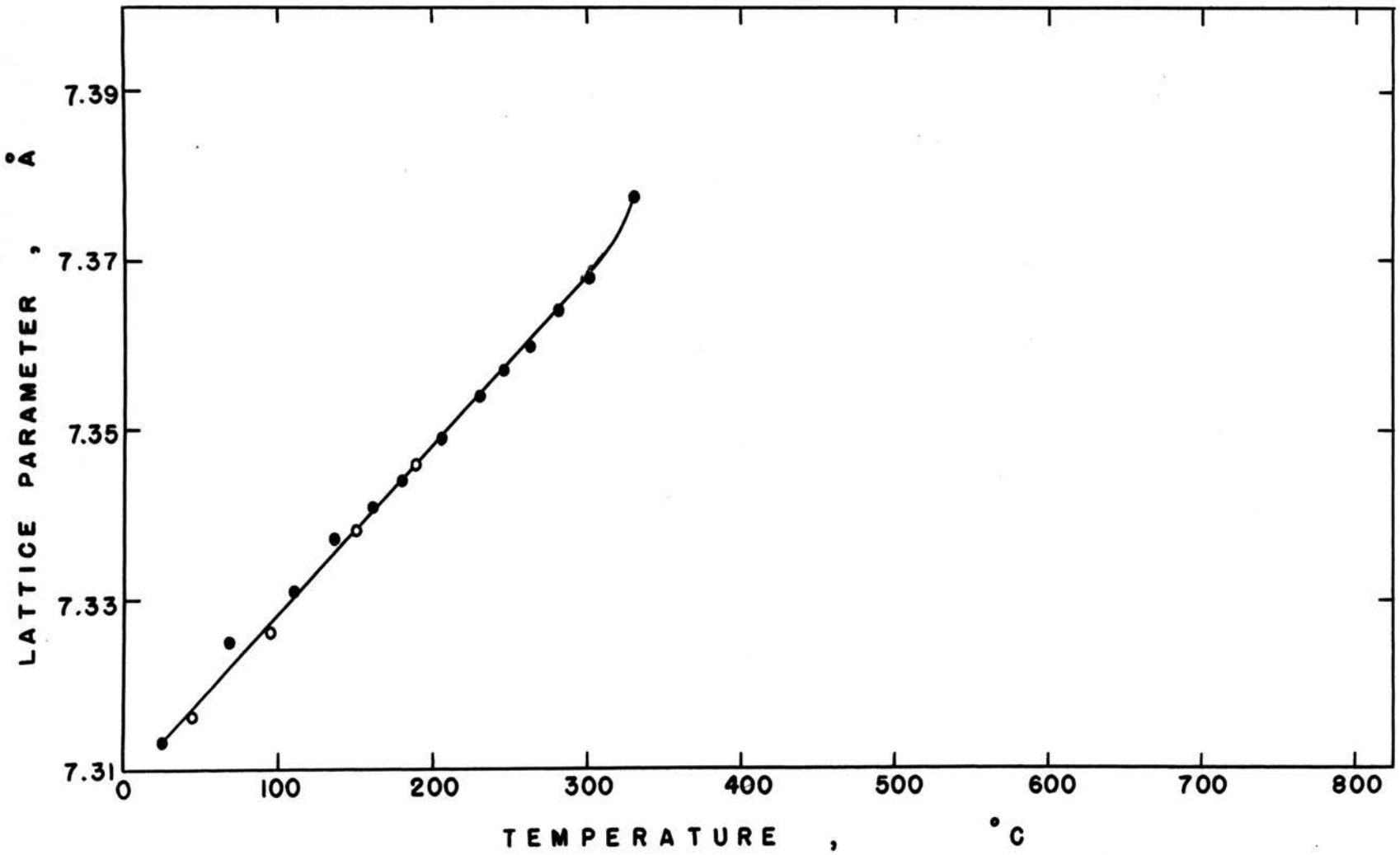

Figure 18. Cubic $BaCl_2$ Lattice Parameter as a Function of Temperature

C. Phase Relationships in the System $SrCl_2$-$BaCl_2$

Three methods were used to determine phase relationships in the $SrCl_2$-$BaCl_2$ system: heating and quenching techniques, high temperature x-ray techniques, and dilatometry. For heating and quenching techniques, samples were equilibrated at the desired temperature, quenched to room temperature, ground, and then scanned. The results show that $SrCl_2$ forms solid solutions having cubic fluorite structure with up to 25 mole percent $BaCl_2$. Above 35 mole percent $BaCl_2$, solid solutions having the $BaCl_2$ orthorhombic structure are formed. X-ray patterns of phases in this system, determined by heating and cooling techniques, are shown in Figure F1 of Appendix F. Lattice parameters of the cubic solid solutions and of the orthorhombic solid solutions of quenched samples are given in Table X and Table XI, respectively. Plots of these data versus $BaCl_2$ content are shown in Figures 19 to 21. The results for the cubic solid solution agree quite closely with those of Brauer and Müller.[43] The lattice parameters in the two solid solution ranges increase with increasing $BaCl_2$ content. The boundaries of these solid solutions, however, are not quite clear. Reasons for this will be given in the discussion section.

Samples with compositions to 90 mole percent $BaCl_2$ were investigated by high temperature X-ray techniques. The results show that at high temperature both cubic and orthorhombic solid solutions transform to hexagonal

TABLE X

Lattice Parameters of Cubic Solid Solutions

Composition ($BaCl_2$ mole%)	Preheat Temperatures and Times 650°C 125 hrs.	710°C 72 hrs.	800°C 24 hrs.	850°C 12 hrs.
0	6.9758	6.9748	6.9758	6.9760
10	7.0074	7.0072	7.0104	7.0104
20	7.0408	7.0451	7.0478	7.0448
25	-	-	7.0565	-
26	-	7.0617	7.0637	-
28	-	7.0767	7.0734	-
30	-	7.0767	7.0767	7.0772
32	-	7.0717	7.0767	-

TABLE XI

Lattice Parameters of Orthorhombic Solid Solutions

Compositions ($BaCl_2$ mole%)	Preheat Temperatures (°C) and Times (hrs.)					
	650 (125)			710 (72)		
	a	b	c	a	b	c
26	7.6708	9.1276	4.6154	-	-	-
28	7.6644	9.1120	4.6176	-	-	-
30	7.6774	9.1296	4.6178	7.6774	9.1144	4.6102
32	7.6840	9.1564	4.6222	-	-	-
35	-	-	-	-	-	-
40	7.7068	9.1588	4.6302	7.7036	9.1740	4.6302
50	7.7300	9.2240	4.6498	7.7234	9.2192	4.6452
60	7.7434	9.2512	4.6718	7.7434	9.2468	4.6648
70	7.7800	9.2972	4.6894	7.7902	9.2832	4.6870
80	7.8206	9.3228	4.7012	7.8104	9.3460	4.7082
90	7.8410	9.3802	4.7154	7.8514	9.3714	4.7122
100	7.8722	9.4250	4.7322	7.8684	9.4236	4.7356

TABLE XI (Cont.)

Compositions ($BaCl_2$ mole%)	Preheat Temperatures (°C) and Times (hrs.)					
	800 (24)			850 (12)		
	a	b	c	a	b	c
26	-	-	-	-	-	-
28	-	-	-	-	-	-
30	7.6700	9.1076	4.6064	7.6612	9.1144	4.6098
32	-	-	-	-	-	-
35	7.6904	9.1364	4.6244	-	-	-
40	7.7116	9.1676	4.6336	7.6904	9.1588	4.6280
50	7.7234	9.2080	4.6474	7.7200	9.1986	4.6486
60	7.7500	9.2536	4.6752	7.7466	9.2536	4.6682
70	7.7834	9.2832	4.6928	7.7968	9.2740	4.6812
80	7.8172	9.3504	4.7094	-	-	-
90	7.8470	9.3802	4.7142	-	-	-
100	7.8722	9.4236	4.7356	-	-	-

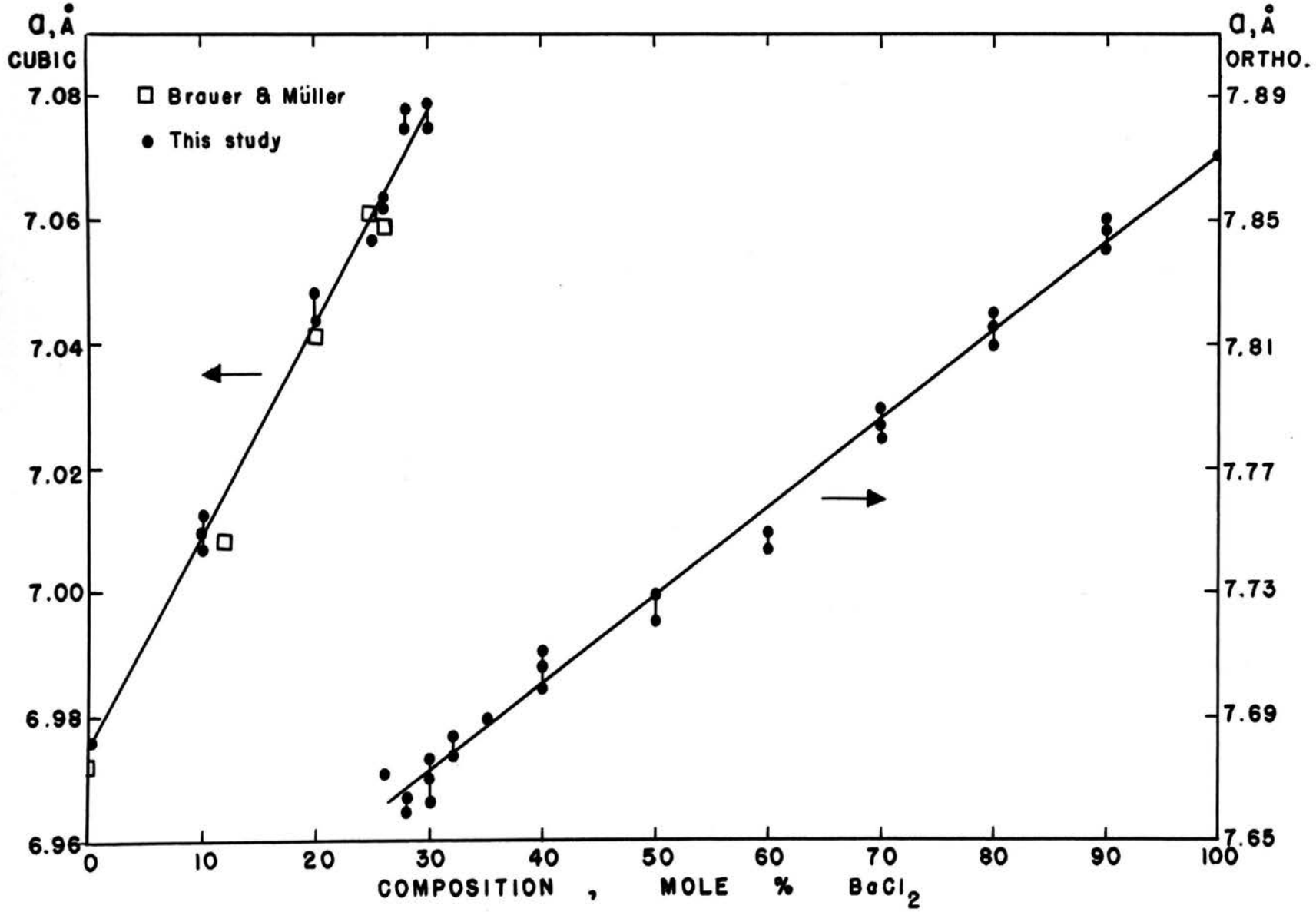

Function 19. The a Parameters of $SrCl_2$-$BaCl_2$ Solid Solutions versus Composition

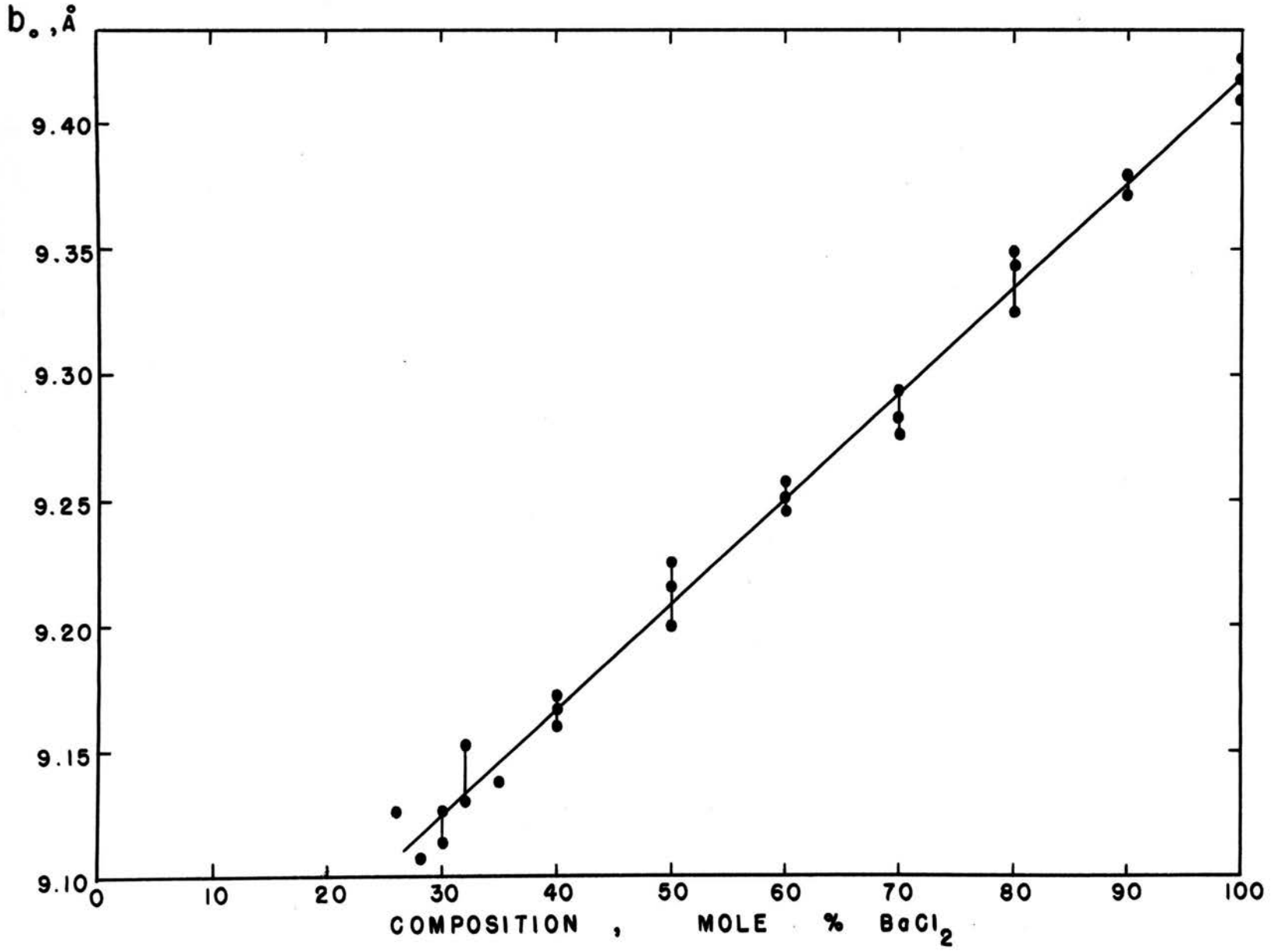

Figure 20. The b Parameter of Orthorhombic Solid Solution versus Composition

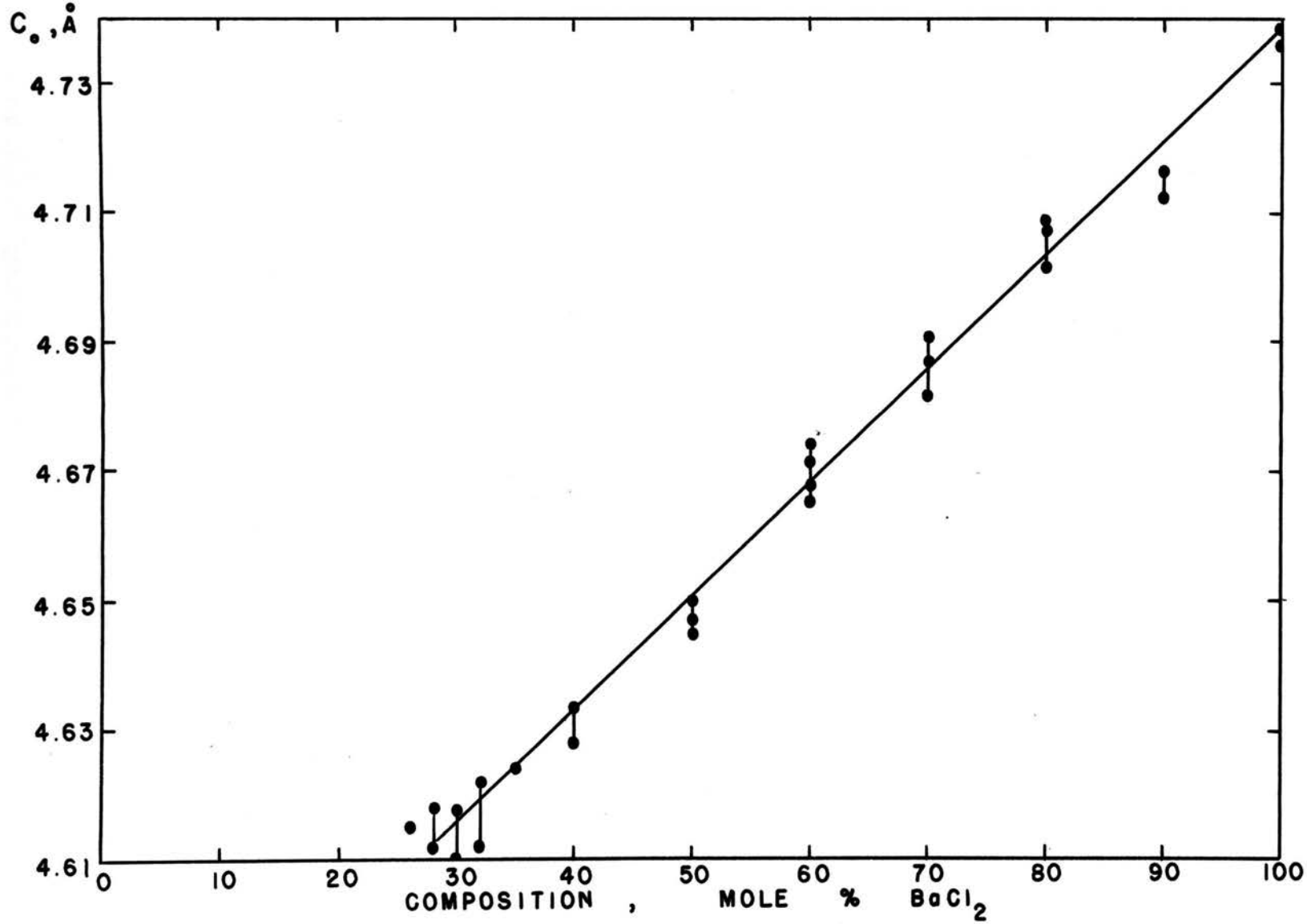

Figure 21. The c Parameter of Orthorhombic Solid Solution versus Composition

structures. The high temperature phase develops with increasing time and temperature. With increasing $BaCl_2$ content, the transformation temperatures of cubic solid solutions decrease, and those of orthorhombic solid solutions increase. The (20.0) and (00.2) lines of the hexagonal solid solution from 0 mole percent to 80 mole percent $BaCl_2$ were measured at 780°C in a dry N_2 atmosphere and lattice parameters were calculated directly. The 2θ angles, d-spacings, and calculated lattice parameters are tabulated in Table XII. The plots of lattice parameters versus temperature are shown in Figures 22 and 23. The lattice parameters of hexagonal solid solutions increase linearly with increasing $BaCl_2$ content.

At 780°C the x-ray patterns of samples with over 60 mole percent $BaCl_2$ initially indicate orthorhombic solid solutions, but after prolonged heating the hexagonal lines emerge slowly. Because the rate of transformation is very low, 2θ data for (20.0) and (00.2) of the hexagonal form of these samples were gathered by heating the samples to higher temperature until the orthorhombic phase converted to the hexagonal form and then cooling to 780°C. Lattice parameters of the hexagonal form of the 90 mole percent $BaCl_2$ solid solutions could not be measured because the sample became a liquid-like crystal in the transformation range, as did pure $BaCl_2$. Actually all of the samples in the system $SrCl_2$-$BaCl_2$ developed liquid-like crystals at temperatures 5° to 30°C below the fusion points. The

TABLE XII

Diffraction Angles, Interplanar Spacings, and Calculated Lattice Parameters for the Hexagonal Phase, Measured at 780°C in the $SrCl_2$-$BaCl_2$ System

Composition ($BaCl_2$ mole%)	$2\theta_{20.0}$	$2\theta_{00.2}$	$d_{20.0}$	$d_{00.2}$	a	c
0	21.28	24.16	4.1752	3.6836	9.6422	7.3672
10	21.18	24.06	4.1946	3.6987	9.6872	7.3974
20	21.11	24.08	4.2084	3.6956	9.7194	7.3912
25	21.05	23.94	4.2202	3.7169	9.7461	7.4338
30	20.98	23.85	4.2342	3.7308	9.7785	7.4616
35	20.94	23.83	4.2422	3.7338	9.7969	7.4676
40	20.84	23.60	4.2623	3.7697	9.8434	7.5394
50	20.79	23.60	4.2824	3.7697	9.8667	7.5394
60	20.78	23.55	4.2745	3.7776	9.8715	7.5552
75	20.60	23.30	4.3114	3.8176	9.9567	7.6352
80	20.43	23.22	4.3469	3.8305	10.0387	7.6610

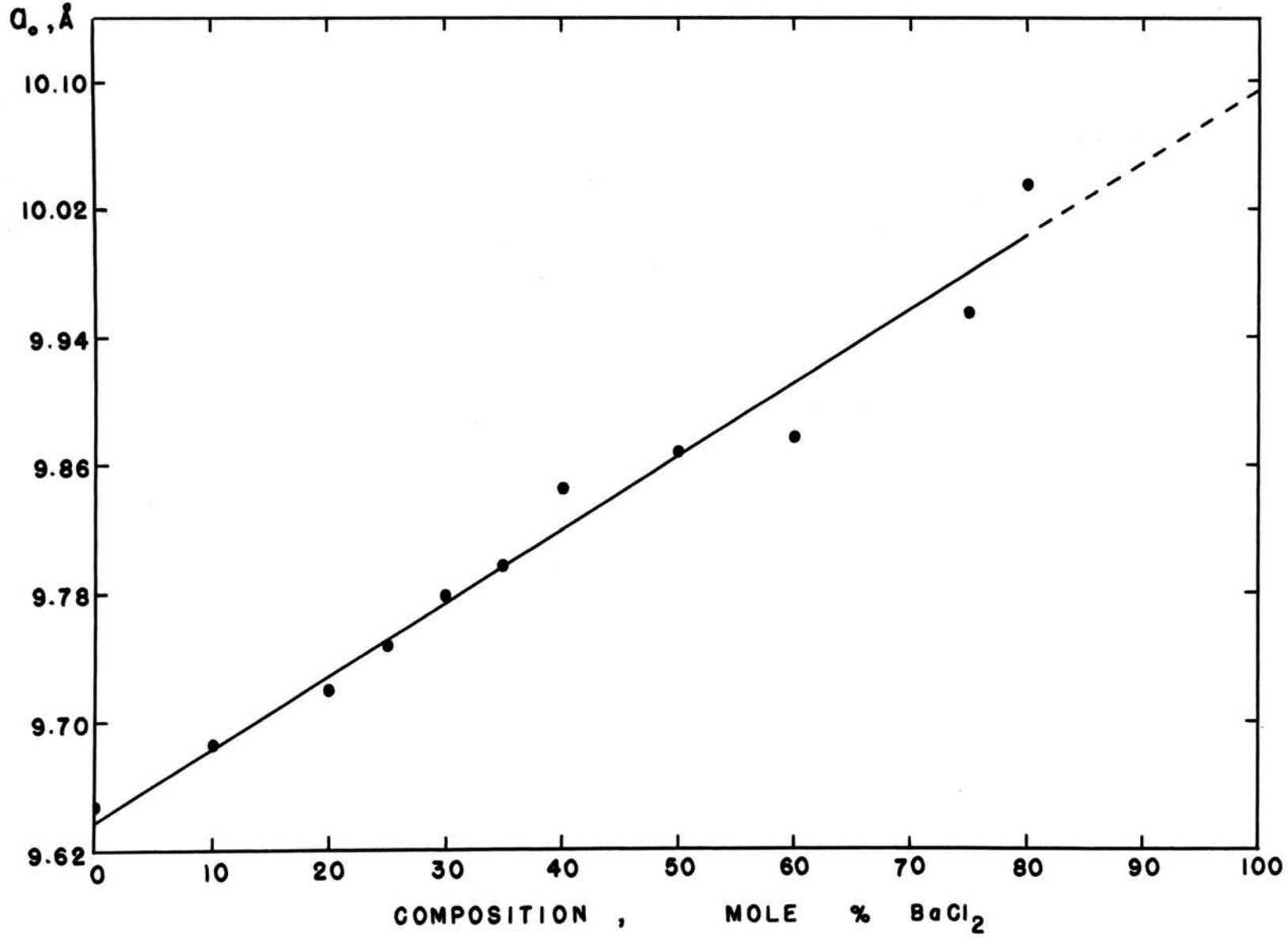

Figure 22. The a Parameter of Hexagonal Solid Solution at 780°C versus Composition

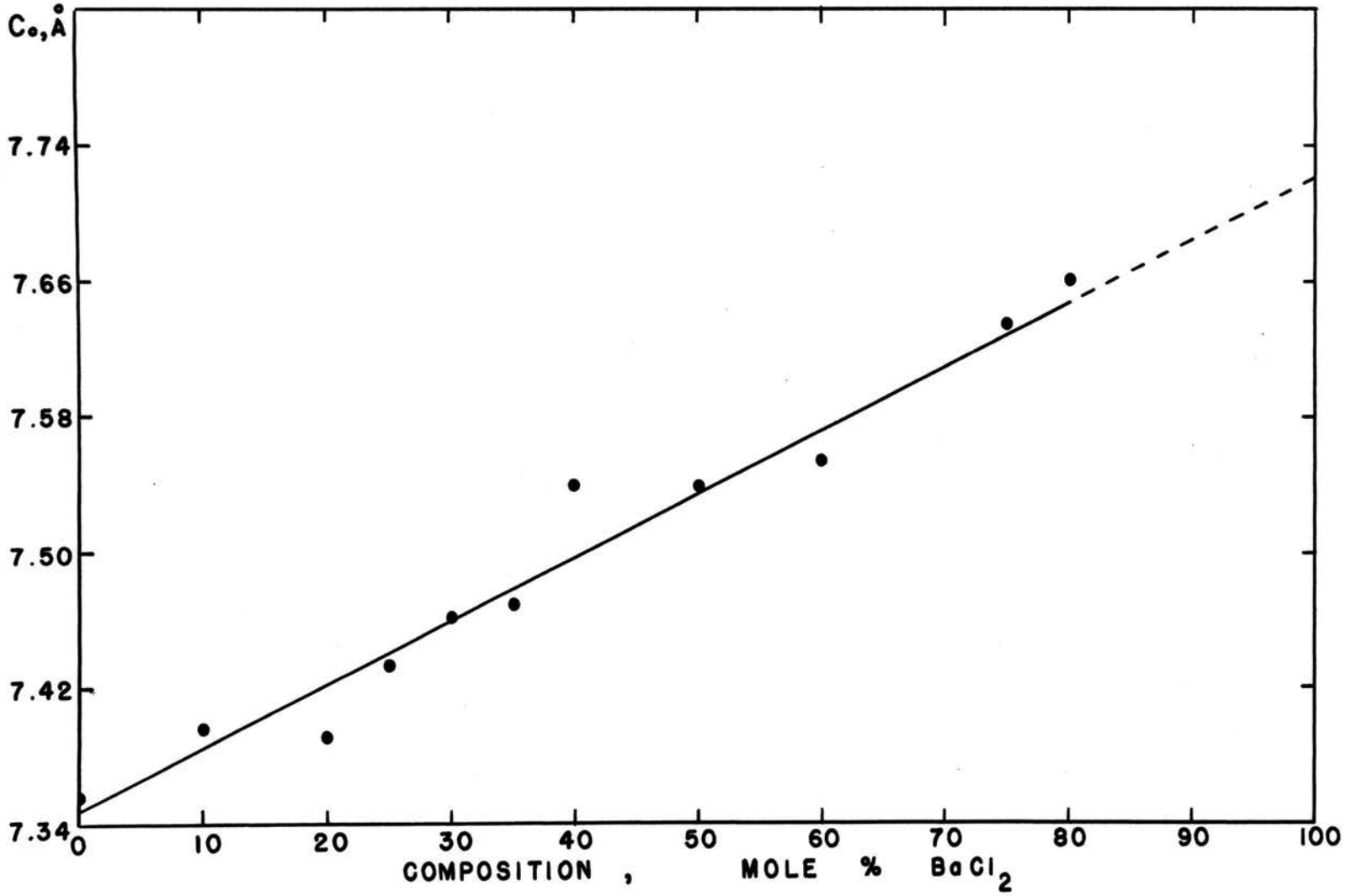

Figure 23. The c Parameter of Hexagonal Solid Solution at 780°C versus Composition

reasons for these phenomenon will be discussed later.

Figures F2 to F4 of Appendix F contain high temperature x-ray patterns, obtained at several temperatures, for the samples $Sr_{0.8}Ba_{0.2}Cl_2$, $Sr_{0.7}Ba_{0.3}Cl_2$, and $Sr_{0.5}Ba_{0.5}Cl_2$. These figures illustrate the development of the high temperature hexagonal phase, showing complete miscibility in the system. Calculation of molar volumes from the measured lattice parameters of all samples shows that the orthorhombic form is 9 to 12% smaller than the cubic and 15 to 20% smaller than the hexagonal form. At the transformation temperature the molar volume of cubic phase is 5-7% smaller than that of hexagonal phase.

Thermodilatometric analyses for this system were made in air between 25° to 780°C of samples with 20 mole percent up to 50 mole percent. The results are shown in Figures 24 to 30 as $L_T/L_{25°}$ values versus temperature; original data are tabulated in Appendix E. Figures E1 and E2, Appendix E also show the second run of samples with 30 and 32 mole percent $BaCl_2$, respectively. Closed circles represent data obtained on heating and open circles on cooling. Although the ascending and descending temperature curves do not superpose at any temperature above 25°C, the sharp change in slope indicates a phase transformation. The sample with cubic solid solution (20 mole percent $BaCl_2$) shows a rather broad transformation range, 600°C to 740°C. The transformation appears to be sharper in orthorhombic solid solutions. On cooling, these samples also

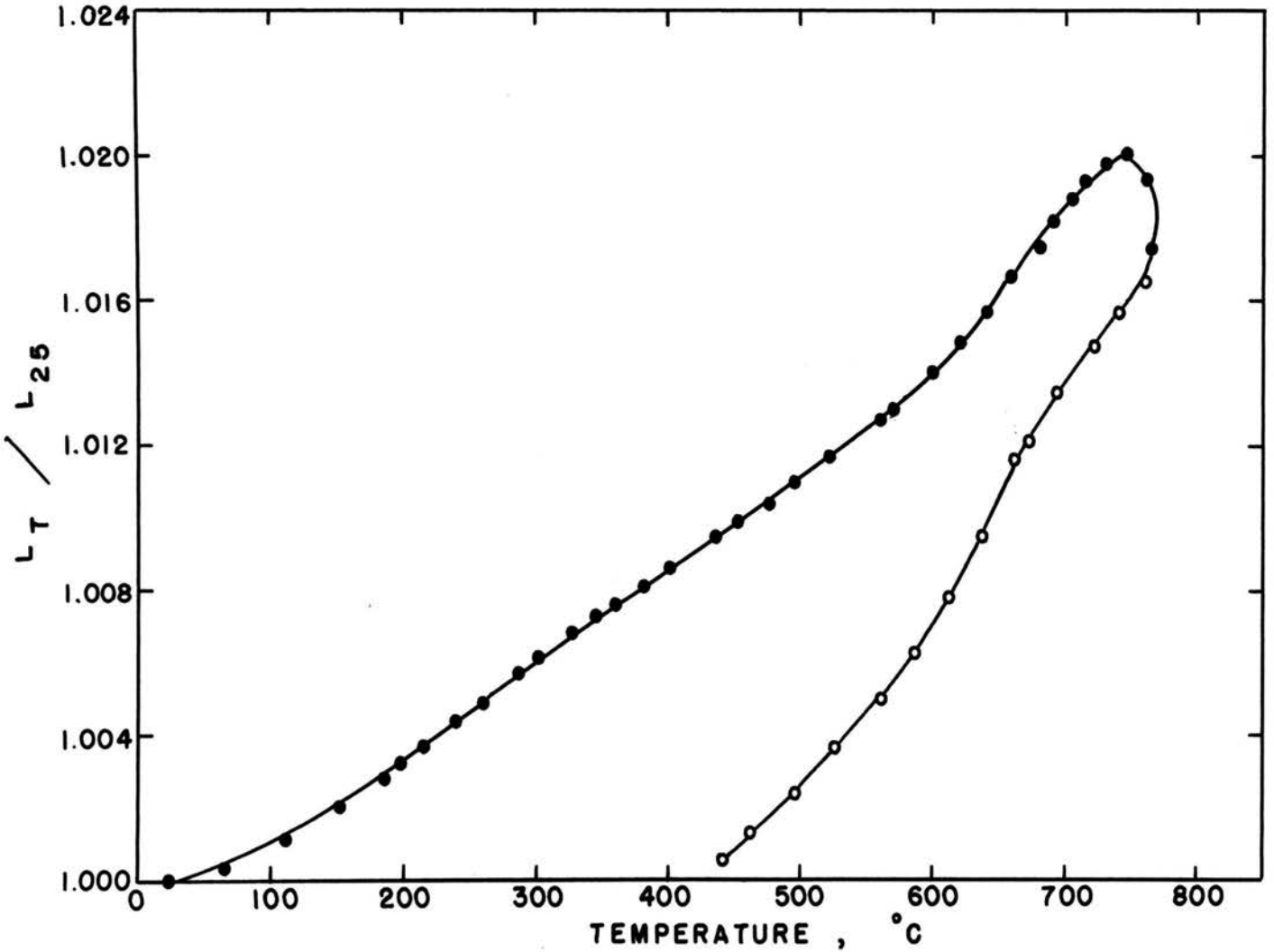

Figure 24. Thermal Expansion and Transformation of Sample with 20 mole % $BaCl_2$ Measured by TDA

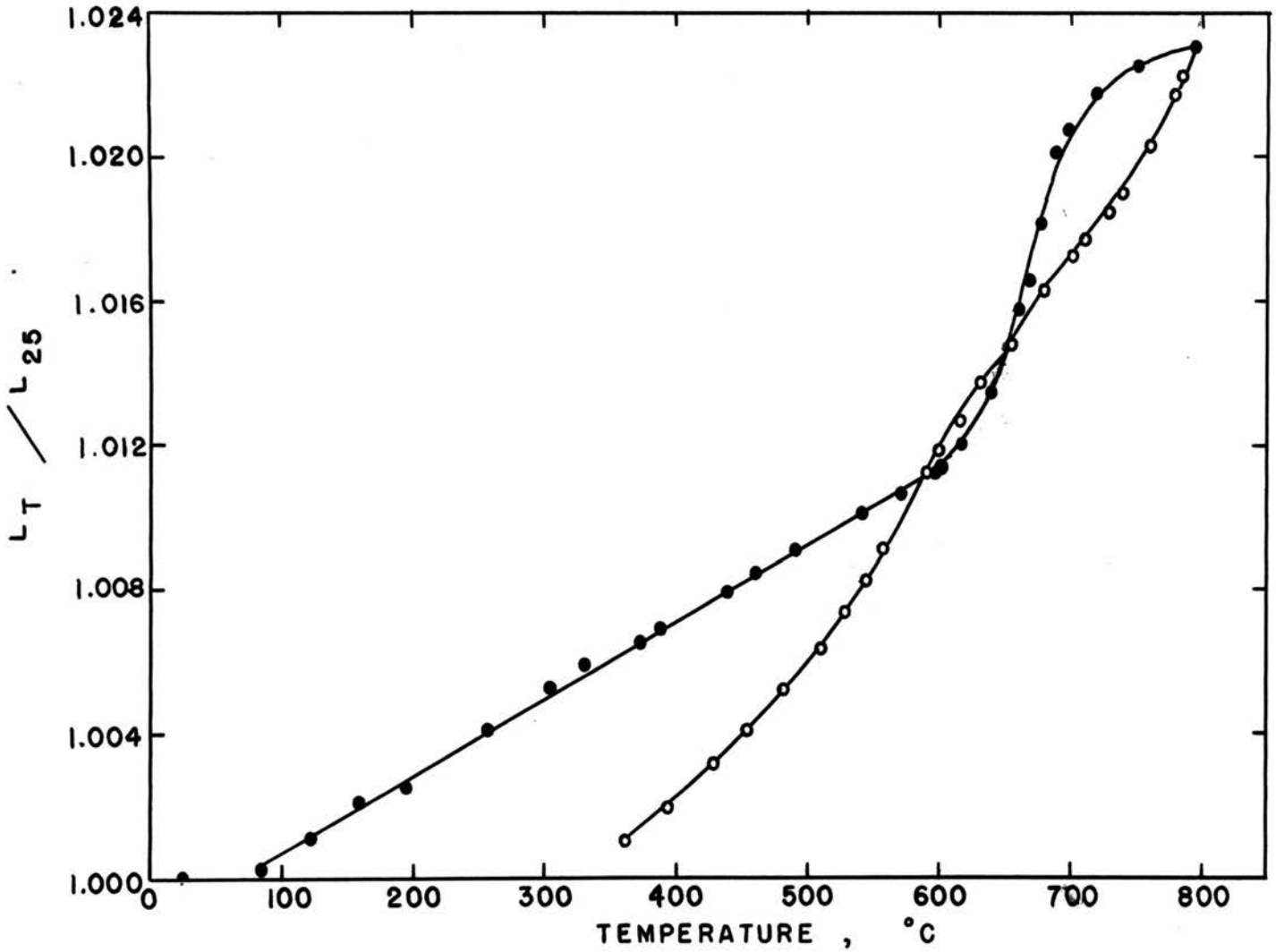

Figure 25. Thermal Expansion and Transformation of Sample with 26 mole % $BaCl_2$ Measured by TDA

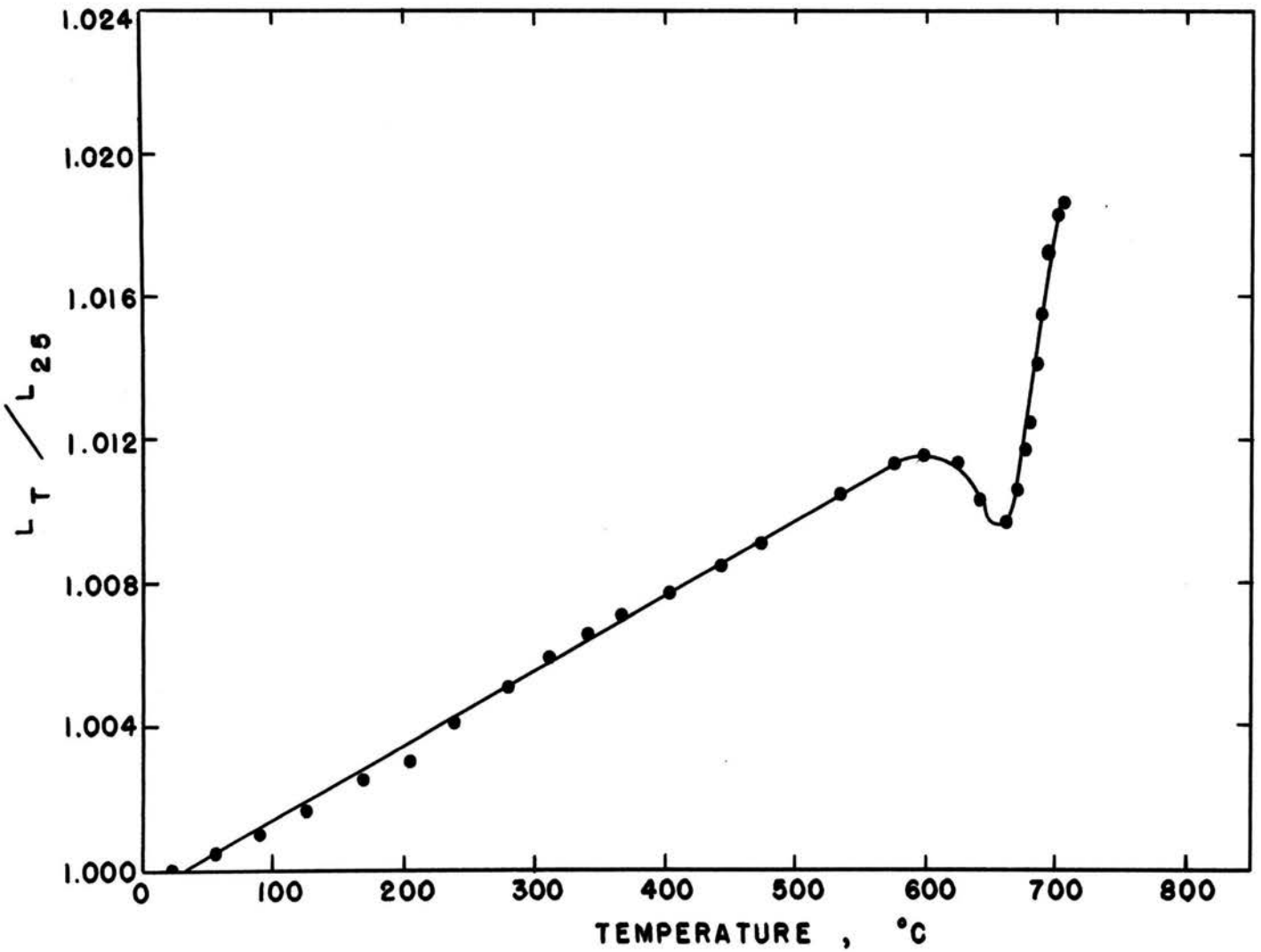

Figure 26. Thermal Expansion and Transformation of Sample with 28 mole % $BaCl_2$ Measured by TDA

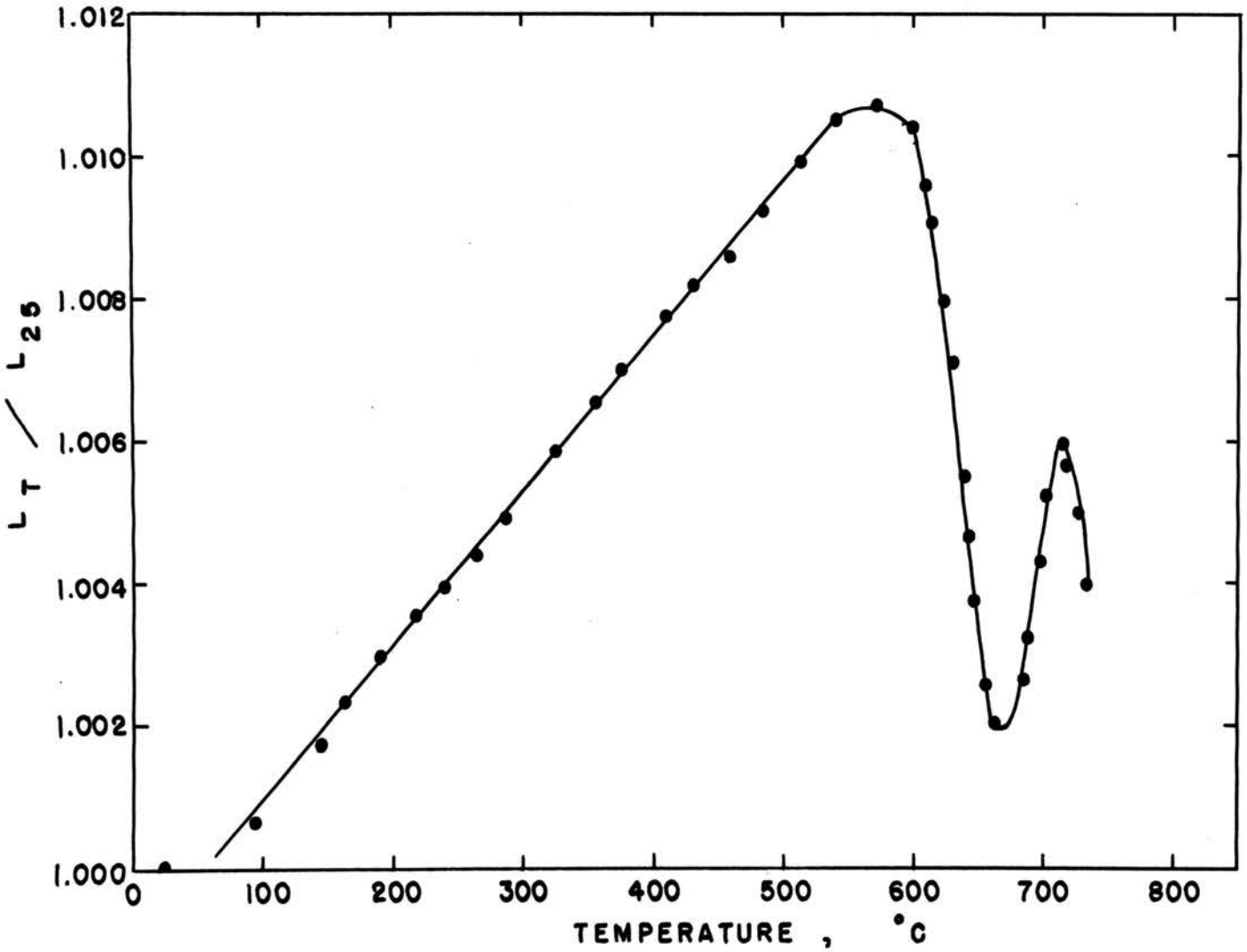

Figure 27. Thermal Expansion and Transformation of Sample with 30 mole % $BaCl_2$ Measured by TDA

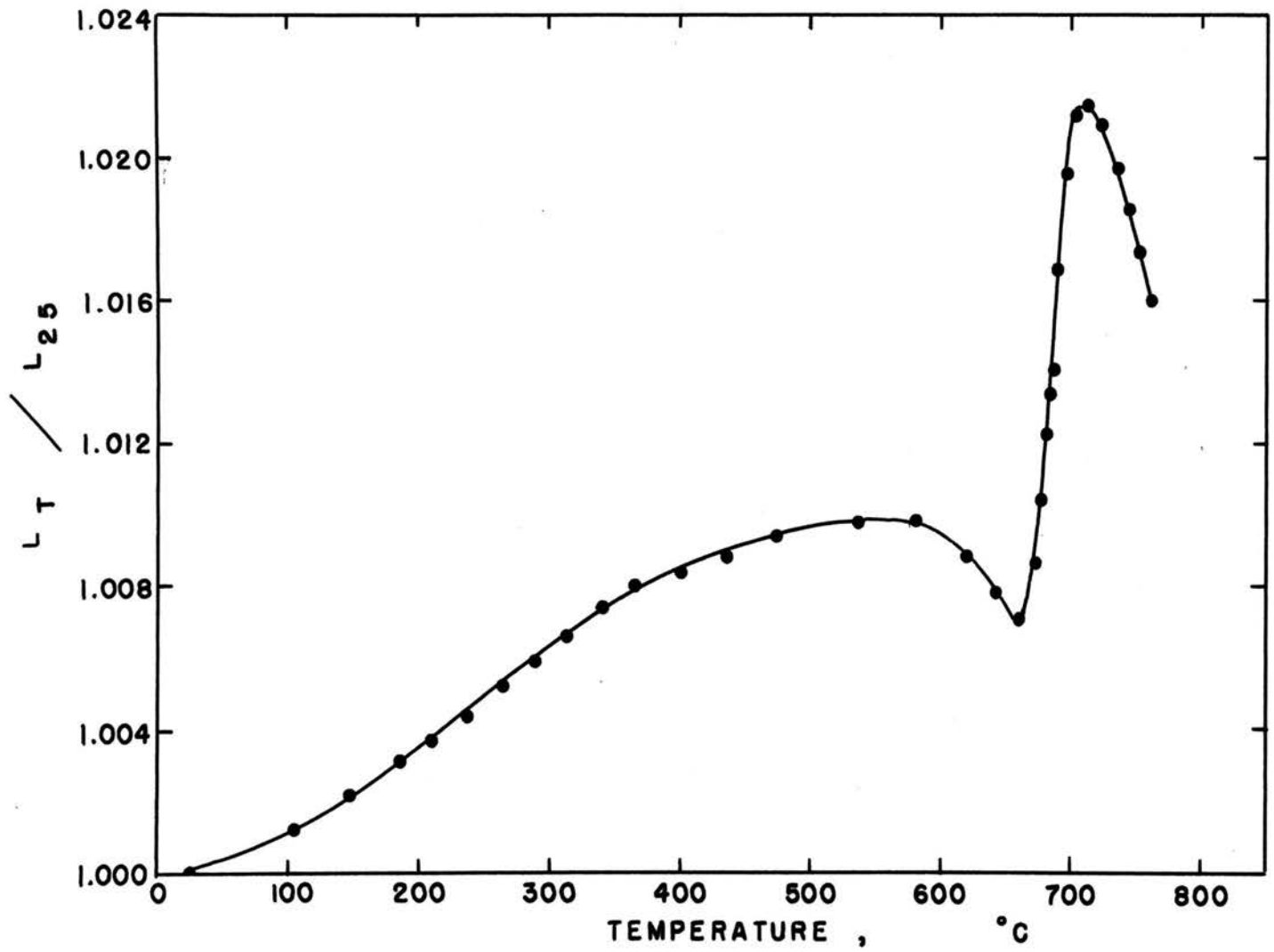

Figure 28. Thermal Expansion and Transformation of Sample with 32 mole % $BaCl_2$ Measured by TDA

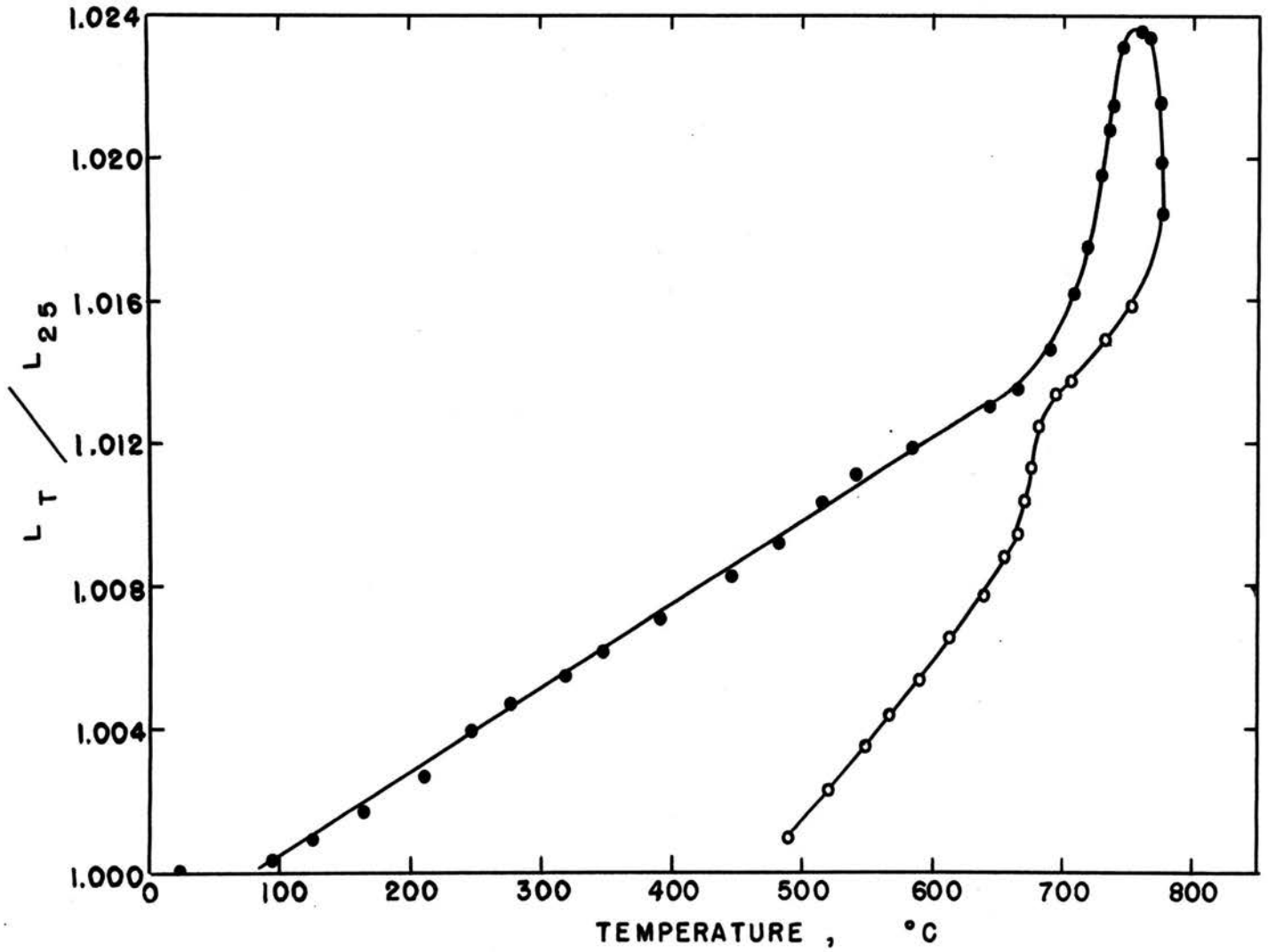

Figure 29. Thermal Expansion and Transformation of Sample with 40 mole % $BaCl_2$ Measured by TDA

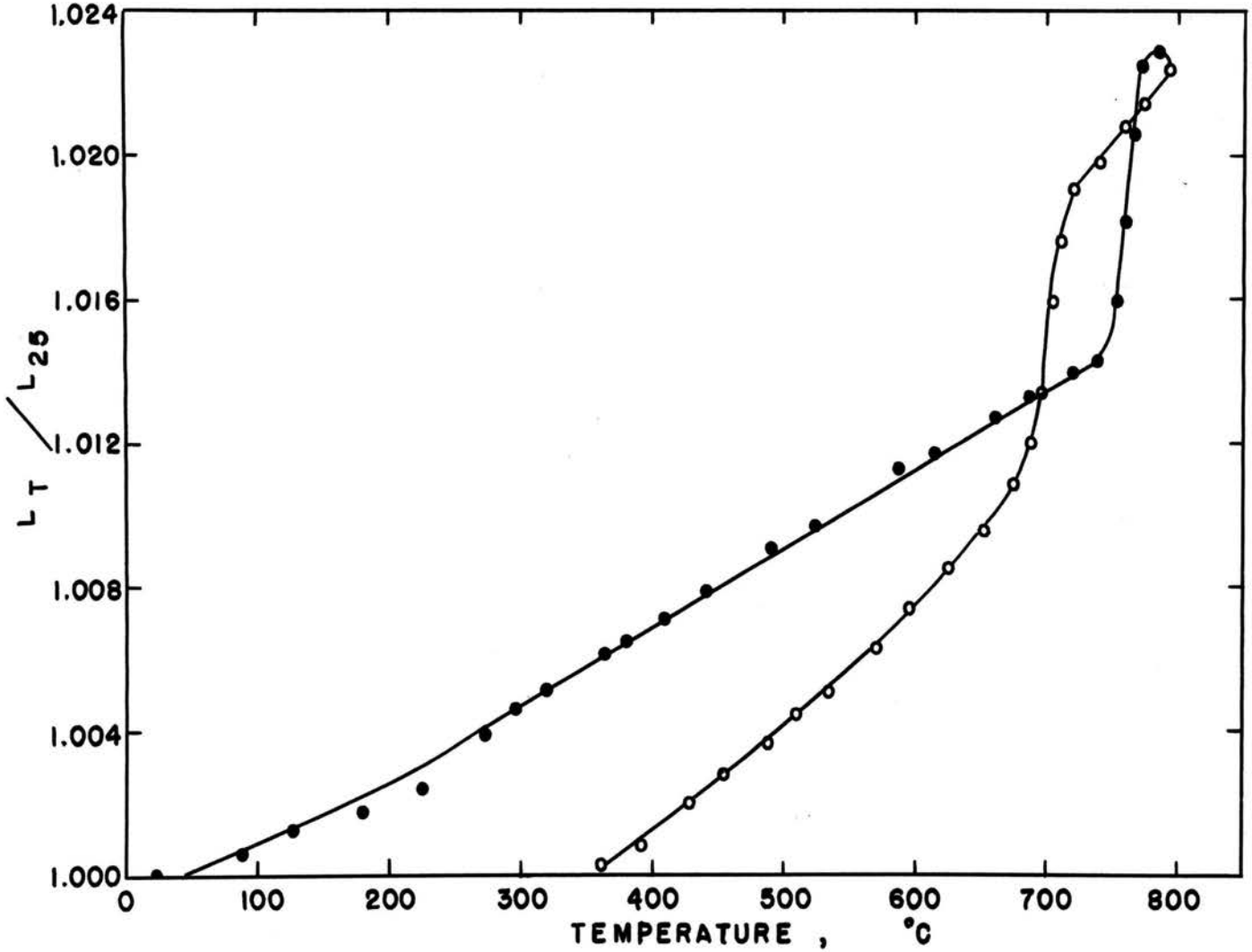

Figure 30. Thermal Expansion and Transformation of Sample with 50 mole % $BaCl_2$ Measured by TDA

transformed.

Typical DTA thermograms of the $SrCl_2$-$BaCl_2$ system are contained in Figure 31. Event temperatures for the system, as determined by DTA and thermodilatometric analysis, are contained in Table XIII. Experimental points for the solidus agree quite closely with those of Vortisch,[39] and of Schei and Flood.[42]

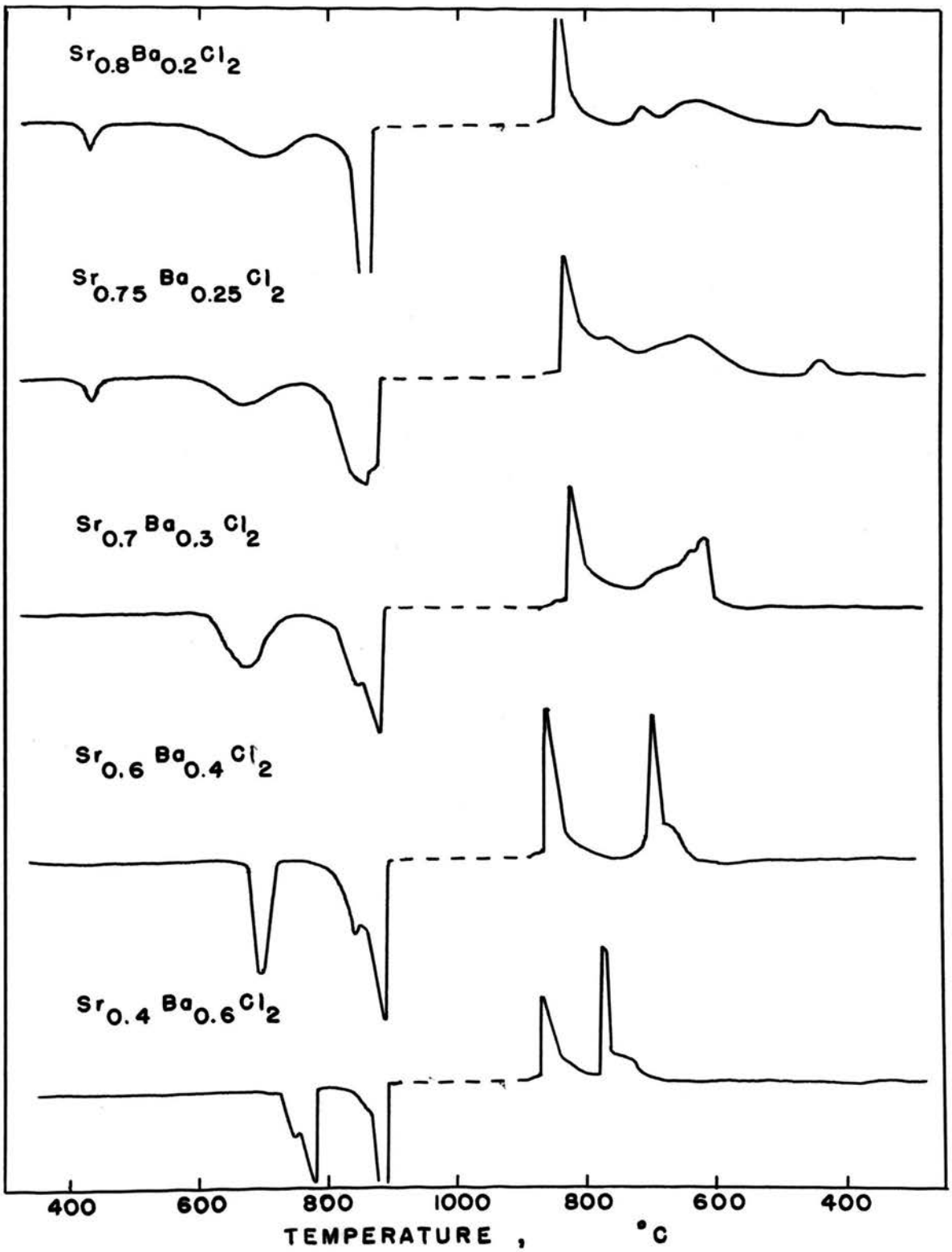

Figure 31. DTA Thermograms for Selected Compositions in the System $SrCl_2$-$BaCl_2$

TABLE XIII

Event Temperatures for the System $SrCl_2$-$BaCl_2$

Composition ($BaCl_2$ mole%)	Low-High Form Transition, Heating		High-Low Form Transition, Cooling		Solidus, Heating	Liquidus, Cooling
	DTA	TDA	DTA	TDA		
0.0	670	-	750	-	875	860
10.0	630	-	718	-	865	850
20.0	600	590	720	710	850	845
25.0	610	-	716	-	845	840
26.0	610	600	700	700	845	845
28.0	610	610	695	-	845	847
30.0	615	(580) (665) (600) (675)	710	-	850	856
32.0	640	(600) (660) 660	710	660	860	862
35.0	650	-	720	-	862	865
40.0	665 670	670	710	690	865	860
50.0	720	735	740	725	870	870

TABLE XIII (Cont.)

Composition ($BaCl_2$ mole%)	Low-High Form Transition, Heating		High-Low Form Transition, Cooling		Solidus, Heating	Liquidus, Cooling
	DTA	TDA	DTA	TDA		
60.0	740	-	780	-	880	875
70.0	780 790	-	820	-	890	887
75.0	810	-	845 850	-	910	910 915
80.0	820	-	870	-	930	927
90.0	850	-	890	-	940	950
100.0	915	-	920	-	960	957

D. Structure of the High Temperature Strontium Chloride

X-ray data for the high-temperature modification of $SrCl_2$ and the complete solid solution series between $SrCl_2$-$BaCl_2$ can be indexed on a hexagonal unit cell with space group $P6_3/mmc$ or $P6_3mc$ as shown in Table VII. An attempt was made to determine the structure of this hexagonal form. It was difficult to obtain precise intensities with the high-temperature diffraction because of nucleation and grain growth. However, from rapid scans and some slow scans approximate data were gathered.

Nothing regarding the high temperature structure of $SrCl_2$ has been found in the literature. Because of the relationship between the cubic fluorite type structure and orthorhombic lead chloride type structure, discussed later, structure models related to the lead chloride structure were devised. The orthorhombic lead chloride structure can be considered as a close-packed deformed hexagonal anion lattice; as a result of the deformation the cations are 9-co-ordinated. The details of this structure were discussed earlier. The orientational relationships between the orthorhombic and the hexagonal structure can be seen on the (010) plane of the orthorhombic structure, as shown in Figure 32. The solid lines show the unit cell of an orthorhombic lead chloride structure, with four molecules per unit cell. The broken lines show the unit cell of a hexagonal structure, with six molecules.

Several models have been devised by arranging cations

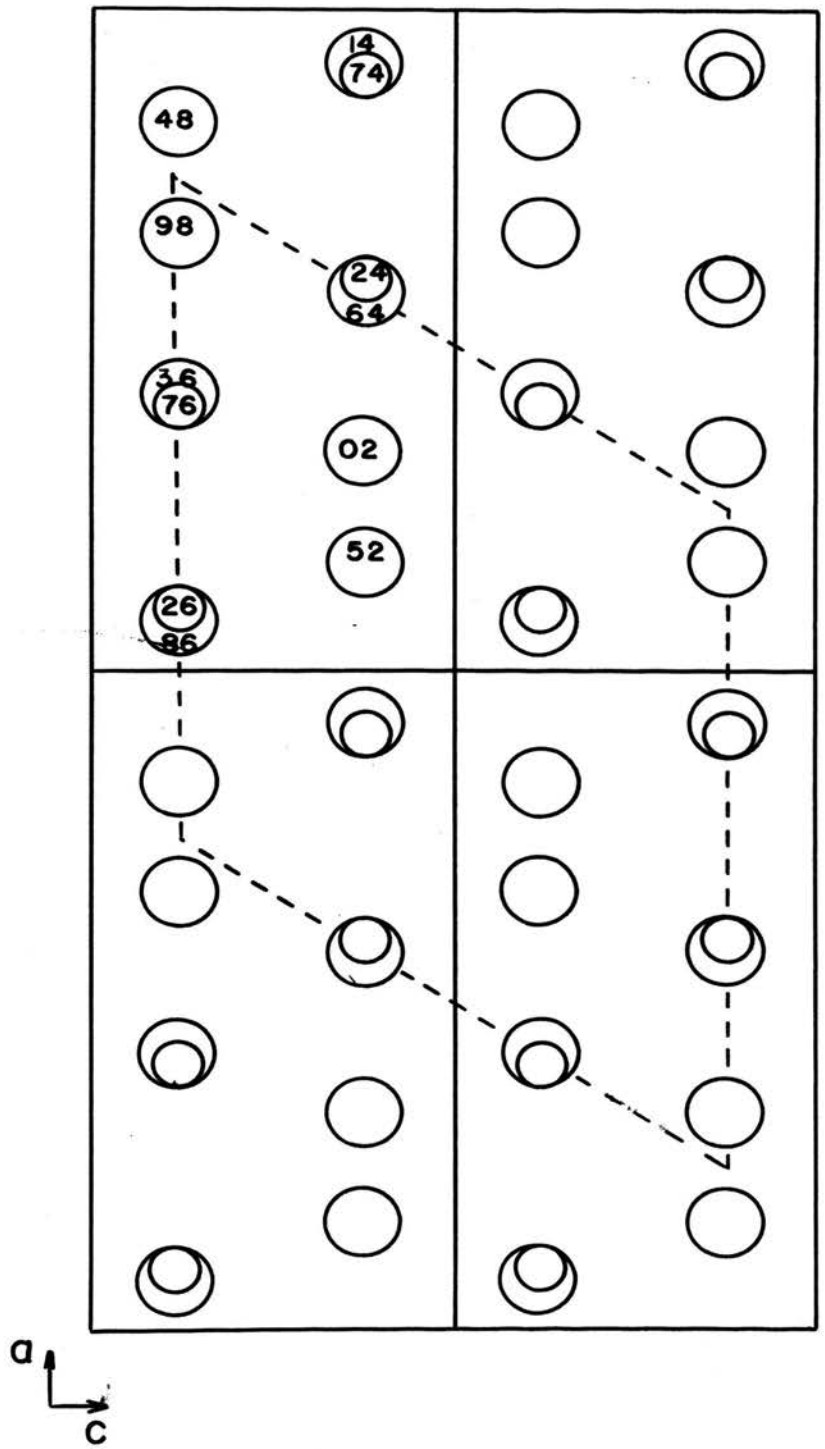

Figure 32. Projection of the Orthorhombic Lead Chloride Structure on (010) Plane Showing the Orientational Relationship with the (00.1) Plane of a Hexagonal Lattice

and anions in positions of space groups $P6_3/mmc$ and $P6_3mc$, and structure factors were calculated. Intensities of lines from 10° to 50° 2θ were calculated for all of the models, according to the expression,

$$I_{hkl} = |F|^2_{hkl} \quad pLp,$$

Where p is the multiplicity of the crystallographic form and Lp is the Lorentz-polarization factor for the diffractometer method. Scattering factors for strontium and chlorine atoms were obtained by linear interpolation from the tables of Cromer and Mann,[52] computed from numerical Hartree-Fock wave functions. All intensities for every model were calculated by using a computer program written by Smith[53] in 1963. The results show that the calculated relative intensities of lines for some models are not even close to the observed intensities. The atomic coordinates for the models exhibiting approximately correct values for most of the observed lines are contained in Table XIV. The calculated relative intensities for these models are listed in Table XV and compared with observed intensities. All relative intensities are based on the (22.0) line. The strong observed intensities for the (20.1), (30.1), (21.2), (10.3), and (20.3) lines of the hexagonal phase are not in agreement with calculated intensities for any model tested. Due to the limitation of time in this study, the refinement of the coordinates of cations and anions in these models can not be done. Unfortunately, the

TABLE XIV

Atomic Coordinates for Models

Every model has the same symmetry transformation of the atomic coordinates as the atomic coordinates as follows:

$x\ 2x\ z;\quad 2\bar{x}\ \bar{x}\ z;\quad x\ x\ z;$

$\bar{x}\ 2\bar{x}\ 1/2 + z;\quad 2x\ x\ 1/2 + 2;\quad \bar{x}\ x\ 1/2 + z$

Model No.	Space Group	Atom	Atom multiplier*	x	y	z
I	$P6_3/mmc$	Sr	1.0000	0.5	0.0	0.0
		Cl	0.3333	0.0	0.0	0.25
		Cl	0.3333	0.3333	0.8667	0.25
		Cl	0.3333	0.3333	0.6667	0.75
		Cl	1.0000	0.1667	0.3333	0.25
II	$P6_3mc$	Sr	1.0000	0.5	0.0	0.25
		Cl	0.3333	0.0	0.0	0.0
		Cl	0.3333	0.3333	0.6667	0.0
		Cl	0.3333	0.3333	0.6667	0.5

TABLE XIV (Cont.)

Model No.	Space Group	Atom	Atom multiplier*	x	y	z
		Cl	1.0000	0.1667	0.3333	0.125
III	$P6_3/mmc$	Sr	1.0000	0.5	0.0	0.25
		Cl	0.3333	0.0	0.0	0.0
		Cl	0.3333	0.3333	0.6667	0.0
		Cl	0.3333	0.3333	0.6667	0.5
		Cl	1.0000	0.1667	0.3333	0.25
IV	$P6_3/mmc$	Sr	1.0000	0.1667	0.3333	0.25
		Cl	0.3333	0.0	0.0	0.0
		Cl	0.3333	0.3333	0.6667	0.0
		Cl	0.3333	0.3333	0.6667	0.5
		Cl	1.0000	0.1667	0.3333	0.75
V	$P6_3mc$	Sr	1.0000	0.1667	0.3333	0.25
		Cl	0.3333	0.0	0.0	0.0
		Cl	0.3333	0.3333	0.6667	0.0

TABLE XIV (Cont.)

Model No.	Space Group	Atom	Atom multiplier*	x	y	z
		Cl	0.3333	0.3333	0.6667	0.5
		Cl	1.0000	0.1667	0.3333	0.625

* Atom multiplier is used to indicate fractional atoms distributed on a set of equivalent points.

TABLE XV

Relative Intensities Compared with the Observed

hkl	observed	Model I	Model II	Model III	Model IV	Model V
10.0	61	43	43	43	40	39
10.1	24	9	4	9	13	20
11.0	-	-	-	-	-	-
20.0	43	80	80	80	69	69
00.2	60	-	10	32	32	10
20.1	127	26	13	26	45	68
11.2	93	40	60	84	84	60
21.1		3	1	3	6	9
30.0	10	-	-	-	-	-
20.2	174	132	91	58	45	23
30.1	110	-	-	-	-	-
22.0	100	100	100	100	100	100

TABLE XV (Cont.)

hkl	observed	Model I	Model II	Model III	Model IV	Model V
21.2	72	19	13	9	7	3
10.3	93	1	-	1	2	8
31.0	5	4	4	4	3	3
30.2	-	17	25	35	35	25
31.1	-	1	-	1	3	4
20.3	60	5	2	5	12	51
40.0	2	13	13	13	10	10
22.2	69	2	14	36	36	14
40.1		4	2	4	10	14
31.2	13	10	7	5	3	2
21.3	2	1	-	1	2	8
32.0	16	2	2	2	2	2
32.1	13	1	-	1	2	2
30.3		-	-	-	-	-

TABLE XV (Cont.)

hkl	observed	Model I	Model II	Model III	Model IV	Model V
00.4	14	14	4	14	14	4

structure of this high temperature $SrCl_2$ is still doubtful. It can be said, however, that the calculated intensities indicate that the assumption of structural similarity between the hexagonal form of $SrCl_2$ and the orthorhombic, pseudohexagonal, $PbCl_2$ structure is valid. The possibility of preferred orientation and recrystallization of thin samples on the platinum strip complicates gathering of valid intensity data necessary for adequate structural analysis. Further effort should be expended to obtain better data using a bulk sample at elevated temperatures.

V. DISCUSSION AND CONCLUSIONS

A. Phase Transformations in Fluorite Structures

CaF_2 and BaF_2 The thermal expansion characteristics of CaF_2, BaF_2 and $SrCl_2$ are very similar. The structures expand normally at low temperatures and depart substantially from linearity at higher temperatures. The lower the melting point of the material is, the lower the temperature at which departure from linearity is observed. Abnormal deviation of expansion from linearity can probably be explained by the formation of defects[8] and by disordering of anions at higher temperatures.[6,11,19] Phase transformations in CaF_2 and BaF_2 were not observed because of reaction of these fluorides with water vapor as discussed in the previous section. The behavior of these materials at high temperature, however, can be related to that of $SrCl_2$, which showed the transformation from cubic to hexagonal structure.

$SrCl_2$ The structure of hexagonal $SrCl_2$ is assumed to be related to the orthorhombic, pseudohexagonal $PbCl_2$ structure, with higher molar volume. Efforts to examine this structure in detail were not successful, primarily because of the difficulty of obtaining data from thin samples at high temperatures. Several general conclusions can be drawn, however, from observed behavior. DTA studies of pure $SrCl_2$ show the initial transformation temperature, on heating, is about 670°C, with the

transformation proceeding over a 100°C temperature range. On cooling, the transformation begins as high as 780°C, continuing over a 200°C temperature range. High temperature X-ray studies of pure $SrCl_2$ indicate that above 480°C anions shift appreciably away from the 1/4 1/4 1/4 positions, resulting in development of faint lines in addition to those of the ideal fluorite structure. The intensities of the lines increase gradually between 480° and 660°C. Disordering of anions, as suggested by many investigators[6,11-13,20,26-30] is believed to be the major structural change occurring in this temperature range. Between 660° and 750°C two-phase coexistence, cubic and hexagonal, is observed. The hexagonal phase increases with increasing temperature and/or time, indicating a nucleation and crystal growth mechanism. The range of transformation, 660° to 750°C, agrees well with that observed by high-temperature calorimetry,[6-7,12,20] 667° to 767°C. It should be noted that the initial transformation temperature observed by DTA is higher than that observed by high temperature X-ray diffractometry because of the relatively high heating rate and the relatively slow nucleation and growth processes. Static methods, such as X-ray diffraction at constant temperature permit the high-temperature phase to nucleate and grow. During the transformation, the rate of expansion of cubic $SrCl_2$ seems to increase anomalously. This can be explained in terms of surface energy effects and a coherent interface with the

hexagonal phase.

The transformation of $SrCl_2$ can be discussed in terms of thermal vibrations of the atoms, which become increasingly anharmonic at higher temperature. Different crystal planes produce preferred vibrational modes and strain in the structure, as observed in neutron diffraction studies of some fluorite compounds,[21-24] which showed slight displacement of anion toward the centers of the interstitial holes at 1/2 1/2 1/2. The molar volume of the hexagonal form is larger than that of the cubic form, so that nucleation of the hexagonal structure in a cubic matrix would produce strain energy. Ubbelohde[54] pointed out that additional terms must be included in the fundamental free energy expressions to account for contributions of internal surface energy at domain boundaries and of the compressive or tensile energy present when a domain of one phase is nucleated within a matrix of the parent phase. On heating pure $SrCl_2$, domains of the less dense hexagonal phase grow under compression in a matrix of the cubic phase. The importance of domain boundary and strain energy is illustrated by the following observations. X-ray diffraction patterns of samples on the Pt strip-heater and of a thin pressed pellet showed that the hexagonal phases persist metastably on cooling. But X-ray patterns of thick pressed pellets or powder samples showed only cubic fluorite phases. Strain energy and/or interaction with the surface of the strip-heater hinders the hexagonal-cubic

transformation on cooling; grinding serves to relieve the strain energy, by forming new surfaces, and the transformation occurs. Quenching a thick pellet from the transformation range to room temperature, however, produces sufficient thermal stress to trigger the transformation, with the thermal stresses acting in the same way as grinding stresses.

$BaCl_2$ Since Gemsky[32] reported that the high-temperature form of $BaCl_2$ is singly-refracting, it has been assumed by subsequent investigators that the cubic structure is the stable form between 925°C and 960°C and that the cubic form produced by dissociation of the dihydrate at low temperatures is metastable. This investigation indicates, however, that in the temperature range 920°-960°C $BaCl_2$ has a liquid-like structure instead of presumed cubic fluorite structure. High temperature X-ray studies of the system $SrCl_2$-$BaCl_2$ show that orthorhombic solid solutions in the $BaCl_2$-rich portion of the system transforms to the hexagonal structure, as does $SrCl_2$. Vortisch,[39] and Schei and Flood[42] reported complete miscibility of the solid phases in this system at high temperatures, as was observed in this study. X-ray diffraction of $BaCl_2$ above 920°C showed two strong peaks at 20.17° and 30.38° 2θ, corresponding to the (20.0) and (30.0) lines of a hexagonal structure. DTA data from this study, ionic conductivity measurements,[38] and heat content measurements[6,12] indicated a first order transition at 920°C,

corresponding to an abrupt change in free energy.

Extrapolation of the Vegard's law plot of lattice parameters of hexagonal solid solutions in ths system $SrCl_2$-$BaCl_2$ (Figures 22 and 23) indicate that at 780°C hexagonal $BaCl_2$ has a=10.098 and c=7.721Å. The calculated density, 3.044 gm/cm^3, is less than the density of liquid $BaCl_2$, 3.160,[51] indicating that the hexagonal form has an open ordered structure and likely to form a liquid-like crystal at higher temperatures. On melting, the structure then loses long range order, becoming a disordered structure, a liquid, denser than the solid. This interpretation correlates well with ionic conductivity, observed by Derrington and O'Keeffe,[38] high for the high temperature phase, changing only slightly on melting.

Thermograms obtained on heating of $BaCl_2$ showed that, after several heating and cooling cycles, the two endothermic peaks for transformation and melting merge, forming one peak at about the transformation temperature. This may be attributed to an increase in defects with each cycle, causing the hexagonal structure to lose long-range order, becoming a liquid.

Cubic $BaCl_2$ was formed by heating the dihydrate of $BaCl_2$ in vacuum at 70°C, as described by Bracket et al.,[34] and by drying the aqueous solution of $BaCl_2$ on a glass slide in air. The cubic form persisted to about 165°C. Nucleation and grain growth appears to be an important feature of the cubic-orthorhombic transformation. The

orthorhombic form increased in quantity with increasing temperature and/or time.

The transformation of cubic fluorite compounds to an orthorhombic $PbCl_2$-type have been observed at high pressures by several investigators.[55-59] X-ray diffraction was used to study transformations of several fluorides at high pressure by Dandekar and Jamieson,[56] and by Smith and Chen.[57] Smith and Chen[57] reported that BaF_2 and SrF_2 transform from the fluorite structure to a structure of lower symmetry, orthorhombic, at about 30 K bar and 60 K-bar, respectively. Dandekar and Jamieson[56] reported the same and, in addition, that CaF_2 transforms at about 80 K bar. They also reported that the observed orthorhombic structure is the $PbCl_2$-type structure. Other investigators studied the transformation by measuring variations of refractive indices with pressure,[55] by measuring changes in dielectric constants (capacitance) and dielectric losses,[58] and by Raman Spectroscopy.[59] It was pointed out by Monberg and Nicol[60] that the two structures are related by a division of the ions in (111) cation planes of the fluorite structure into two equal groups and insertion of each group into adjacent but non-equivalent (111) anion planes to form the (001) planes of the orthorhombic structure, causing an increase of the cation near-neighbor coordination from 8 to 9. The details of this relationship are discussed in reference [59].

In 1970, Samara[58] studied the phase transition in BaF_2 by measuring changes in dielectric constants (capacitances) and dielectric losses as functions of pressure and temperature. He reported that, with increasing pressure at 22°C, the transition occurs at 26.8 K bar. The transition pressure decreases with increasing temperature, and at sufficiently high pressure the transition can be induced by raising the temperature. He also reported that the pressure hysteresis of the transition decreases with increasing temperature. The temperature dependence of the transition pressure of BaF_2 from Samara's work is shown in Figure 33. It can be seen that if the transition of BaF_2 occurred at the lower pressure at 22°C it would also occur at higher temperature at 1 atm. pressure. This shows conclusively that the cubic form of $BaCl_2$ is the stable low temperature form and that the orthorhombic form is the high-temperature form.

On a purely geometric basis, $BaCl_2$, with a 0.75 radius ratio,[4] should have occurred as a cubic fluorite structure at room temperature rather than as an orthorhombic $PbCl_2$ structure. Naray -Szabo[3] described orthorhombic $BaCl_2$ as a result of the large radius of Ba^{+2}, requiring a coordination higher than 8 as in the fluorite structure. It should be noted, however that BaF_2, with a 0.99 radius ratio,[4] is stable as the cubic fluorite structure rather than the orthorhombic $PbCl_2$ structure. Brackett et al.[34] described the orthorhombic $PbCl_2$-type

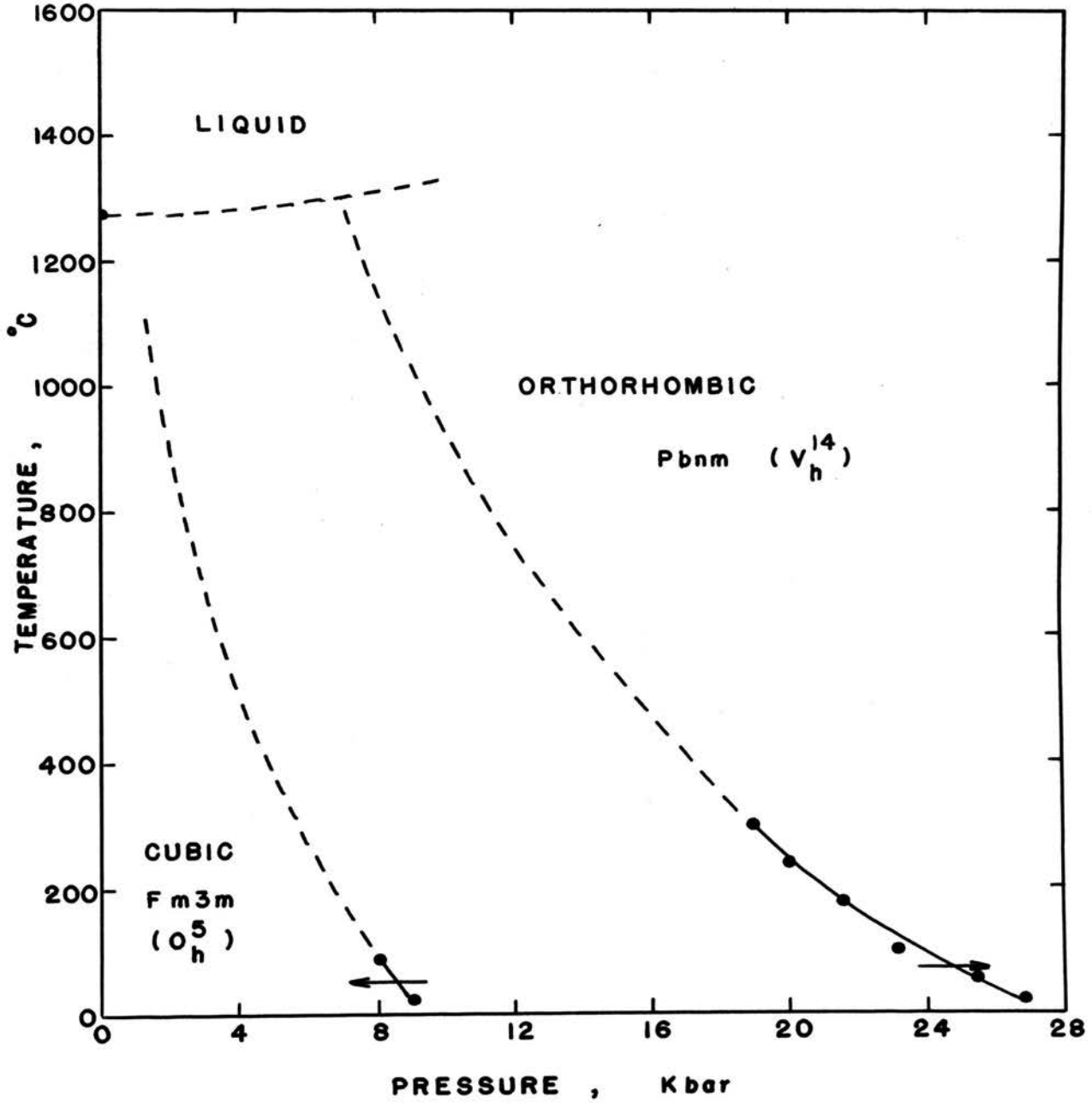

Figure 33. Temperature - Pressure Phase Diagram for BaF_2: From Samara[58] (1970)

structure, moreover, as having cations with only seven near anion neighbors, forming a trigonal pyramid, and with two other anions at much greater distances.

Further evidence of the stability of cubic $BaCl_2$ at low temperatures is the extrapolation of the lattice parameters of cubic solid solutions (Figure 34), showing that the extrapolated lattice constant for cubic $BaCl_2$ at 25°C is 7.316 Å, in excellent agreement with the observed value, 7.3145 Å. It is apparent therefore, that strong evidence exists for placing the transformation from cubic $BaCl_2$, stable at low temperatures, to orthorhombic $BaCl_2$ at approximately 165°C. Because of the molar volume relationships, however, with the low-temperature form being less dense, the orthorhombic form persists on cooling to room temperature. The stable cubic form can be formed only by heating $BaCl_2 \cdot 2H_2O$ in vacuum or by evaporating an aqueous solution on a glass slide or a Pt strip.

From this information, a reasonable conclusion can be drawn that $BaCl_2$ occurs in three forms: cubic, orthorhombic, and hexagonal. The cubic form is stable below about 165°C and transforms irreversibly to the orthorhombic form; at 920°C the orthorhombic form is changed to a highly disordered hexagonal form.

This interpretation of the cubic fluorite and orthorhombic $PbCl_2$ structures as the low-and high-temperature forms, respectively, leads to a conflict with the

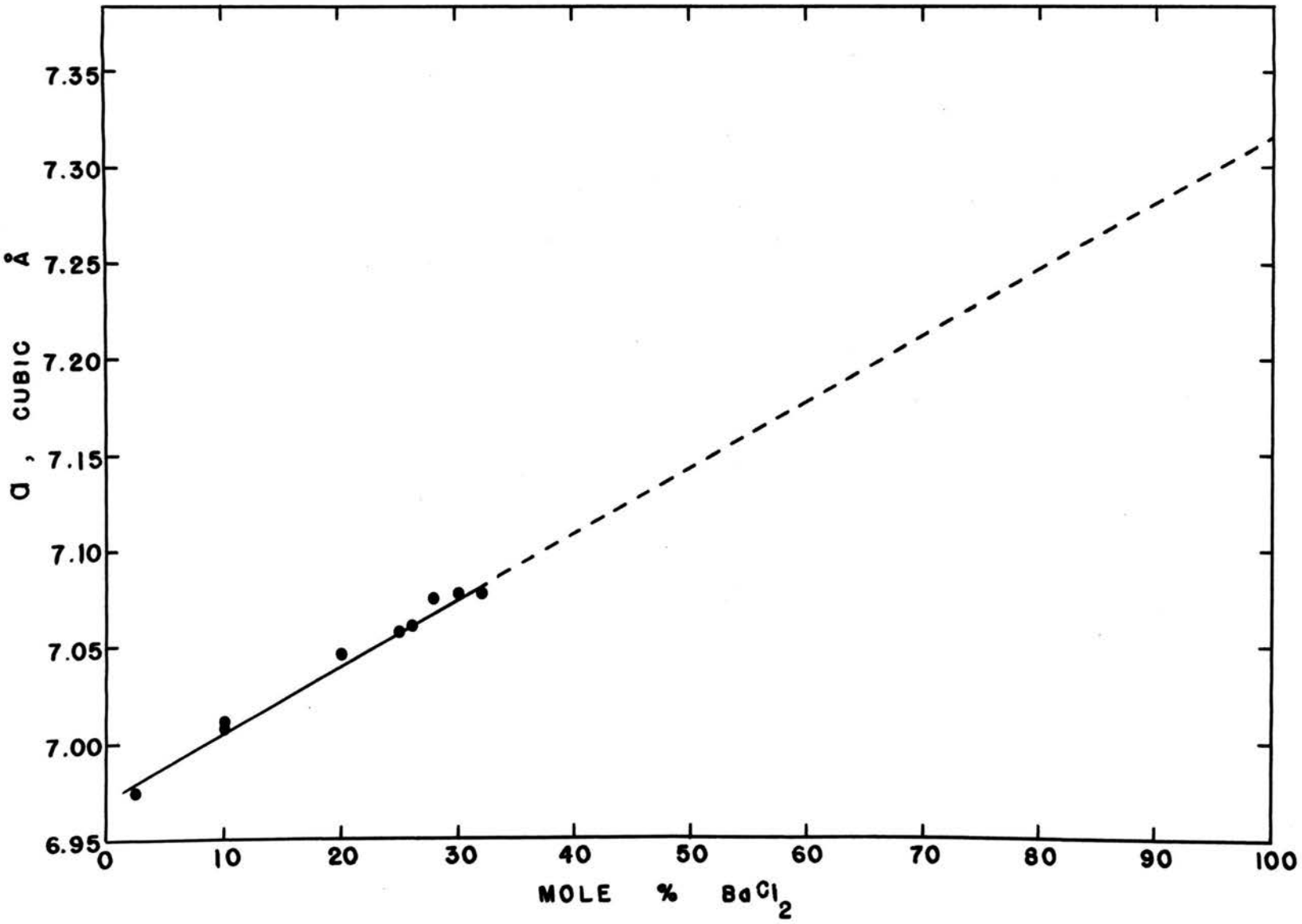

Figure 34. Extrapolation of the a Parameter of Cubic Solid Solutions in the System $SrCl_2$-$BaCl_2$

literature.[17,30,33-36,55-57,59-60] Several investigators[17,33-36] referred to the cubic $BaCl_2$ as a high temperature phase, even though they observed it at low temperature, simply because of Gemsky's work. Gemsky[32], in 1913, referred to the modification observed between 925° and 960°C as singly refracting; later investigators have apparently interpreted that to mean cubic. There is no doubt that this modification is a highly disordered hexagonal structure, similar to the hexagonal form of $SrCl_2$. Others[30,55-57,59-60] referred to the cubic fluorite phase on the basis of observations of PbF_2. It has been reported that there are two forms of PbF_2, cubic and orthorhombic.[61-62] The cubic form was reported as a high temperature form, with a transformation point at 315°C, by Sauka[61] in 1949. He also reported that the cubic form of PbF_2 can be obtained and maintained at lower temperature, as confirmed by several other investigators.[30,55,59] Schmidt and Vedam[55] suggested that the observed transformation of PbF_2 at 4.8 K bar at 23°C is a reversal of the transformation of the metastable cubic phase to the stable orthorhombic phase. Which form of PbF_2 is the stable form at low temperature remains in doubt. Temperature-pressure relationships for PbF_2 have not yet been studied. It can be concluded from the study that cubic fluorite compounds can change to the orthorhombic $PbCl_2$ structure, to a hexagonal structure, or to disordered structure, depending on pressure, temperature, and the chemistry of compound. At high temperatures,

defects in the form of vacancies play an important role in the solid-solid transformations and in melting. The transformations of these fluorite compounds occur by the changes in the coordination of the nearest neighbor (first coordination), resulting from movement of anions in the open fluorite structure.

B. $SrCl_2$-$BaCl_2$ Phase Relationships

X-ray analyses of heated and quenched samples revealed that $SrCl_2$ forms cubic solid solution with up to 25 mole percent $BaCl_2$ and orthorhombic solid solutions beyond 35 mole percent $BaCl_2$. The lattice parameters of cubic solid solutions are in good agreement with those reported by Brauer and Müller.[43] Between 25 mole percent and 35 mole percent $BaCl_2$ two phases, cubic and orthorhombic solid solutions, were observed. High temperature X-ray studies showed that at higher temperatures complete solid solution, having a hexagonal structure, occurs. Between 5 and 30°C below the fusion points, all samples in the system $SrCl_2$-$BaCl_2$, developed liquid-like crystals, with densities lower than the corresponding liquid phases.

Butler and Sorrell[63] state

> "In systems with two different metal ions in chemical combination with a common anion, subsolidus equilibrium depends on differences in metallic character of the cations, as indicated by electronegativities, ionic radii, etc. If the electronegativities are similar, as with Ba^{+2} and Sr^{+2}, complete solid solution is expected at all temperatures."

The system $SrCl_2$-$BaCl_2$ should, therefore, exhibit complete solid solution at all temperatures. Though $BaCl_2$ has three forms: cubic, orthorhombic, and hexagonal, there are only two forms in $SrCl_2$, cubic and hexagonal. Existence of orthorhombic $BaCl_2$ can be explained in terms of the polarizability of the Ba^{+2} ion. It is expected that at higher pressures cubic $SrCl_2$ would transform to the

orthorhombic structure, and at lower pressures the cubic $BaCl_2$ range should be wider.

Lattice parameters for cubic and orthorhombic solid solutions between 25 mole percent to 35 mole percent $BaCl_2$ are not quite constant, as expected for a stable two phase region. The intensities of the X-ray lines moreover were not observed to vary uniformly with composition making precise boundaries difficult to define. The non-uniformity of data within the two phase region is most likely the result of the presence of metastable orthorhombic phase. The phase diagram proposed for the system $SrCl_2$-$BaCl_2$, based on the experimental work reported here, is shown in Figure 35. Solid circles or squares represent data obtained on heating and open circles or squares represent those obtained on cooling. Event temperatures are listed in Table XIII. The data for the solidus line, obtained from temperatures of initial deviation from the base lines of thermograms, agree well with those of Vortisch,[39] and of Schei and Flood.[42] Transformation temperatures of the orthorhombic solid solutions, determined by DTA, are higher than expected. Transformation temperatures obtained from annealed orthorhombic solid solutions can be expected, however, to be lower.

At high temperatures the system shows complete miscibility in both liquid and solid phases, with a freezing point minimum of 845°C at about 28 mole percent $BaCl_2$. At lower temperatures, samples with more than

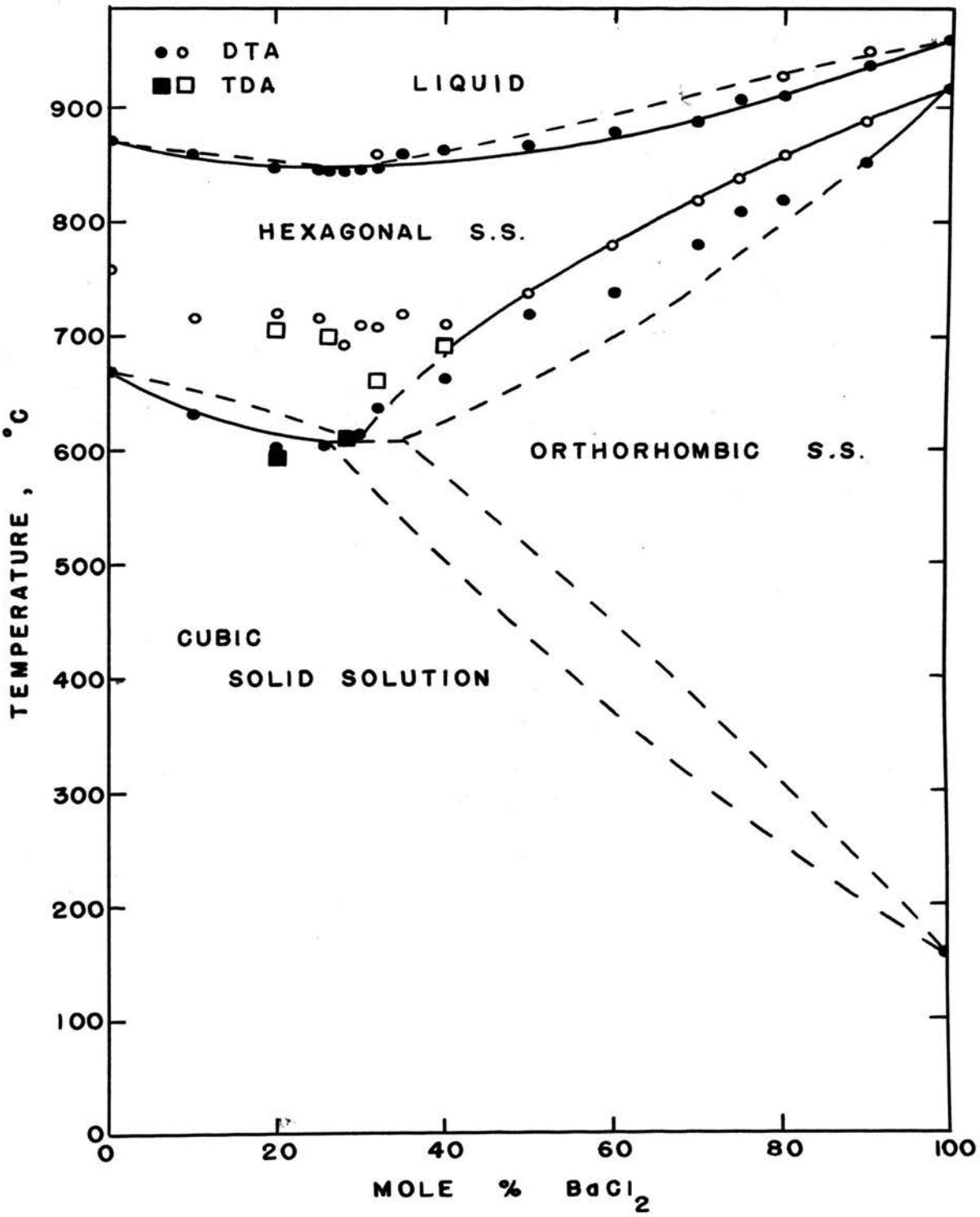

Figure 35. Proposed Phase Diagram of the System $SrCl_2$-$BaCl_2$

35 mole percent $BaCl_2$ form orthorhombic solid solutions and those with less than 25 mole percent $BaCl_2$ form cubic solid solutions. There are two phases with transformation temperatures at about 610°C in the region 25-35 mole percent $BaCl_2$. The orthorhombic solid solutions should transform to cubic solid solutions at lower temperatures, but they were not observed to do so. This is attributed to metastable persistence of orthorhombic solid solutions on cooling.

VI. APPENDICES

APPENDIX A

Thermal Expansion Data for Cubic Fluorite Type Materials and Orthorhombic $BaCl_2$

The tables included in this appendix contain raw and calculated data based on high temperature x-ray diffraction. The lattice parameter of the cubic phase is the average value calculated from the d-spacings of (111), (200), (220), and (311) lines. The lattice parameters of orthorhombic $BaCl_2$ are calculated directly from the d-spacings of the (200), (040), and (002) lines. The cooling data were obtained from samples not previously heated through the transformation range.

TABLE AI

Diffraction Angles, Interplanar Spacings, and Calculated Lattice Parameters of Cubic CaF_2

Temp., °C.	$2\theta_{111}$	$2\theta_{220}$	$2\theta_{311}$	d_{111}	d_{220}	d_{311}	a, Å
Heating Data							
25	28.30	47.06	55.81	3.1534	1.9310	1.6472	5.4617
100	28.24	46.97	55.71	3.1600	1.9344	1.6502	5.4731
200	28.17	46.87	55.58	3.1677	1.9383	1.6537	5.4847
300	28.10	46.73	55.45	3.1754	1.9438	1.6571	5.4960
400	28.05	46.62	55.30	3.1810	1.9483	1.6612	5.5096
500	27.97	46.50		3.1899	1.9529		5.5236
575	27.90	46.41	55.03	3.1977	1.9564	1.6687	5.5345
600	27.88	46.35		3.2000	1.9588		5.5403
675	27.84	46.27	54.89	3.2045	1.9621	1.6726	5.5480
700	27.80	46.19	54.80	3.2090	1.9653	1.6751	5.5560
750	27.78	46.16	54.73	3.2113	1.9665	1.6771	5.5621

TABLE AI (Cont.)

Temp.,°C.	$2\theta_{111}$	$2\theta_{220}$	$2\theta_{311}$	d_{111}	d_{220}	d_{311}	a,Å
800	27.72	26.08	54.63	3.2181	1.9697	1.6799	5.5723
850	27.69	46.00	54.53	3.2215	1.9729	1.6828	5.5805
875	27.65		54.50	3.2261		1.6836	5.5839
930	27.61		54.37	3.2306		1.6873	5.5960
950	27.59		54.34	3.2329		1.6882	5.5995
980	27.54		54.27	3.2387		1.6904	5.6064
1052	27.46		54.03	3.2479		1.6972	5.6289
1151	27.38		53.88	3.2573		1.7015	5.6420
Cooling Data							
750	27.78	46.14	54.73	3.2113	1.9673	1.6771	5.5620
650		46.29	54.89		1.9613	1.6726	5.5471
450	27.99	46.57		3.1876	1.9503		5.5163
350	28.09	46.69	55.37	3.1765	1.9454	1.6595	5.5024

TABLE AI (Cont.)

Temp.,°C.	$2\theta_{111}$	$2\theta_{220}$	$2\theta_{311}$	d_{111}	d_{220}	d_{311}	a,Å
250	28.15	46.80	55.52	3.1699	1.9408	1.6551	5.4897
150	28.19	46.89	55.62	3.1655	1.9375	1.6524	5.4801
50	28.27	47.01	55.76	3.1567	1.9329	1.6485	5.4675
25	28.28	47.04	55.80	3.1556	1.9317	1.6477	5.4637

TABLE AII

Diffraction Angles, Interplanar Spacings, and Calculated Lattice Parameters of Cubic BaF_2

Temp.,°C.	$2\theta_{111}$	$2\theta_{200}$	$2\theta_{220}$	d_{111}	d_{200}	d_{220}	a,Å
Heating Data							
28	24.875	28.80	41.175	3.5794	3.0998	2.1923	6.2000
86	24.835	28.75	41.135	3.5850	3.1051	2.1948	6.2088
170	24.79	28.715	41.055	3.5914	3.1088	2.1984	6.2181
200	24.775	28.685	41.04	3.5932	3.1120	2.1992	6.2227
278	24.745	28.65	40.97	3.5978	3.1157	2.2032	6.2315
360	24.68	28.59	40.885	3.6071	3.1221	2.2072	6.2442
400	24.67	28.56	40.835	3.6086	3.1253	2.2100	6.2506
454	24.62	28.52	40.79	3.6158	3.1296	2.2126	6.2592
500	24.62	28.51	40.76	2.6158	3.1307	2.2136	6.2614
550	24.56	28.45	40.695	3.6249	3.1369	2.2170	6.2738

TABLE AII (Cont.)

Temp.,°C.	$2\theta_{111}$	$2\theta_{200}$	$2\theta_{220}$	d_{111}	d_{200}	d_{220}	a,Å
568	24.555	28.425	40.665	3.6252	3.1398	2.2188	6.2760
600	24.53	28.41	40.64	3.6289	3.1415	2.2200	6.2804
650	24.49	28.37	40.58	3.6347	3.1456	2.2230	6.2912
688	24.48	28.34	40.53	3.6362	3.1491	2.2259	6.2960
700	24.465	28.325	40.50	3.6383	3.1507	2.2273	6.2998
750	24.44	28.30	40.45	3.6420	3.1534	2.2297	6.3065
760	24.43	28.27	40.43	3.6435	3.1567	2.2312	6.3108
800	24.40	28.25	40.37	2.6479	3.1589	2.2341	6.3178
850	24.36	28.23	40.34	3.6538	3.1618	2.2357	6.3238
860	24.36	28.20	40.32	3.6538	3.1644	2.2368	6.3281
900	24.31	28.12	40.225	3.6612	3.1732	2.2421	6.3416
935	24.265			3.6678			6.3528
950	24.245		40.125	3.6709		2.2472	6.3560

TABLE AII (Cont.)

Temp.,°C.	$2\theta_{111}$	$2\theta_{200}$	$2\theta_{220}$	d_{111}	d_{200}	d_{220}	a,Å
975			40.115			2.2483	6.3592
980			40.10			2.2485	6.3597
1000			40.065			2.2510	6.3668
1020	24.19		40.04	3.6791		2.2518	6.3724
1040	24.18		29.99	3.6807		2.2545	6.3767
1070	24.12			3.6896			6.3906
Cooling Data							
882			40.265			2.2403	6.3365
800	24.40	28.25	40.41	3.6479	3.1589	2.2325	6.3150
650	24.52		40.585	3.6303		2.228	6.2870
300	24.73	28.64	40.94	3.6000	3.1168	2.2043	6.2350

TABLE AIII

Diffraction Angles, Interplanar Spacings, and Calculated Lattice Parameters of Cubic $SrCl_2$

Temp., °C.	$2\theta_{111}$	$2\theta_{220}$	$2\theta_{311}$	d_{111}	d_{220}	d_{311}	a, Å
Heating Data							
25	22.07	36.43	43.01	4.0275	2.4662	2.1031	6.9758
48		36.40	42.97		2.4682	2.1048	6.9808
123		36.33	42.885		2.4727	2.1087	6.9940
160		36.295	42.85		2.4750	2.1104	6.9994
200	21.95	36.23	42.80	4.0492	2.4774	2.1127	7.0072
224		36.23	42.77		2.4795	2.1142	7.0120
268		36.175	42.705		2.4830	2.1172	7.0220
300	21.87	36.15	42.66	4.0638	2.4846	2.1193	7.0275
357		36.075	42.585		2.4896	2.1228	7.0405
380	21.83	36.045	42.55	4.0712	2.4916	2.1246	7.0465

TABLE AIII (Cont.)

Temp.,°C.	$2\theta_{111}$	$2\theta_{220}$	$2\theta_{311}$	d_{111}	d_{220}	d_{311}	a,Å
400	21.83	36.025	42.525	4.0712	2.4929	2.1257	7.0502
415	21.82	36.005	42.50	4.0730	2.4943	2.1270	7.0545
420	21.815	36.005	42.50	4.0739	2.4943	2.1270	7.0550
427	21.81	36.00	42.48	4.0749	2.4947	2.1278	7.0560
440	21.795	35.975	42.47	4.0776	2.4963	2.1284	7.0606
458	21.78	35.945	42.43	4.0804	2.4983	2.1303	7.0654
470	21.77	35.93	42.42	4.0823	2.4994	2.1308	7.0676
500	21.75	35.90	42.36	4.0860	2.5014	2.1337	7.0767
523	21.73	35.86	42.33	4.0897	2.5041	2.1351	7.0813
536	21.72	35.85	42.305	4.0916	2.5047	2.1363	7.0853
562	21.70	35.81	42.27	4.0953	2.5075	2.1380	7.0909
598	21.66	35.76	42.20	4.1028	2.5108	2.1414	7.1012
600		35.755	42.195		2.5111	2.1417	7.1030

TABLE AIII (Cont.)

Temp.,°C.	$2\theta_{111}$	$2\theta_{220}$	$2\theta_{311}$	d_{111}	d_{220}	d_{311}	a,Å
618		35.725	42.17		2.5132	2.1428	7.1080
638	21.62	35.69	42.13	4.1103	2.5156	2.1448	7.1135
650	21.62	35.67	42.10	4.1103	2.5169	2.1464	7.1188
665		35.65	42.07		2.5183	2.1477	7.1234
684		35.61	42.02		2.5211	2.1501	7.1304
698		35.57	41.97		2.5238	2.1526	7.1383
710		35.54	41.94		2.5259	2.1541	7.1443
720		35.51	41.90		2.5279	2.1560	7.1500
735		35.45			2.5321		7.1619
Cooling Data							
336	21.87	36.09	42.61	4.0638	2.4886	2.1217	7.0380
292		36.15	42.67		2.4846	2.1189	7.0276
245		36.20	42.73		2.4813	2.1160	7.0180

TABLE AIII (Cont.)

Temp.,°C.	$2\theta_{111}$	$2\theta_{220}$	$2\theta_{311}$	d_{111}	d_{220}	d_{311}	a,Å
174		36.27	42.825		2.4767	2.1115	7.0031
100		36.355	42.92		2.4711	2.1071	6.9893
25	22.07	36.43	43.01	4.0275	2.4662	2.1031	6.9758

TABLE AIV

Diffraction Angles and Interplanar Spacings of the (200), (002), and (040) Lines of Orthorhombic $BaCl_2$

Temp., °C.	$2\theta_{200}$	$2\theta_{002}$	$2\theta_{040}$	d_{200}	d_{002}	d_{040}
Heating Data						
25	22.60	38.00	38.20	3.9342	2.3678	2.3559
125	22.51	37.84	38.07	3.9497	2.3775	2.3636
202	22.44	27.75	38.00	3.9619	2.3829	2.3678
303	22.32	37.63	37.99	3.9829	2.3903	2.3684
330	22.28	37.61	37.93	3.9900	2.3915	2.3720
388	22.25	37.51	37.90	3.9953	2.3976	2.3738
462	22.19	37.39	37.85	4.0059	2.4050	2.3769
573	22.11	37.21	37.78	4.0203	2.4163	2.3811
686	21.98	37.00	37.70	4.0437	2.4295	2.3862
785	21.92	36.81	37.60	4.0547	2.4416	2.3921

TABLE AIV (Cont.)

Temp., °C.	$2\theta_{200}$	$2\theta_{002}$	$2\theta_{040}$	d_{200}	d_{002}	d_{040}
871	21.82			4.0730		
Cooling Data						
638	22.05	37.08	37.69	4.0311	2.4244	2.3866
498	22.09	37.23	37.79	4.0239	2.4150	2.3805
286	22.27	37.57	37.92	3.9917	2.3939	2.3726

TABLE AV

Calculated Lattice Parameters for Orthorhombic $BaCl_2$

Based on Data of Table AIV

Temp., °C.	a, Å	b, Å	c, Å
Heating Data			
25	7.8684	9.4236	4.7356
125	7.8994	9.4544	4.7550
202	7.9238	9.4712	4.7658
303	7.9658	9.4736	4.7806
330	7.9800	9.4880	4.7830
388	7.9906	9.4952	4.7952
462	8.0118	9.5076	4.8100
573	8.0406	9.5244	4.8326
686	8.0874	9.5448	4.8590
785	8.1094	9.5684	4.8832

TABLE AV (Cont.)

Temp., °C.	a, Å	b, Å	c, Å
871	8.1460		
Cooling Data			
638	8.0622	9.5464	4.8488
498	8.0478	9.5220	4.8300
286	7.9834	9.4904	4.7878

TABLE AVI

Diffraction Angles, Interplanar Spacings, and Calculated Lattice Parameters of Cubic $BaCl_2$

Temp., °C.	$2\theta_{111}$	$2\theta_{220}$	$2\theta_{311}$	d_{111}	d_{220}	d_{311}	a, Å
Heating Data							
25	21.02	34.68	40.92	4.2262	2.5865	2.2054	7.3145
68	20.99	34.63	40.86	4.2322	2.5901	2.2085	7.3248
110	20.98	34.60	40.82	4.2342	2.5923	2.2105	7.3314
136	20.95	34.58	40.79	4.2402	2.5938	2.2121	7.3367
160	20.94	34.56	40.77	4.2422	2.5952	2.2131	7.3400
180	20.935	34.54	40.75	4.2432	2.5967	2.2142	7.3432
206	20.92	34.52	40.72	4.2442	2.5981	2.2157	7.3486
230	20.91	34.49	40.69	4.2482	2.6003	2.2173	7.3539
247		34.48	40.67		2.6011	2.2183	7.3573
264		34.46	40.66		2.6025	2.2189	7.3597

TABLE AVI (Cont.)

Temp.,°C.	$2\theta_{111}$	$2\theta_{220}$	$2\theta_{311}$	d_{111}	d_{220}	d_{311}	a,Å
282		34.44	40.63		2.6040	2.2204	7.3636
303		34.42	40.61		2.6055	2.2215	7.3680
330		34.39			2.6077		7.3757
Cooling Data							
188		34.53	40.73		2.5974	2.2152	7.3468
150		34.57	40.79		2.5945	2.2121	7.3367
96		34.62	40.85		2.5909	2.2090	7.3264
46		34.67	40.91		2.5872	2.2059	7.3161

APPENDIX B

X-Ray Patterns of Cubic Fluorite Type Materials

X-ray patterns of CaF_2, BaF_2, $SrCl_2$, and $BaCl_2$ are contained in this appendix. All patterns were obtained by scanning the samples at room temperature, using CuKα radiation.

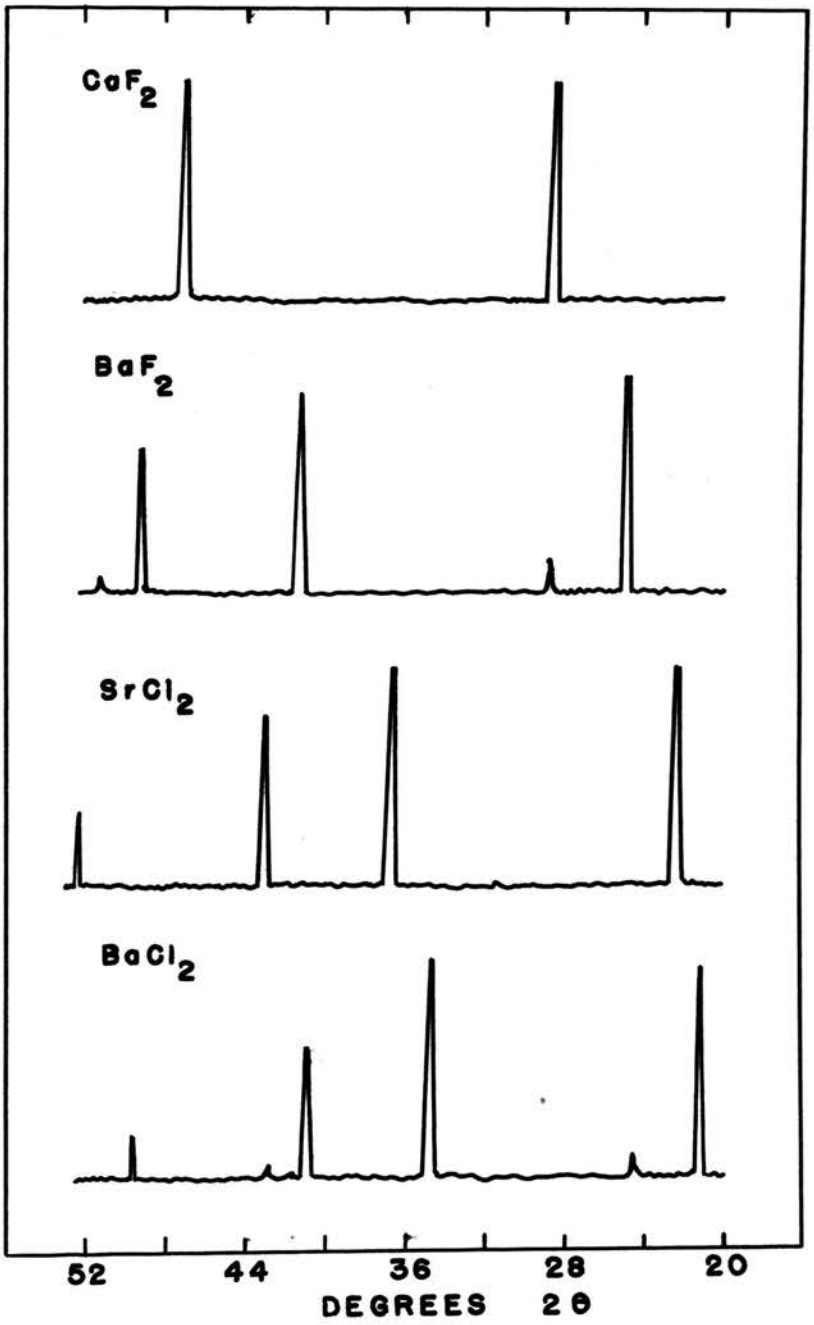

Figure B1. X-Ray Diffraction Patterns for CaF_2 BaF_2, $SrCl_2$, and Cubic $BaCl_2$; CuKα Radiation

APPENDIX C

Thermal Expansion Data for Hexagonal $SrCl_2$

TABLE CI

Diffraction Angles, Interplanar Spacings, and Calculated Lattice Parameters of Hexagonal $SrCl_2$

Temp.,°C.	$2_{20.0}$	$2_{00.2}$	$d_{20.0}$	$d_{00.2}$	a,Å	c,Å
Heating Data						
25	21.66	24.68	4.1028	3.6071	9.4750	7.2142
354	21.50	24.49	4.1329	3.6347	9.5445	7.2694
523	21.41	24.38	4.1501	3.6508	9.5842	7.3016
716	21.35	24.26	4.1616	3.6686	9.6108	7.3372
723	21.32	24.23	4.1674	3.6731	9.6242	7.3462
730	21.30	24.22	4.1713	3.6746	9.6332	7.3492
750	21.31	24.23	4.1693	3.6731	9.6286	7.3462
770	21.28	24.21	4.1752	3.6761	9.6422	7.3522
780	21.28	24.16	4.1752	3.6836	9.6422	7.3672
820	21.27	24.16	4.1771	3.6836	9.6466	7.3672

TABLE CI (Cont.)

Temp.,°C.	$2\theta_{20.0}$	$2\theta_{00.2}$	$d_{20.0}$	$d_{00.2}$	a,Å	c,Å
830	21.25	24.14	4.1810	3.6866	9.6556	7.3732
840	21.26	24.10	4.1790	3.6926	9.6510	7.3852
860	21.24	24.12	4.1829	3.6896	9.6600	7.3792
Cooling Data						
740	21.31	24.23	4.1693	3.6731	9.6286	7.3462
697	21.33	24.31	4.1655	3.6612	9.6198	7.3224
650	21.34	24.30	4.1635	3.6627	9.6152	7.3254
630	21.36	24.28	4.1597	3.6656	9.6064	7.3312
600	21.37	24.33	4.1578	3.6582	9.6020	7.3164
570	21.40	24.33	4.1520	3.6582	9.5886	7.3164
500	21.43	24.39	4.1463	3.6494	9.5755	7.2988
440	21.46	24.44	4.1405	3.6420	9.5621	7.2840
302	21.54	24.51	4.1253	3.6318	9.5270	7.2636

TABLE CI (Cont.)

Temp., °C.	$2\theta_{20.0}$	$2\theta_{00.2}$	$d_{20.0}$	$d_{00.2}$	a, Å	a, Å
290	21.53	24.48	4.1272	3.6362	9.5314	7.2724
122	21.61	24.65	4.1121	3.6115	9.4990	7.2230

APPENDIX D

Calculated Molar Volumes of Cubic and Hexagonal $SrCl_2$

TABLE DI

Lattice Parameters and Calculated Molar Volume Data for Cubic $SrCl_2$

Temp., °C.	a, Å	Molar Volume, cm^3/mole
25	6.9758	51.110
123	6.9940	51.511
200	7.0072	51.803
263	7.0220	52.132
357	7.0405	52.545
400	7.0502	52.763
470	7.0676	53.155
523	7.0813	53.464
562	7.0909	53.682
600	7.1030	53.957
638	7.1135	54.197
665	7.1234	54.423
698	7.1383	54.766
710	7.1443	54.904
720	7.1500	55.035
735	7.1619	55.311

TABLE DII

Lattice Parameters and Calculated Molar Volume Data for Hexagonal $SrCl_2$

Temp., °C	a, Å	c, Å	Molar Volume, cm^3/mole
25	9.4750	7.2142	56.299
122	9.4990	7.2230	56.653
302	9.5270	7.2636	57.308
440	9.5621	7.2840	57.893
500	9.5755	7.2988	58.174
600	9.6020	7.3164	58.637
697	9.6198	7.3224	58.903
716	9.6108	7.3372	58.912
730	9.6332	7.3492	59.283
750	9.6286	7.3462	59.202
770	9.6422	7.3522	59.418
780	9.6422	7.3672	59.540
820	9.6466	7.3672	59.594
830	9.6556	7.3732	59.754
840	9.6510	7.3852	59.794
860	9.6600	7.3792	59.857

APPENDIX E

Thermal Expansion Data for the System $SrCl_2$-$BaCl_2$

All of the thermal expansion data, determined by thermodilatometric analysis, for the system $SrCl_2$-$BaCl_2$ are contained in this appendix. The plots of L_T/L_{25} versus temperature for second runs of the samples with 30 mole percent and 32 mole percent $BaCl_2$ are also included. Preliminary heating temperatures and times, and sample lengths at room temperature are indicated.

TABLE EI

Dilatometry Data of $SrCl_2$ Preheated at 800°C. for 24 hours; Sample 0.309 in. at 25°C.

Heating Temp., °C.	L_T/L_{25}	Cooling Temp., °C.	L_T/L_{25}
25	1.00000		
100	1.00099		
123	1.00149		
151	1.00228		
160	1.00270		
173	1.00297		
176	1.00323		
192	1.00369		
204	1.00383		
213	1.00422		
221	1.00445		
238	1.00507		
243	1.00524		
250	1.00534		
258	1.00547		
274	1.00577		
293	1.00617		
298	1.00636		
305	1.00663		
313	1.00683		

TABLE EI (Cont.)

Heating Temp.,°C.	L_T/L_{25}	Cooling Temp.,°C.	L_T/L_{25}
327	1.00712		
434	1.00944		
445	1.00968		
460	1.00984		
478	1.01015		
496	1.01050		
511	1.01071		
523	1.01092		
537	1.01105		
541	1.01132		
564	1.01155		
577	1.01172		
586	1.01182		
605	1.01196		
621	1.01200		
629	1.01165		
632	1.01136		
640	1.01107		
646	1.01075		
652	1.01036		
664	1.00995		
674	1.00970		
686	1.00954		

TABLE EI (Cont.)

Heating Temp.,°C.	L_T/L_{25}	Cooling Temp.,°C.	L_T/L_{25}
695	1.00945		
700	1.00900		
714	1.00920		
722	1.00965		
729	1.00982		
734	1.00995		
761	1.00903		
764	1.00777		
770	1.00628		
773	1.00440		

TABLE EII

Dilatometry Data of Rerun of $SrCl_2$ Sample Previously Heated (Table EI), Containing Metastable Hexagonal Form; Sample 0.315 in. at 25°C.

Heating Temp.,°C.	L_T/L_{25}	Cooling Temp.,°C.	L_T/L_{25}
66	1.00041	741	1.01247
94	1.00027	735	1.01187
115	1.00066	727	1.01148
131	1.00105	715	1.01071
146	1.00150	703	1.01020
162	1.00180	687	1.00949
174	1.00212	679	1.00888
184	1.00238	669	1.00834
189	1.00254	663	1.00789
202	1.00290	652	1.00744
209	1.00303	647	1.00880
217	1.00325	633	1.00664
224	1.00338	620	1.00600
238	1.00361	605	1.00542
244	1.00384	592	1.00490
265	1.00442	581	1.00452
276	1.00465	572	1.00416
291	1.00494	548	1.00367
301	1.00514	539	1.00332
343	1.00595	532	1.00303

TABLE EII (Cont.)

Heating Temp., °C.	L_T/L_{25}	Cooling Temp., °C.	L_T/L_{25}
351	1.00605	522	1.00265
361	1.00640	512	1.00229
376	1.00651	503	1.00210
394	1.00693	495	1.00184
412	1.00748	487	1.00158
423	1.00774	480	1.00139
432	1.00793	471	1.00122
438	1.00806	462	1.00093
467	1.00906	391	0.99931
488	1.00945	384	0.99905
503	1.00984	371	0.99886
516	1.01020	352	0.99815
528	1.01055	341	0.99779
536	1.01075		
549	1.01098		
578	1.01182		
589	1.01208		
601	1.01234		
614	1.01263		
616	1.01279		
636	1.01289		
648	1.01306		
661	1.01335		

TABLE EII (Cont.)

Heating Temp., °C.	L_T/L_{25}	Cooling Temp., °C.	L_T/L_{25}
670	1.01367		
683	1.01374		
690	1.01387		
717	1.01452		
723	1.01475		
743	1.01476		
757	1.01404		

TABLE EIII

Dilatometry Data of $BaCl_2$ Preheated at 800°C. for 24 hours; Sample 0.308 in. at 25°C.

Heating Temp.,°C.	L_T/L_{25}	Cooling Temp.,°C.	L_T/L_{25}
72	1.00039	766	1.01526
160	1.00310	758	1.01483
172	1.00330	752	1.01454
183	1.00357	746	1.01411
191	1.00380	741	1.01392
200	1.00403	727	1.01358
211	1.00423	705	1.01300
220	1.00446	690	1.01240
230	1.00473	671	1.01170
241	1.00499	662	1.01141
268	1.00556	647	1.01088
282	1.00592	631	1.01039
289	1.00602	605	1.00959
302	1.00639	595	1.00952
312	1.00662	584	1.00903
323	1.00688	574	1.00854
337	1.00722	564	1.00840
347	1.00751	550	1.00797
359	1.00781	537	1.00758
378	1.00821	530	1.00728
399	1.00864	512	1.00688

TABLE EIII (Cont.)

Heating Temp.,°C.	L_T/L_{25}	Cooling Temp.,°C.	L_T/L_{25}
405	1.00874	458	1.00578
415	1.00911	448	1.00555
423	1.00934	442	1.00535
435	1.00957	434	1.00512
443	1.00977	410	1.00456
454	1.01000		
468	1.01037		
488	1.01080		
514	1.01133		
526	1.01163		
540	1.01200		
557	1.01220		
580	1.01270		
596	1.01288		
624	1.01351		
655	1.01378		
664	1.01400		
680	1.01411		
708	1.01461		
718	1.01488		
732	1.01505		
746	1.01518		
756	1.01525		

TABLE EIII (Cont.)

Heating Temp.,°C.	L_T/L_{25}	Cooling Temp.,°C.	L_T/L_{25}
771	1.01539		
777	1.01540		

TABLE EIV

Dilatometry Data of 20 mole percent $BaCl_2$ Sample Preheated at 800°C. for 24 hours;
Sample 0.326 in. at 25°C.

Heating Temp.,°C.	L_T/L_{25}	Cooling Temp.,°C.	L_T/L_{25}
66	1.00040	761	1.01655
113	1.00110	740	1.01562
153	1.00210	721	1.01469
185	1.00282	710	1.01444
199	1.00317	693	1.01354
216	1.00376	670	1.01215
240	1.00438	660	1.01162
260	1.00492	645	1.01033
288	1.00579	638	1.00956
301	1.00616	632	1.00928
329	1.00676	623	1.00857
346	1.00723	613	1.00786
363	1.00761	601	1.00699
381	1.00811	595	1.00680
398	1.00858	586	1.00625
416	1.00901	574	1.00563
437	1.00949	561	1.00501
452	1.00983	546	1.00436
477	1.01036	541	1.00429
495	1.01093	526	1.00361

TABLE EIV (Cont.)

Heating Temp., °C.	L_T/L_{25}	Cooling Temp., °C.	L_T/L_{25}
519	1.01164	512	1.00299
534	1.01208	496	1.00240
559	1.01258	480	1.00181
571	1.01299	476	1.00168
586	1.01343	464	1.00128
602	1.01399	439	1.00047
622	1.01479		
631	1.01520		
640	1.01566		
650	1.01613		
662	1.01665		
670	1.01706		
681	1.01752		
692	1.01814		
705	1.01879		
717	1.01935		
730	1.01979		
744	1.02001		
754	1.01983		
761	1.01904		
763	1.01741		

TABLE EV

Dilatometry Data of 26 mole percent $BaCl_2$ Sample Preheated at 800°C. for 24 hours;
Sample 0.284 in. at 25°C.

Heating Temp.,°C.	L_T/L_{25}	Cooling Temp.,°C.	L_T/L_{25}
83	1.00036	786	1.02223
123	1.00108	780	1.02170
138	1.00183	774	1.02113
158	1.00212	761	1.02028
178	1.00238	754	1.02003
193	1.00249	746	1.01946
213	1.00300	740	1.01904
255	1.00411	730	1.01851
284	1.00486	711	1.01779
305	1.00537	700	1.01726
332	1.00598	692	1.01704
371	1.00656	681	1.01633
387	1.00699	669	1.01566
416	1.00764	656	1.01481
439	1.00800	642	1.01416
462	1.00847	633	1.01384
490	1.00909	624	1.01335
514	1.00959	614	1.01264
541	1.01004	599	1.01192
555	1.01040	586	1.01121
570	1.01070	584	1.01107

TABLE EV (Cont.)

Heating Temp.,°C.	L_T/L_{25}	Cooling Temp.,°C.	L_T/L_{25}
588	1.01100	566	1.00976
602	1.01140	557	1.00908
618	1.01197	543	1.00827
639	1.01304	540	1.00816
643	1.01318	528	1.00745
662	1.01565	519	1.00692
671	1.01654	508	1.00642
674	1.01742	497	1.00592
678	1.01809	479	1.00517
684	1.01908	472	1.00485
688	1.02003	465	1.00460
691	1.02025	454	1.00414
696	1.02053	442	1.00375
702	1.02099	429	1.00321
707	1.02142	408	1.00250
720	1.02184	397	1.00217
732	1.02217	390	1.00199
750	1.02242	372	1.00146
759	1.02264	361	1.00099
772	1.02286		
785	1.02304		
790	1.02304		

TABLE EVI

Dilatometry Data of 28 mole percent $BaCl_2$ sample preheated at 800°C. for 24 hours;
Sample 0.322 in. at 25°C.

Heating Temp.,°C.	L_T/L_{25}	Cooling Temp.,°C.	L_T/L_{25}
55	1.00040		
91	1.00098		
128	1.00165		
168	1.00248		
205	1.00296		
222	1.00362		
238	1.00413		
257	1.00463		
280	1.00508		
300	1.00565		
311	1.00597		
327	1.00635		
341	1.00663		
363	1.00708		
383	1.00737		
405	1.00778		
425	1.00823		
443	1.00855		
472	1.00906		
486	1.00935		

TABLE EVI (Cont.)

Heating Temp.,°C.	L_T/L_{25}	Cooling Temp.,°C.	L_T/L_{25}
533	1.01052		
546	1.01090		
576	1.01129		
596	1.01158		
624	1.01131		
633	1.01082		
640	1.01026		
647	1.00983		
653	1.00971		
660	1.00971		
664	1.01009		
669	1.01056		
671	1.01115		
674	1.01177		
680	1.01243		
683	1.01324		
686	1.01420		
689	1.01420		
691	1.01628		
694	1.01725		
697	1.01787		
702	1.01840		
707	1.01865		

TABLE EVII

Dilatometry Data of 30 mole percent $BaCl_2$ Sample Preheated at 815°C. for 8 hours;

Sample 0.351 in. at 25°C.

Heating Temp., °C.	L_T/L_{25}	Cooling Temp., °C.	L_T/L_{25}
94	1.00067		
125	1.00115		
147	1.00181		
153	1.00201		
161	1.00236		
191	1.00300		
202	1.00324		
218	1.00353		
240	1.00394		
263	1.00441		
286	1.00490		
309	1.00528		
325	1.00586		
356	1.00656		
377	1.00703		
412	1.00776		
431	1.00820		
459	1.00861		
486	1.00925		
514	1.00995		
540	1.01053		

TABLE EVII (Cont.)

Heating Temp.,°C.	L_T/L_{25}	Cooling Temp.,°C.	L_T/L_{25}
574	1.01072		
600	1.01042		
610	1.00957		
614	1.00909		
618	1.00886		
624	1.00798		
630	1.00710		
635	1.00670		
640	1.00551		
642	1.00466		
647	1.00372		
652	1.00307		
565	1.00258		
664	1.00202		
683	1.00268		
687	1.00325		
693	1.00383		
695	1.00406		
698	1.00431		
701	1.00483		
704	1.00523		
707	1.00557		
710	1.00577		

TABLE EVII (Cont.)

Heating Temp., °C.	L_T/L_{25}	Cooling Temp., °C.	L_T/L_{25}
712	1.00592		
721	1.00575		
731	1.00499		
733	1.00442		
737	1.00408		

TABLE EVIII

Dilatometry Data for 30 mole percent $BaCl_2$ Sample after the Previous Run (Table EVII);
Sample 0.292 in. at 25°C.

Heating Temp., °C.	L_T/L_{25}	Cooling Temp., °C.	L_T/L_{25}
75	1.00062		
131	1.00147		
153	1.00193		
188	1.00249		
202	1.00267		
211	1.00292		
222	1.00347		
245	1.00410		
275	1.00476		
292	1.00518		
339	1.00599		
362	1.00669		
399	1.00757		
414	1.00809		
433	1.00861		
458	1.00927		
471	1.00949		
500	1.01019		
514	1.01060		
533	1.01113		

TABLE EVIII (Cont.)

Heating Temp., °C.	L_T/L_{25}	Cooling Temp., °C.	L_T/L_{25}
565	1.01152		
578	1.01180		
593	1.01194		
619	1.01199		
631	1.01152		
649	1.01112		
657	1.01081		
674	1.01062		
683	1.01107		
690	1.01169		
695	1.01251		
699	1.01303		
702	1.01358		
704	1.01457		
708	1.01556		
713	1.01646		
717	1.01660		
725	1.01712		
735	1.01678		
737	1.01647		
742	1.01616		
750	1.01521		
755	1.01436		

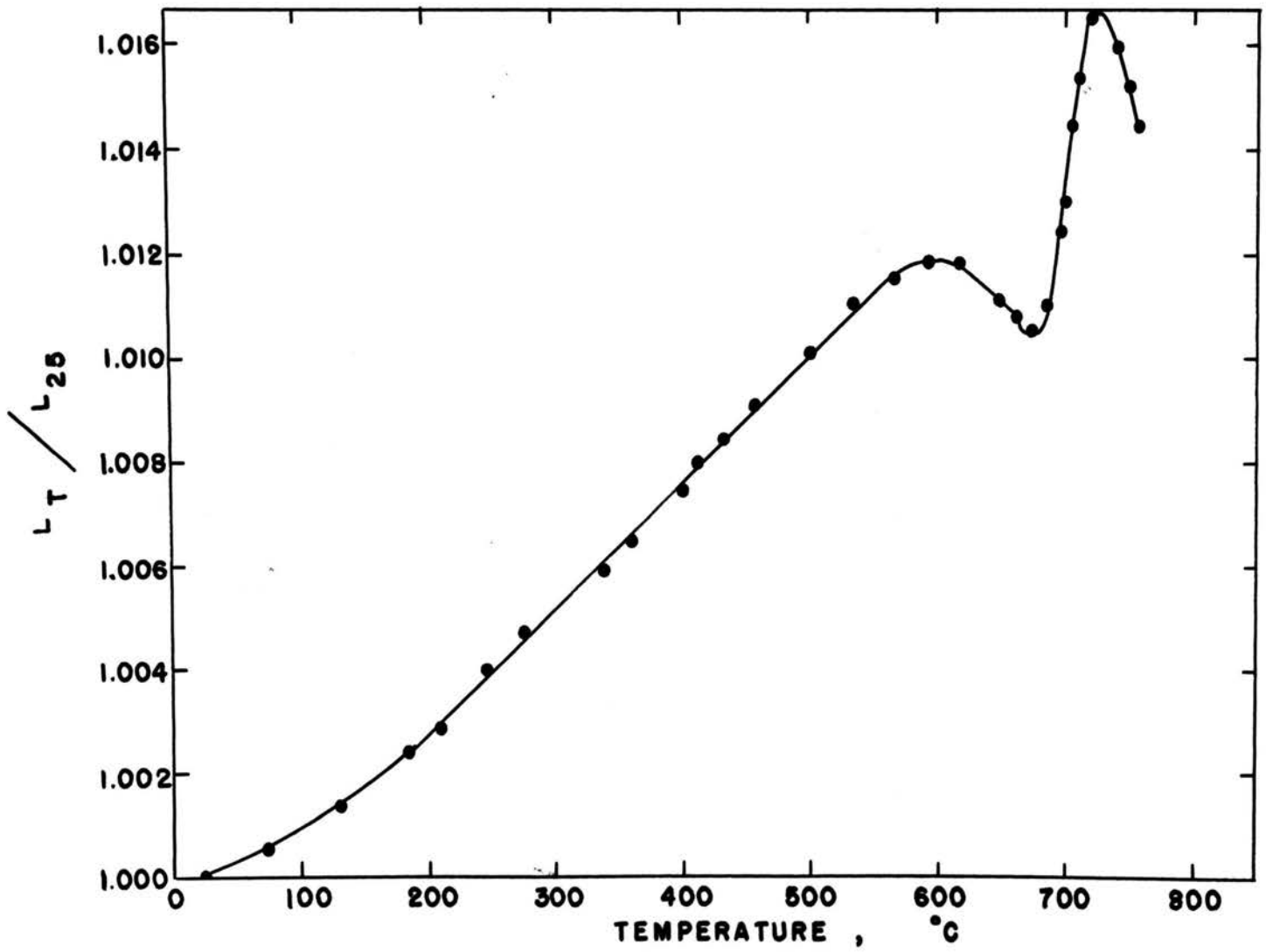

Figure E1. Thermal Expansion of 30 mole % $BaCl_2$ Sample on the Second Run Measured by TDA

TABLE EIX

Dilatometry Data of 32 mole percent $BaCl_2$ Sample Preheated at 815°C. for 8 hours;
Sample 0.365 in. at 25°C.

Heating Temp.,°C.	L_T/L_{25}	Cooling Temp.,°C.	L_T/L_{25}
57	1.00038		
105	1.00123		
131	1.00179		
146	1.00226		
166	1.00255		
184	1.00322		
209	1.00372		
235	1.00445		
263	1.00534		
274	1.00555		
288	1.00593		
301	1.00634		
312	1.00665		
327	1.00710		
341	1.00749		
366	1.00800		
378	1.00814		
399	1.00834		
406	1.00851		
419	1.00862		

TABLE EIX (Cont.)

Heating Temp.,°C.	L_T/L_{25}	Cooling Temp.,°C.	L_T/L_{25}
435	1.00882		
455	1.00927		
473	1.00945		
497	1.00968		
535	1.00989		
579	1.00988		
596	1.00989		
608	1.00957		
619	1.00894		
630	1.00826		
637	1.00821		
642	1.00780		
652	1.00737		
660	1.00710		
668	1.00782		
673	1.00861		
676	1.01048		
680	1.01136		
682	1.01232		
685	1.01336		
687	1.01410		
692	1.01684		
697	1.01959		

TABLE EIX (Cont.)

Heating Temp.,°C.	L_T/L_{25}	Cooling Temp.,°C.	L_T/L_{25}
700	1.02035		
704	1.02118		
710	1.02143		
724	1.02083		
730	1.02048		
737	1.01961		
740	1.01933		
745	1.01854		
750	1.01791		
753	1.01737		
756	1.01699		
760	1.01606		
763	1.01532		

TABLE EX

Dilatometry Data of 32 mole percent $BaCl_2$ Sample after the previous Run (Table EIX);

Sample 0.360 in. at 25°C.

Heating Temp.,°C.	L_T/L_{25}	Cooling Temp.,°C.	L_T/L_{25}
63	1.00039	722	1.01725
80	1.00068	707	1.01616
97	1.00108	693	1.01549
119	1.00153	671	1.01448
141	1.00190	661	1.01395
155	1.00233	654	1.01347
173	1.00273	645	1.01283
198	1.00332	640	1.01238
209	1.00361	636	1.01174
222	1.00392	631	1.01062
235	1.00437	629	1.01032
251	1.00482	625	1.00948
265	1.00516	621	1.00884
282	1.00570	614	1.00826
298	1.00612	609	1.00778
325	1.00666	596	1.00672
335	1.00698	584	1.00613
361	1.00757	578	1.00601
376	1.00797	559	1.00500
406	1.00854	542	1.00460

TABLE EX (Cont.)

Heating Temp., °C.	L_T/L_{25}	Cooling Temp., °C.	L_T/L_{25}
423	1.00894	533	1.00440
445	1.00947	523	1.00424
477	1.00988	510	1.00382
488	1.01008	496	1.00354
496	1.01025	480	1.00309
523	1.01077	457	1.00242
532	1.01096	391	1.00185
560	1.01153	377	1.00150
571	1.01184	290	1.00109
586	1.01232	258	1.00071
598	1.01266	176	0.99995
620	1.01315	127	0.99940
635	1.01349		
650	1.01383		
664	1.01431		
675	1.01515		
685	1.01585		
688	1.01629		
694	1.01752		
700	1.01863		
703	1.01974		
707	1.02086		
710	1.02142		

TABLE EX (Cont.)

Heating Temp.,°C.	L_T/L_{25}	Cooling Temp.,°C.	L_T/L_{25}
722	1.02237		
735	1.02234		
743	1.02199		
746	1.02160		
750	1.02066		
757	1.01938		

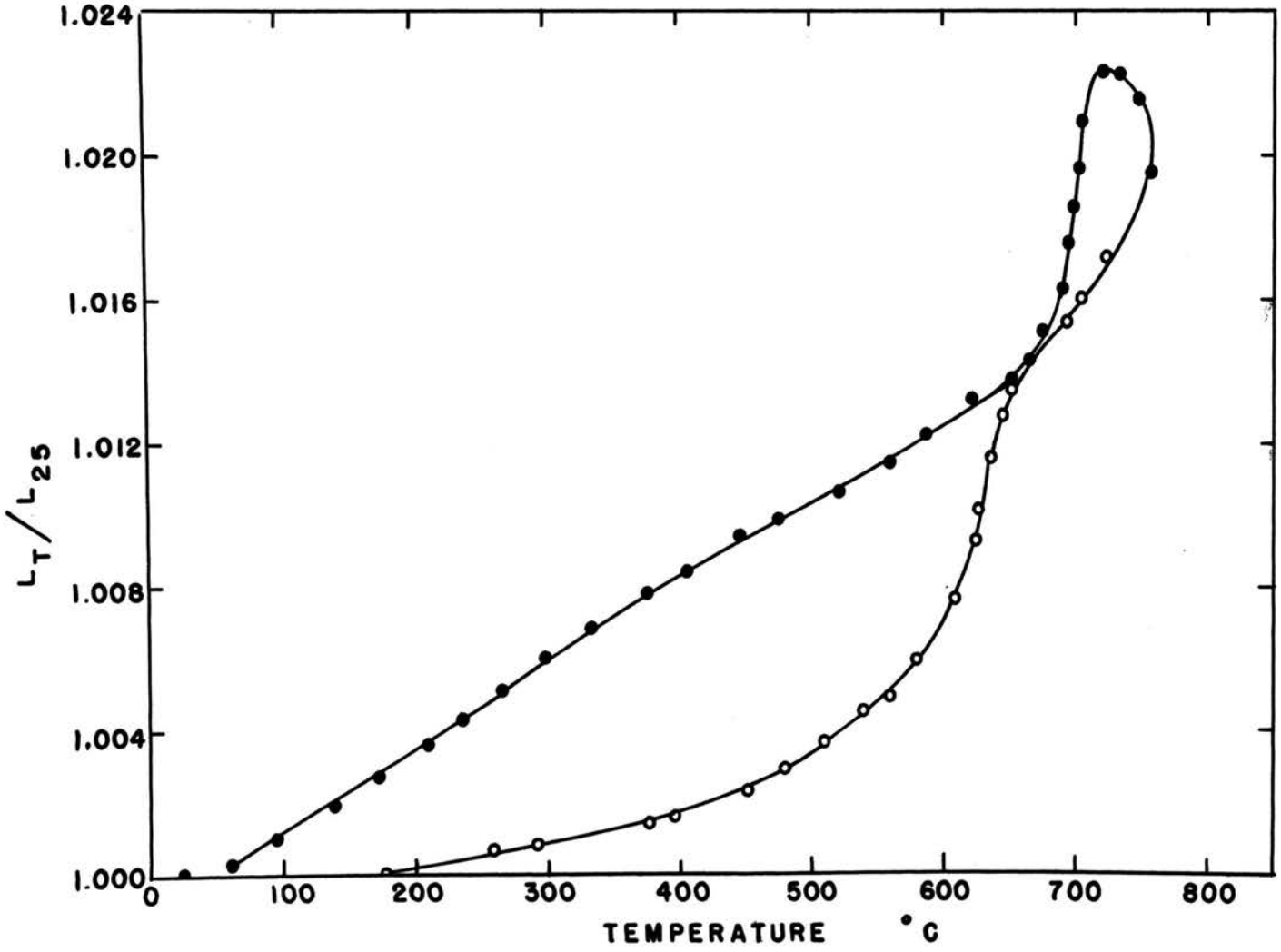

Figure E2. Thermal Expansion of 32 mole % $BaCl_2$ Sample on the Second Run Measured by TDA

TABLE EXI

Dilatometry Data of 40 mole percent $BaCl_2$ Sample Preheated at 815°C. for 24 hours;
Sample 0.355 in. at 25°C.

Heating Temp.,°C.	L_T/L_{25}	Cooling Temp.,°C.	L_T/L_{25}
93	1.00036	757	1.01588
127	1.00102	744	1.01565
165	1.00169	730	1.01490
186	1.00215	717	1.01431
210	1.00275	707	1.01371
223	1.00344	694	1.01351
245	1.00401	686	1.01302
260	1.00436	681	1.01254
274	1.00476	676	1.01138
287	1.00505	670	1.01040
317	1.00548	664	1.00955
335	1.00589	661	1.00912
347	1.00623	654	1.00870
371	1.00669	647	1.00819
391	1.00713	639	1.00779
416	1.00768	623	1.00694
446	1.00825	614	1.00662
465	1.00869	601	1.00594
482	1.00926	591	1.00537
501	1.00983	575	1.00467
515	1.01032	566	1.00457

TABLE EXI (Cont.)

Heating Temp.,°C.	L_T/L_{25}	Cooling Temp.,°C.	L_T/L_{25}
524	1.01080	558	1.00409
543	1.01120	548	1.00354
583	1.01187	532	1.00278
595	1.01216	521	1.00224
642	1.01306	514	1.00209
663	1.01349	503	1.00152
674	1.01386	494	1.00095
685	1.01435	471	0.99985
690	1.01463		
699	1.01506		
703	1.01565		
708	1.01622		
713	1.01678		
718	1.01746		
722	1.01777		
725	1.01842		
729	1.01947		
733	1.02029		
735	1.02074		
737	1.02144		
741	1.02235		
744	1.02311		
748	1.02334		

TABLE EXI (Cont.)

Heating Temp., °C.	L_T/L_{25}	Cooling Temp., °C.	L_T/L_{25}
752	1.02368		
762	1.02368		
766	1.02337		
769	1.02295		
771	1.02174		
774	1.01952		
775	1.01828		

TABLE EXII

Dilatometry Data of 50 mole percent $BaCl_2$ Sample Preheated at 815°C. for 24 hours;

Sample 0.351 in. at 25°C.

Heating Temp.,°C.	L_T/L_{25}	Cooling Temp.,°C.	L_T/L_{25}
88	1.00061	790	1.02248
127	1.00137	775	1.02139
180	1.00166	759	1.02078
204	1.00198	740	1.01983
223	1.00242	720	1.01903
272	1.00387	714	1.01828
296	1.00457	710	1.01762
319	1.00515	705	1.01586
335	1.00550	696	1.01346
363	1.00614	687	1.01203
381	1.00657	682	1.01151
409	1.00710	676	1.01094
428	1.00748	666	1.01045
440	1.00786	654	1.00959
461	1.00844	649	1.00953
492	1.00911	636	1.00913
524	1.00981	624	1.00858
541	1.01030	611	1.00789
588	1.01127	595	1.00734
613	1.01173	584	1.00708

TABLE EXII (Cont.)

Heating Temp., °C.	L_T/L_{25}	Cooling Temp., °C.	L_T/L_{25}
632	1.01214	570	1.00639
662	1.01273	544	1.00549
687	1.01314	535	1.00509
704	1.01349	523	1.00494
721	1.01384	510	1.00439
736	1.01391	488	1.00372
740	1.01419	474	1.00326
744	1.01462	455	1.00282
749	1.01522	441	1.00262
754	1.01591	427	1.00198
757	1.01677	405	1.00137
759	1.01714	393	1.00074
762	1.01805	362	1.00027
766	1.01962	351	1.00009
767	1.02047	327	0.99974
769	1.02147	188	0.99907
773	1.02247		
777	1.02262		
784	1.02279		
790	1.02279		
792	1.02268		

APPENDIX F

X-Ray Patterns of Phases and of Selected Compositions in the System $SrCl_2$-$BaCl_2$

X-ray patterns obtained at room temperature for phases and high-temperature x-ray scans of samples in the system $SrCl_2$-$BaCl_2$ are contained in this appendix. Heating and quenching techniques were used to determine phases in the system. High temperature techniques were employed for determination of thermal expansion and for study transformations in the system $SrCl_2$-$BaCl_2$.

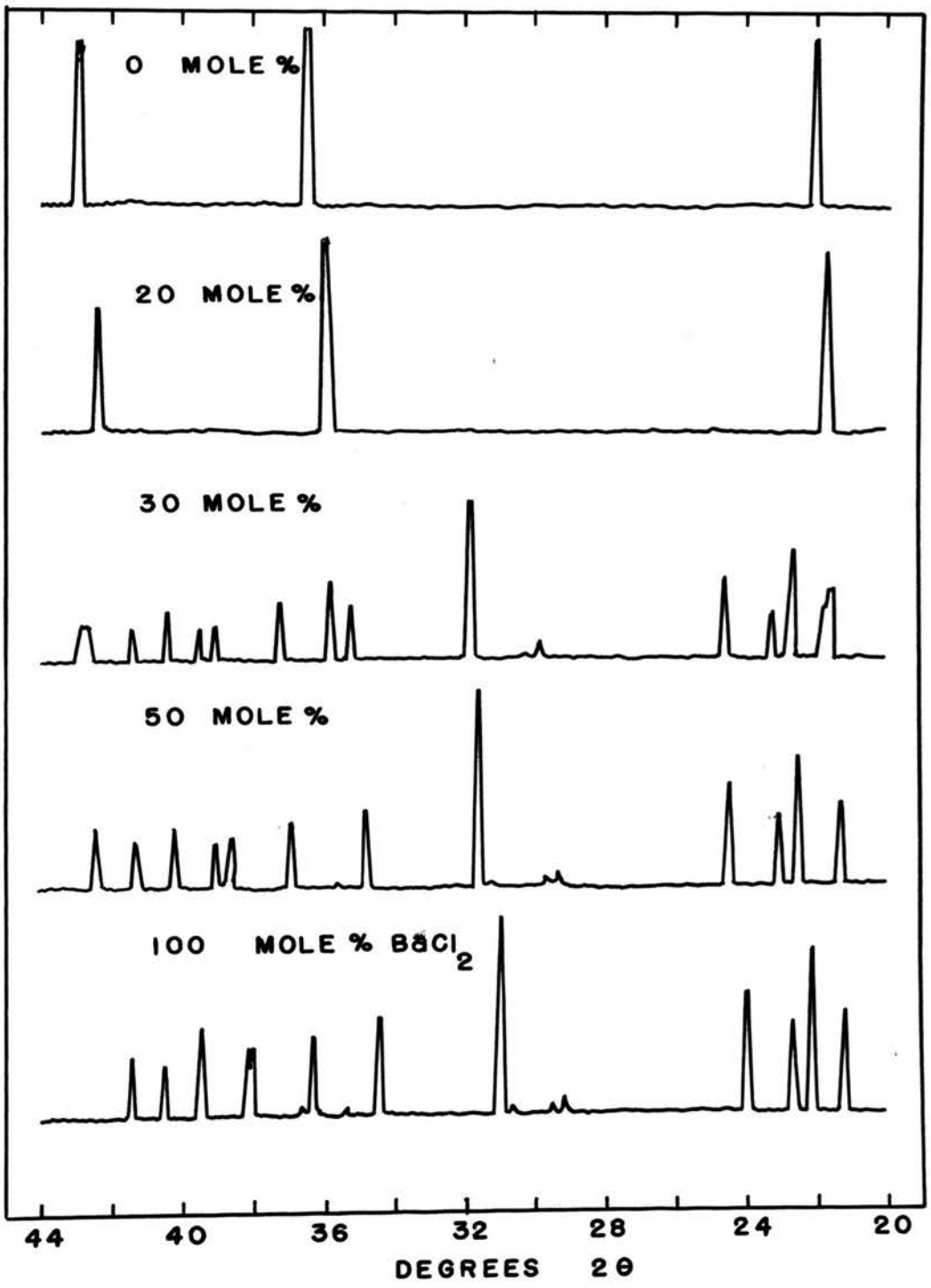

Figure F1. X-Ray Patterns of Phases in the System $SrCl_2$-$BaCl_2$; CuKα Radiation

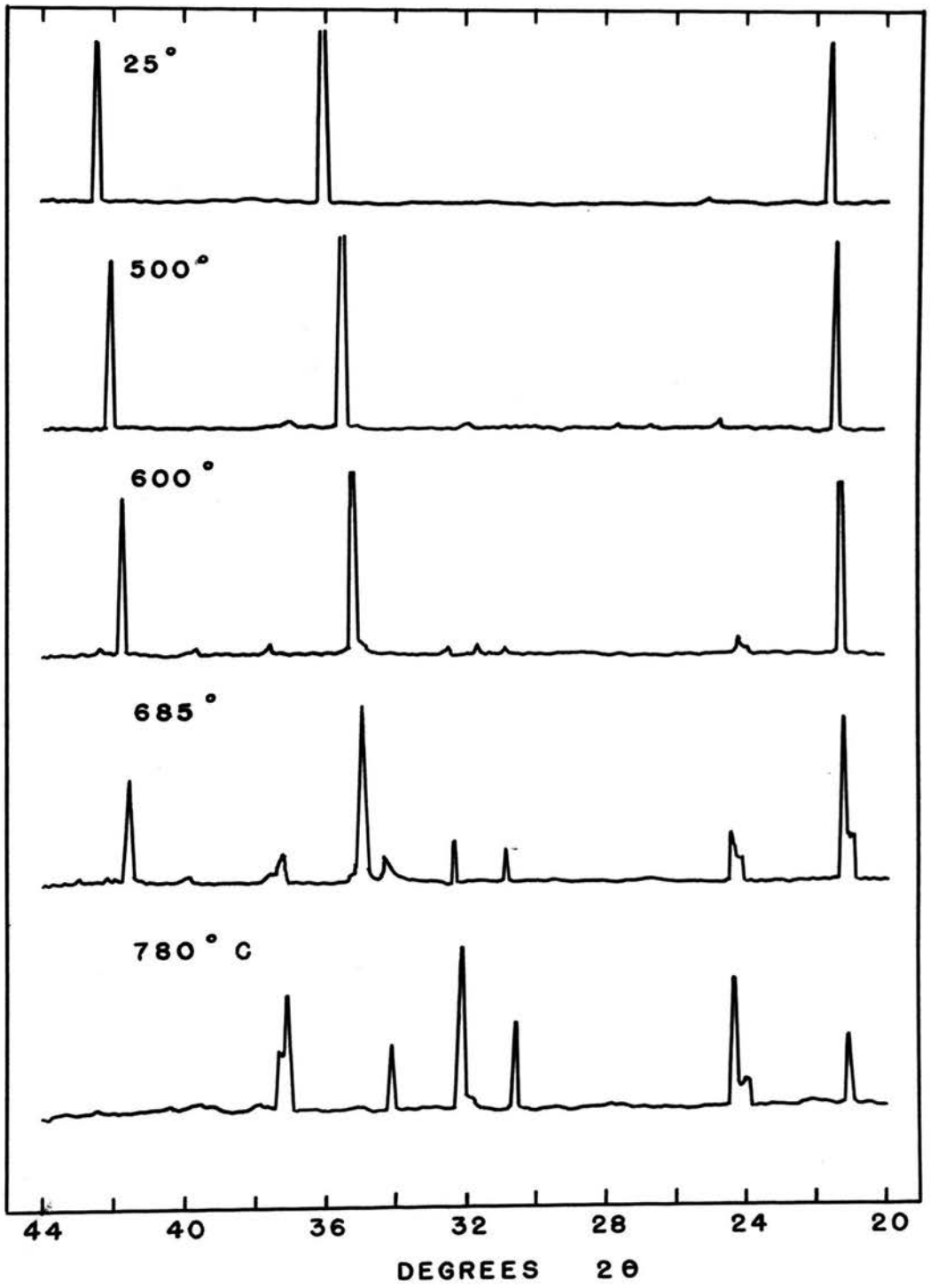

Figure F2. High Temperature X-Ray Patterns at Selected Temperatures on Heating of $Sr_{0.8}Ba_{0.2}Cl_2$; CuKα Radiation

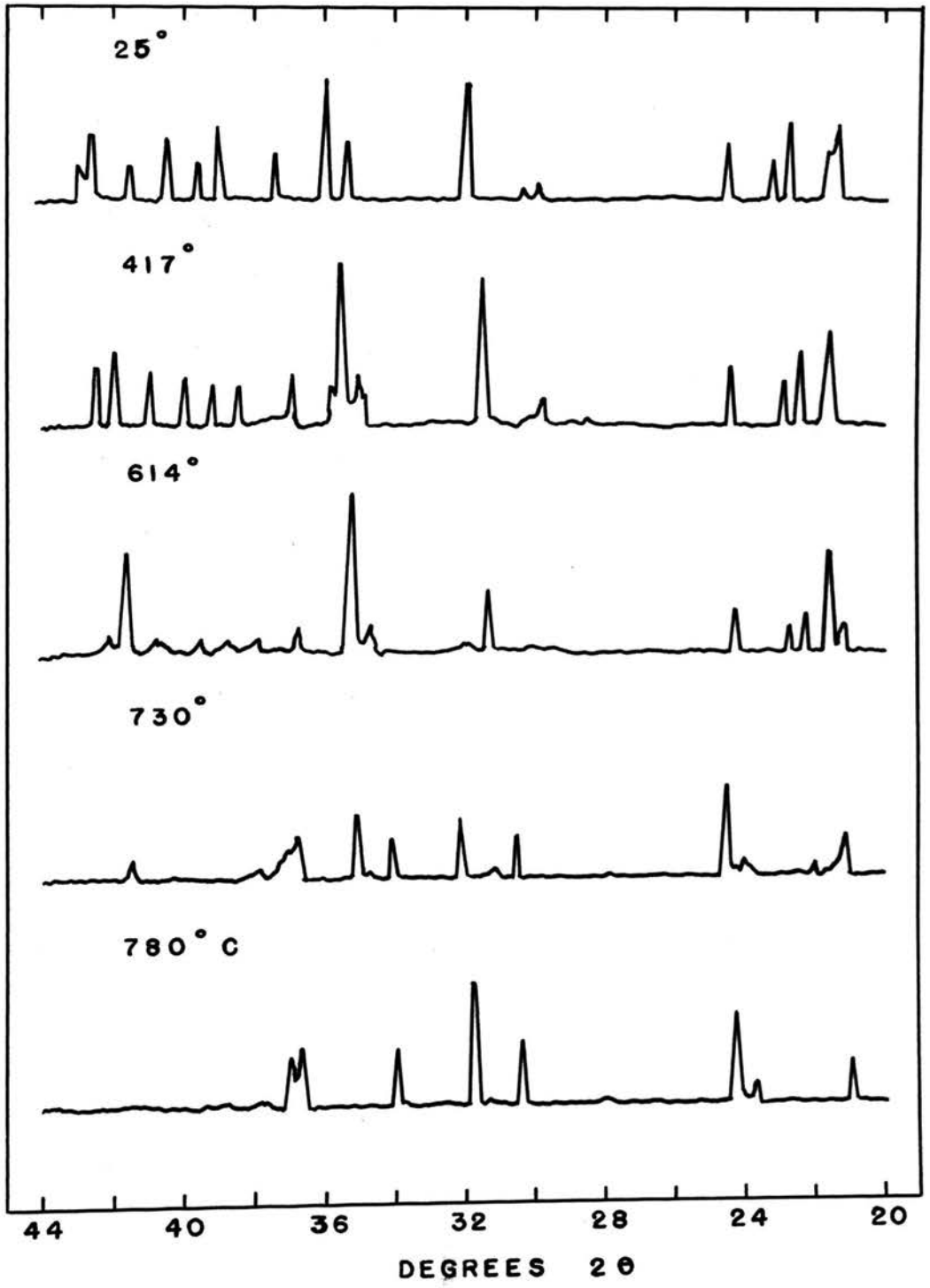

Figure F3. High Temperature X-Ray Patterns at Selected Temperatures on Heating of $Sr_{0.7}Ba_{0.3}Cl_2$; CuKα Radiation

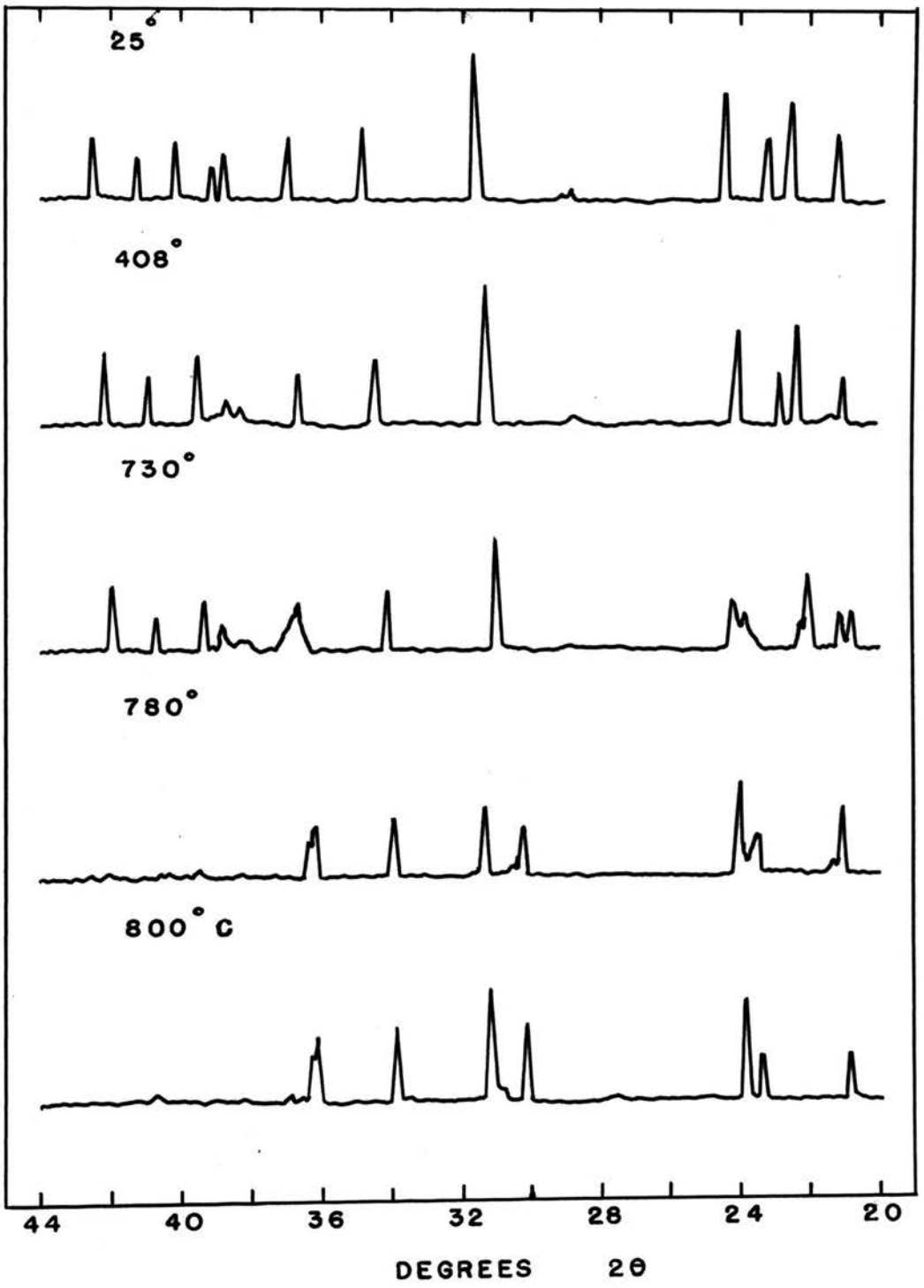

Figure F4. High Temperature X-Ray Patterns at Selected Temperatures on Heating of $Sr_{0.5}Ba_{0.5}Cl_2$; CuKα Radiation

VII. BIBLIOGRAPHY

1. W. L. Bragg, "The Analysis of Crystals by the X-Ray Spectometer," Proc. Roy. Soc. (London), 89A, 468 (1914).

2. R. W. G. Wyckoff; pp. 239-44 in Crystal Structure, 2nd Edition, Vol. 1, Interscience Publishers, Div. of John Wiley & Sons, New York, (1963).

3. Naray-Szabo, I.; pp. 58, & 192-247 in Inorganic Crystal Chemistry, Akademiai Kiado, Budapest, (1969).

4. R. C. Evans; pp. 145-63 in An Introduction to Crystal Chemistry, 2nd Edition, Cambridge University Press, New York, (1966).

5. B. F. Naylor, "Heat Contents at High Temperatures of Magnesium and Calcium Fluorides," J. Am. Chem. Soc., 67, 150-2 (1945).

6. A. S. Dworkin and M. A. Bredig, "The Heats of Fusion and Transition of Alkaline Earth and Rare Earth Metal Halides," J. Phys. Chem., 67, 697-8 (1963).

7. A. S. Dworkin and M. A. Bredig, "Heat Content and Entropy of Strontium Chloride from 298° to 1200°K," J. Chem. Eng. Data, 8 (3), 416-7 (1963).

8. R. Szwarc, "The Defect Contribution to the Excess Enthalpy of Uranium Dioxide-Calculation of the Frenkel Energy," J. Phys. Chem. Solids, 30 705-11 (1969).

9. R. A. Hein, L. H. Sjodahl and R. Szwarc, "Heat Content of Uranium Dioxide from 1200° to 3100°K," J. Nu l. Mat., 25, 99-102 (1968).

10. R. A. Hein, P. N. Flagella, and J. B. Conway, "High-Temperature Enthalpy and Heat of Fusion of UO_2," J. Am. Ceram. Soc., 51, 291-2 (1968).

11. M. A. Bredig, "The Order-Disorder (Lambda) Transition in Uranium Dioxide and Other Solids of the Fluorite Type of Structure,"; pp. 183-91 in COLLOQUE INTERNATIONAL SUR L'ETUDE DES TRANSFORMATIONS CRISTALLINES A HAUTE TEMPERATURE AU DESSUS DE 2000 K, EDITIONS DU C.N.R.S., Paris, (1972); ORNL-4437, (1969).

12. G. J. Janz, F. J. Kelly and J. L. Perano, "Melting and Pre-Melting Effects in the Alkaline Earth Halides," Trans. Faraday Soc., 59, 2718-22 (1963).

13. A. S. Dworkin and M. A. Bredig, "Diffuse Transition and Melting in Fluorite and Anti-Fluorite Type of Compounds: Heat Content of Potassium Sulfide From 298 to 1260°K," J. Phys. Chem., 72, 1277-81 (1968).

14. International Tables for X-ray Crystallography, Vol. 1, Edited by N. F. M. Henry and K. Lonsdale, The Kynoch Press, Birmingham, (1952).

15. H. E. Swanson and E. Tatge, "Standard X-ray Diffraction Powder Patterns," Nat. Bur. Stand. (U.S.) Circ. No. 539, Vol. I, P. 69-72 (1953).

16. H. E. Swanson, R. K. Fuyat, and G. M. Ugrinic, "Standard X-ray Diffraction Powder Patterns," Nat. Bur. Stand. (U.S.) Circ. No. 539, Vol. IV, P. 40(1955).

17. H. E. Swanson, H. F. McMurdie, M. C. Morris, E. H. Evans, and B. Paretzkin, "Standard X-ray Diffraction Powder Patterns," Nat. Bur. Stand. (U.S.), Monogr. 25-Section 9, P. 11-13 (1971).

18. J. C. Southard, "A Modified Calorimeter for High Temperatures. The Heat Content of Silica, Wollastonite and Thorium Dioxide Above 25°," J. Am. Chem. Soc., 63, 3142-6 (1941).

19. U. Croatto and M. Bruno, "Crystalline Structures with Lattice Disturbances. III. Strontium Chloride," Gazz. chim ital., 76, 246-54 (1946).

20. R. I. Efremova and E. V. Matizen, "Enthalpy of Barium Fluoride, Strontium Chloride, and Strontium Fluoride at High Temperatures," Izv. Sib. Otd. Akad. Nauk SSSR., Ser. Khim. Nauk., 1, 3-12 (1970).

21. B. T. M. Willis, "The Anomalous Behaviour of the Neutron Reflexions of Fluorite," Acta Cryst., 18, 75-6 (1965).

22. M. J. Cooper, K. D. Rouse and B. T. M. Willis, "Neutron Diffraction Studies of Anharmonic Temperature Factors in BaF_2," Acta Cryst., A24, 484-93 (1968).

23. M. J. Cooper and K. D. Rouse, "A Neutron Diffraction Study of SrF_2 and CaF_2," Acta Cryst., A27, 622-8 (1971).

24. B. T. M. Willis, "Neutron Diffraction Studies of the Actinide Oxides II. Thermal Motions of the Atoms in Uranium Dioxide and Thorium Dioxide Between Room

Temperature and 1100°C," Proc. Roy. Soc., A, 274, 134-44 (1963).

25. V. R. Belosludov, R. I. Efremova and E. V. Matizen, "Phase Transition in a Fluorite-Type Lattice," Fiz. Tverd. Tela, 16 (5), 1311-8 (1974).

26. R. W. Ure Jr., "Ionic Conductivity of Calcium Fluoride Crystals," J. Chem. Phys., 26 (6), 1363-73 (1957).

27. E. Barsis and A. Taylor, "Lattice Disorder in Some CaF_2-Type Crystals," J. Chem. Phys., 45, 1154-62 (1966).

28. G. M. Hood and J. A. Morrison, "Ionic Conduction and Diffusion in Single Crystals of $SrCl_2$," J. Appl. Phys., 38, 4796-802 (1967).

29. L. E. Nagel and M. O'Keeffe, "Highly-Conducting Fluorides Related to Fluorite and Tysonite," pp. 165-72 in Fast Ion Transport in Solids, edit. by W. van Gool, North-Holland, Amsterdam, (1973).

30. C. E. Derrington and M. O'Keeffe, "Anion Conductivity and Disorder in Lead Fluoride," Nature Physical Science, 246, 44-6 (1973).

31. H. Matzke, "Fluorine Self-Diffusion in CaF_2 and BaF_2," J. Mat'l. Sci., 5, 831-6 (1970).

32. H. Gemsky, "Crystallographic and Thermal Investigation of the Ternary System: Barium Chloride, Potassium Chloride, and Sodium Chloride," Jahrb. Min. Beil.-Bd., 36, 513-58 (1913).

33. W. Döll and W. Klemm, "Measurements on the Bivalent and the Quadrivalent Compounds of the Rare Earths. VII. The Structure of Several Dihalides," Z. anorg. allgem. Chem., 241, 239-58 (1939).

34. E. B. Brackett, T. E. Brackett and R. L. Sass, "The Crystal Structures of Barium Chloride, Barium Bromide, and Barium Iodide," J. Phys. Chem., 67, 2132-5 (1963).

35. K. Sahl, "Refinement of the Crystal Structures of $PbCl_2$ (Cotunnite), $BaCl_2$, | $PbSO_4$ (Anglesite), and $BaSO_4$ (Barite)," Beitr. Mineral. Petrog., 9, (2), 111-32 (1963).

36. J. Solans-Huguet and M. Font-Altaba, "X-ray Diffraction Diagram of Anhydrous Barium Chloride," Anales Real Soc. Espan. Fis. Quim. Madrid, 64, (5), 425-9 (1968).

37. B. K. Vainshtein, "Electronographic Determination of the Structure of Barium Chloride," Dokl. Akad. Nauk SSSR, 60, 1169-71 (1948).

38. C. E. Derrington and M. O'Keeffe, "The Solid Electrolyte Behavior of Barium Chloride and Strontium Bromide," paper submitted to Solid State Comm. (1974).

39. E. Vortisch, "Mixed Crystals in the Ternary Systems Formed by Strontium Chloride, Barium Chloride, and Sodium Chloride or Potassium Chloride," Jahrb. Min. Beil.-Bd., 38, 185-272 (1914).

40. E. M. Levin, C. R. Robbins and H. F. McMurdie; pp. 395 in Phase Diagrams for Ceramists, Edited and Published by The American Ceramic Society, INC. (1964).

41. A. G. Bergman and G. A. Bukhalova, "Exchange Decomposition in the Absence of Solvent-Complex Formation, Solid Solutions, and Exchange Decomposition in Melts of Strontium and Barium Fluorides and Chlorides," Zhur. Obsh. Khim., 19, 603-11 (1949).

42. A. Schei and H. Flood, "The Phase Diagram of the System $SrCl_2$-$BaCl_2$," Acta Chem. Scand., 14, 2067-70 (1960).

43. G. Brauer and O. Müller, "The Crystal Chemistry of Strontium Chloride," Z. anorg. u. allgem. chem., 295, 218-26 (1958).

44. J. H. Maurer and R. J. Ackermann, "A High-Temperature, Controlled Atmosphere X-Ray Diffractometer Attachment," Argonne National Laboratory Report, ANL-7257. (1967).

45. X-ray Powder Data File, Sets 1-5 (Revised), American Society for Testing Materials, Philadelphia (1960).

46. American Institute of Physics Handbook, McGraw-Hill Book Company, Inc. New York, (1957).

47. C. A. Sorrell and R. J. Ackermann, Unpublished data.

48. C. Frondel, "The System of Mineralogy," Vol. III, pp. 117-9, Silica Minerals, Wiley, New York, (1962).

49. C. A. Sorrell, H. U. Anderson and R. J. Ackermann, "Thermal Expansion and the α-β Transformation in Quartz: II Dilatometric Studies," paper submitted to J. Phys. Chem. Solids (1974).

50. O. J. Whittemore Jr. and N. N. Ault, "Thermal Expansion of Various Ceramic Materials to 1500°C," J. Am. Ceram. Soc., 39 (12), 443-4 (1956).

51. K. Grjotheim, H. A. Ikeuchi, S. Dhabanandana and J. Krogh-Moe, "The Solution of Alkaline Earth Metals in Their Molten Halides. III. The Densities of Melts in the Systems Barium-Barium Chloride, Barium-Barium Bromide and Strontium-Strontium Chloride," Acta Chem. Scand., 25 (9), 3415-20 (1971).

52. D. T. Cromer and J. B. Mann, "X-Ray Scattering Factors Computed from Numerical Hartree-Fock Wave Functions," Los Alamos Scientific Laboratory Report, LA-3816 UC-34 Physics TID-4500 (1968).

53. D. K. Smith, "A Fortran Program for Calculating X-Ray Powder Diffraction Patterns," Report of Lawrence Radiation Laboratory, University of California, UCRL-7196 (1963).

54. A. R. Ubbelohde, "Thermal Transformations in Solids," Quart. Rev. 11, 246-72 (1957).

55. E. D. D. Schmidt and K. Vedam, "Variation of the Refractive Indices of CaF_2, BaF_2 and β-PbF_2 with Pressure to 7 kb," J. Phys. Chem. Solids, 27, 1563-6 (1966).

56. D. P. Dandekar and J. C. Jamieson, "High Pressure Phases of RX_2 Fluorides," Trans. Amer. Crystallogr. Ass. 5, 19-27 (1969).

57. H. I. Smith and J. H. Chen, "High-Pressure Investigations of the Repulsive Potential and Phase Transitions in CaF_2, SrF_2, and BaF_2," Bull. Am. Phys. Soc. 11, 414 (1966).

58. G. A. Samara, "Pressure-Induced Phase Transitions in Solids: BaF_2," Phys. Rev. B10, 4194-8 (1970).

59. J. R. Kessler, E. Monberg and M. Nicol, "Studies of Fluorite and Related Divalent Fluoride Systems at High Pressure by Raman Spectroscopy," J. of Chem. Phys. 60, (12), 5057-65 (1974).

60. E. M. Monberg and M. Nicol, "Vibrational Raman Spectrum of Orthorhombic $BaBr_2$," J. of Chem. Phys. 60, (12), 5054-6 (1974).

61. Y. Sauka, "Crystal Modifications of Lead Fluoride," Zh. Obshch. Khim. 19, 1453-8 (1949).

62. J. A. A. Ketelaar, "The Crystal Structure of PbF_2," Z Krist. 84, 62-4 (1932)

63. J. C. Butler and C. A. Sorrell, "Subsolidus Formation of Binary Solid Solutions of Barium, Strontium, and Lead Sulfates and Fluorides," High Temp. Science, 4, (2), 128-40 (1972).

VIII. VITA

Damri Sukhotanang was born on September 6, 1949, in Petchburi, Thailand. He received his elementary and secondary education in that town.

He attended college at Chulalongkorn University, Bangkok, Thailand, receiving a Bachelor of Science degree with Second Class Honours in Ceramics Technology, Department of Chemical Technology, in April 1969. In May 1972, he received a Master of Science degree in Ceramic Engineering from the University of Missouri - Rolla, Rolla, Missouri.

He was employed as an instructor by the Department of Chemical Technology, Faculty of Science, Chulalongkorn University, Bangkok, Thailand, during the period June 1969 to June 1970. During the fall semester of the 1973-74 academic year, he was a Resident Associate with the Chemistry Division, Argonne National Laboratory, Argonne, Illinois.

He has been enrolled in the Graduate School of the University of Missouri - Rolla, continuing graduate study in the Department of Ceramic Engineering since August, 1972 and has held a scholarship from Thailand.

He is a member of the American Ceramic Society and Keramos.